Decentralized Control of Multi-Agent Dynamic Games

J. Postma

Master of Science Thesis

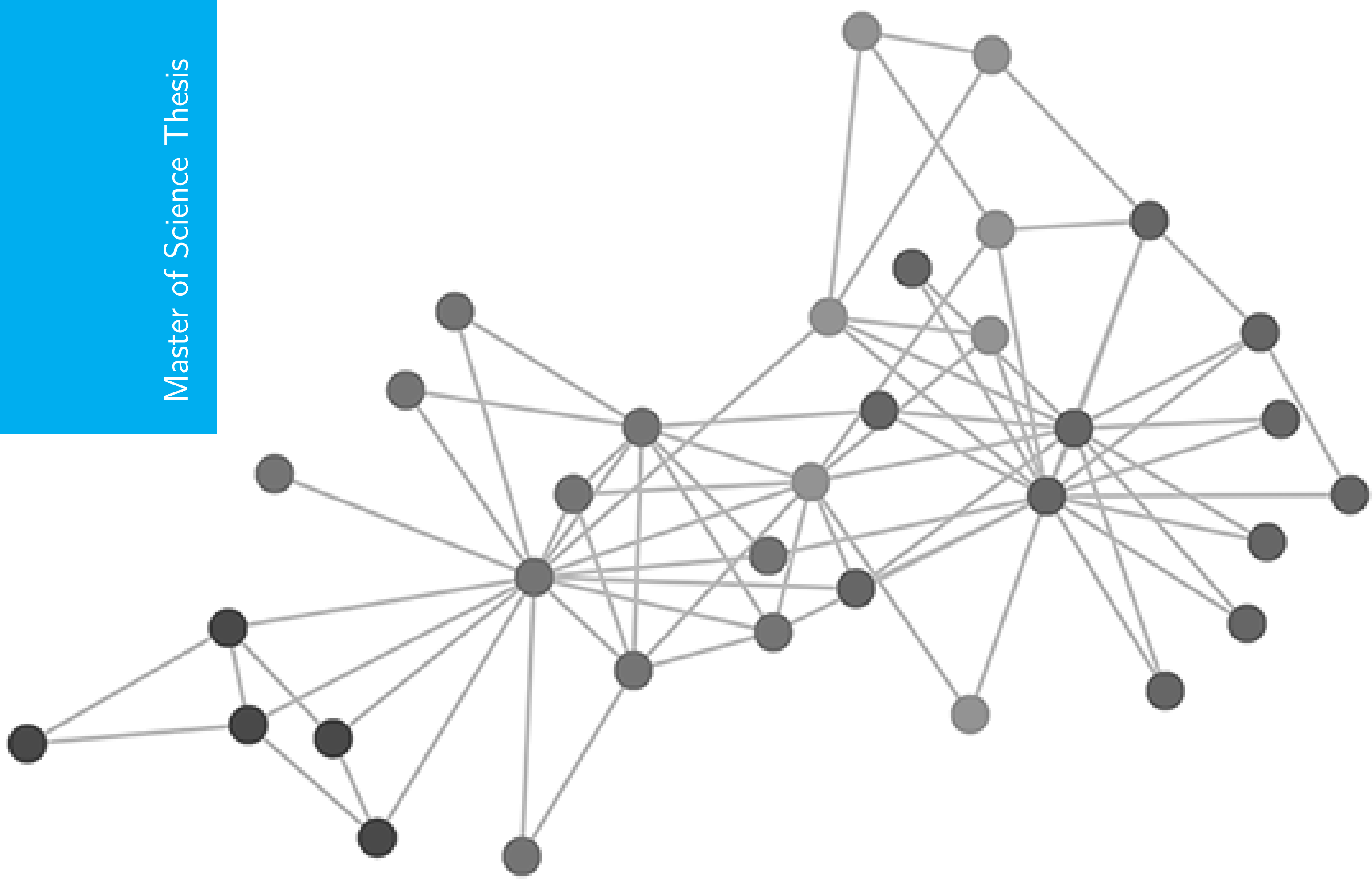

TU Delft
Delft University of Technology

Delft Center for Systems and Control

Decentralized Control of Multi-Agent Dynamic Games

Master of Science Thesis

For the degree of Master of Science in Systems and Control at Delft University of Technology

J. Postma

February 15, 2020

Faculty of Mechanical, Maritime and Materials Engineering (3mE) · Delft University of Technology

SUPERVISORS:
prof. G. Giordano
Dr.ir. S. Grammatico

Abstract

The field of network systems and multi-agent games has been characterised by a growing interest in the recent years. Findings in the study of network systems provide elegant ways of decentralizing controllers such that large systems can be controlled globally resorting to an ensemble of local control inputs, each acting on a small sub-portion of the overall system. These findings can be applied to the field of game theory, resulting in the concept of multi-agent network games. Recent studies have analysed this topic and proposed methods to find the equilibria of network games.

This thesis deals with these topics, and in particular it provides control methods to steer multi-agent games to the Nash equilibrium in a decentralized way whilst being subject to intrinsic dynamics.

The research will cover three distinct problems: first a networked system will be considered with games that consist of a cost-function that only depends on the agent state as well as the states of the neighbouring agents. Secondly the report introduces aggregate games with cost-functions that rely on the average of all subsystems and will find this average by means of an algorithm derived from the concept of consensus. Lastly a system subject to games with cost-functions that are dependent on agents not necessarily in the neighbour set is introduced, solved by means of a decentralized estimation method. For all of these problems the study provides distinct controllers.

The controllers converge to the Nash equilibrium and are proven to be stable. Furthermore examples are provided for each of the three scenarios. The results are applied to a case study, where a wind farm consisting of multiple pitch-controlled wind turbines is considered. Applying the control actions to this wind farm case results in the wind turbines being steered to their Nash equilibrium.

Table of Contents

Preface

This report is written to conclude the Master's degree in Systems & Control at the 3mE faculty of the TUDelft. Not being specialized in the topics I would be tackling during the last year or so (specifically game theory and decentralized control), this research provided to be a decent challenge. Thanks to my supervisors Giulia Giordano and Sergio Grammatico this challenge was not unsurpassable.

During my research time I decided to work at Allseas Engineering BV, an offshore company situated in delft (near the IKEA). Even though my work there is not related at all to this research, it helped me a lot during the process of graduating. It provided a healthy distraction; where I could take a study break whilst still being productive in a way. During my time working there I've been asked numerous times whether I'm graduated already, or when told 'no' they would ask me how long it will take. Which inspired me to keep working on this research, in view of finally starting a long-awaited career.

Part I

Introduction

Chapter 1

General Context

This chapter will introduce and give detail about the main fields discussed in this research. For the modelling and control of large scale systems, a useful approach is to divide the system into multiple subsystems. For example a power grid can be divided into subsystems (power storage nodes), which communicate with one another through links (power lines). This is referred to as a networked system consisting of nodes and edges; subsystems and links respectively. With the introduction of networked systems, approaches to design controllers following a similar structure were researched. This gave the rise to network decentralized controllers, i.e. a control structure that does not require a central all-knowing computer but instead consists of controllers which can be designed locally. An example of this is a swarm of cooperating drones with the goal to avoid collision with each other. For each of the drones a local controller can be designed which is only based on their near neighbours. Designing controllers in such a way reduces the controller complexity significantly and as such the scalability issues present in centralized controllers are not as prevalent in their decentralized counterparts. Relevant studies were done in the field of network systems [1], with findings in state agreement problems for multi-agent system coordination; [2], [3], [4] and [5]. Furthermore research on network-decentralized control was done, where a control action for a subsystem is based only on the subsystem's state and information from the subsystems it communicates with. Subjects within this topic range from network-decentralized stability [6], robust control [7] and network-decentralized state estimation [8].

In addition to a network decentralized approach, which provides a scalable solution for increasing network sizes, the field of game theory can be discussed. Multi-agent games describe the field of a set of participants (agents) with each a certain optimal decision which is based on the decision of the other participants (the game). The problem of steering multi-agent games to an equilibrium has been of interest in recent years. From systems describing Cournot competitions, to more general systems with imposed dynamics. One of the first occurences of finding equilibrium problems in multi-agent games were introduced in [9] and henceforth referred to as Nash equilibrium problems. Since then the Nash equilibrium problems were extended to generalized Nash equilibrium problems as in [10] and [11], where the focus of the research was to prove the existence of an equilibrium for competitive economic systems. After the introduction of generalized Nash equilibrium problems, numerous studies on the subject were done as discussed in [12]. The application of generalized Nash equilibrium extends to multi-agent network games as in [13] and [14], both introducing equilibrium finding algorithms. Furthermore dynamical steering of economic model to a supply-demand equilibrium was investigated in [15], such a model is referred to as a Cournot competition.

This thesis aims to extend the current research on network decentralized multi agent games. Solving a game theoretic problem and steering each of the agents to the game equilibrium, referred to as the Nash Equilibrium, has been researched extensively. However, this does not hold for the addition of dynamics to the agents and the resulting stability problems. Each of the agents might be a stable system with well defined local controllers. However, certain cross agent interactions exist as a result of the overarching game theoretic problem, which could introduce instabilities. This research addresses these difficulties and provides multiple controllers for different game theoretic scenarios.

Chapter 2

Literature Review

This chapter revisits the literature review that preceded this research, reported in Appendix A. In this review we discussed the terms network systems, network decentralized control, multi agent games, and it provided the problem statement for this research. Appendix A-1 provides details about network systems; it introduces the concept of graphs with relevant properties, which provides a solid basis for the chapter thereafter. Appendix A-2 explains the main concepts of consensus theory, mainly the sections about continuous-time consensus, Appendix A-2-2, provide beneficial background knowledge for this research. Following that, Appendix A-3 describes network decentralized control approaches, providing useful tools and methods to prove the stabilizability of network systems. Appendix A-4 goes into detail about game theory, starting with general definitions and followed by control approaches to steer the game to its Nash Equilibrium. In Appendix A-5 a brief summary of all the chapters is provided. As a short summary we focus on the concepts of continuous time consensus and multi agent game theory.

Literature review: continuous time consensus

In this section we briefly summarize the concepts discussed in the aforementioned literature review, as included in Appendix A. We mainly focus on continuous time consensus which will find its uses during this research. Consider a network system with nodes and edges as the example depicted in Figure 2-1. For this network we define the set of nodes as $\mathcal{V} = \{1, \dots, N\}$ where N is the number of nodes. The set of edges is defined as $\mathcal{E} \subset \mathcal{V} \times \mathcal{V}$. We note that there exists an edge between nodes i and j iff $\{i, j\} \in \mathcal{E}$; where $\{\cdot, \cdot\}$ denotes an unordered pair and $(\cdot, \cdot)$ an ordered pair. Combining the set of nodes and edges results in the definition of a graph, which in this research will be represented by $\mathcal{G}(\mathcal{V}, \mathcal{E})$. Furthermore we define $\mathcal{N}_i$ as the neighbour set of node i which contains all nodes about which node i receives information; i.e. if $(i, j) \in \mathcal{E}$ then $j \in \mathcal{N}_i$. Throughout this research we consider undirected graphs, meaning that $j \in \mathcal{N}_i$ implies $i \in \mathcal{N}_j$; or $(i, j) \in \mathcal{E}$ implies $(j, i) \in \mathcal{E}$.

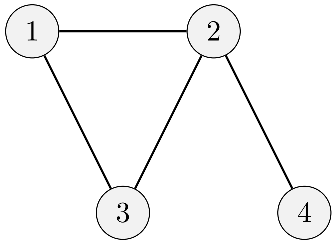

Figure 2-1: Example of an undirected graph with $N = 4$ nodes (grey numbered circles) and 4 edges (black solid lines). The set of nodes is defined as $\mathcal{V} = \{1, 2, 3, 4\}$ and the set of edges as $\mathcal{E} \in \{\{1, 2\}, \{1, 3\}, \{2, 3\}, \{2, 4\}\}$. The neighbour sets are equal to $\mathcal{N}_1 = \{2, 3\}$, $\mathcal{N}_2 = \{1, 3, 4\}$, $\mathcal{N}_3 = \{1, 2\}$, $\mathcal{N}_4 = \{2\}$.

With the preliminary definitions of graph theory done, we can shift our focus on the concepts of consensus. As a decentralized approach to find the weighted average of agent states, the field of consensus provides useful results for the design of decentralized controllers. Each individual agent aims to find the weighted average by means of the information sent through the graph edges. We introduce the adjacency matrix $A_{\mathcal{G}}$ as a systematic way to represent the information distribution, specifically:

$$\{A_{\mathcal{G}}\}_{ij} = \mathbb{e}_i^\top A_{\mathcal{G}} \mathbb{e}_j = \begin{cases} a_{ij} & \text{if } j \in \mathcal{N}_i \\ 0 & \text{otherwise} \end{cases} \tag{2-1}$$

With $a_{ij} \in \mathbb{R}_{>0}$ a certain weight associated with the corresponding edge. For the graph depicted in Figure 2-1 given equal edge weights of 1 (an un-weighted graph) this results in

$$A = \begin{bmatrix} 0 & 1 & 1 & 0 \\ 1 & 0 & 1 & 1 \\ 1 & 1 & 0 & 0 \\ 0 & 1 & 0 & 0 \end{bmatrix}$$

We use the adjacency matrix to construct the Laplacian matrix $L_{\mathcal{G}}$, the fundamental matrix for continuous time consensus, as $L_{\mathcal{G}} = \text{diag}(A_{\mathcal{G}} \mathbb{1}_N) - A_{\mathcal{G}}$. Following the findings from [1], this leads us to the continuous time consensus algorithm of

$$\dot{\mathbf{z}}(t) = -L_{\mathcal{G}} \mathbf{z}(t) \tag{2-2}$$

where $\mathbf{z}(t)$ is the collection of the agents beliefs of the average, with $\mathbf{z}(0)$ equal to the (initial) values of the agents.

This approach is limited to a static case, where the agents find the weighted average of the constant valued agent states. This research will require a consensus algorithm that finds the weighted average of continuously changing values, as such these findings are extended upon in Chapter 4.

Literature review: game theory

This section will briefly discuss the game theoretic notations and definitions introduced in the literature review and reused in this research. We define a generalized Nash equilibrium problem (GNEP) for each agent v as

$$\forall v: \quad \min_{y_v} \theta_v(y_v, \mathbf{y}_{-v}) \;\text{ s.t. }\; y_v \in Y_v(\mathbf{y}_{-v}) \tag{2-3}$$

In other words, each agent has a certain cost function θ_v they want to minimize. This function is dependent on the agent's state y_v as well as the collection of all other agent states $\mathbf{y}_{-v}$, where $\mathbf{y}_{-v}$ is defined as the vector of all states where the state of agent v is omitted. Since agent v can only directly influence its own state y_v, the cost function will be minimized with respect to y_v only. Furthermore a constraint set of the form $y_v \in Y_v(\mathbf{y}_{-v})$ exists; the strategy set of agent v. For this research however we omit the constraint (i.e. we set $Y_v(\mathbf{y}_{-v}) = \mathbb{R}$). We furthermore define the Nash equilibrium as $\mathbf{y}^\star$ and as such we find

$$\forall v: \quad y_v^\star \in \arg\min_{\zeta_v} \theta_v(\zeta_v, \mathbf{y}_{-v}^\star) \tag{2-4}$$

This implies that in order to find the Nash equilibrium of agent v, we need to know the Nash equilibria of the other agents $\mathbf{y}_{-v}^\star$. However, the same holds for all other agents and as a result finding the Nash equilibrium is not as straightforward.

Chapter 3

Overview

This chapter will provide an overview of this report. Continuing this part of the report Chapter 4 will extend the preliminary results needed for this research.

After that, Part II will contain the main findings of the research. This part starts off with the problem definition in Chapter 5. Following this we propose a controller in Section 6-1 which steers the system to its Nash equilibrium under the assumption of a fully connected graph. Dropping this assumption in Chapter 7, we alter the controller to be applicable to aggregate games using the preliminary results from Chapter 4. We end the part with Chapter 8 introducing a decentralized state estimation method, which can be applied to the results of Chapter 7.

In the following part, Part III, we introduce an illustrative case study. This part contains Chapter 9 in which we describe a wind farm model with the main goal of maximizing output power whilst minimizing the strain on the individual wind turbines.

After this case study Part IV will conclude the research. In this part we will discuss the results (Chapter 10), provide some conclusions (Chapter 11), and we end the part by giving suggestions of future research problems (Chapter 12).

Chapter 4

Preliminary findings: consensus on time-varying signals

To extend the background knowledge for this research, this chapter will provide some preliminary results on time-varying consensus. For simplicity we can assume that all agents have access to all other agents' information, i.e. a fully connected graph; as done in Chapter 6. However, this assumption gets more limiting the higher the number of participants. As such we introduce a (undirected) communication graph $\mathcal{G}_c(\mathcal{V}, \mathcal{E}_c)$ with $\mathcal{V} \in \{1, \ldots, N\}$ the set of agents and $\mathcal{E}_c \in \mathcal{V} \times \mathcal{V}$ the set of edges. In essence, if $\{v, j\} \in \mathcal{E}_c$ then agent v has access to the output of agent j, y_j. We define the set of neighbours of agent v as $\mathcal{N}_{c,v} = \{j \in \mathcal{V} \mid \{v, j\} \in \mathcal{E}_c\}$.

In view of decentralization of the system, the control action can only be based on the agents in the neighbour set, i.e.

$$u_v(t) := u_v(y_v, \{y_j\}_{j \in \mathcal{N}_{c,v}}) \tag{4-1}$$

Similarly the cost-functions of the agents are based on the output of the other agents. However, the cost functions do not necessarily follow the same topology as the communication graph. As such we introduce a second (possibly directed) graph describing the dependency of the cost-function θ_v on the other agents. We define this graph as $\mathcal{G}_\theta(\mathcal{V}, \mathcal{E}_\theta)$ and the neighbour set $\mathcal{N}_{\theta,v} = \{j \in \mathcal{V} \mid (v, j) \in \mathcal{E}_\theta\}$, with the cost functions defined as

$$\theta_v(t) := \theta_v(y_v, \{y_j\}_{j \in \mathcal{N}_{\theta,v}}) \tag{4-2}$$

To illustrate this difference in graph topologies, Figure 4-1 shows both graphs with the solid line representing $\mathcal{G}_c$ and the dashed lines as $\mathcal{G}_\theta$.

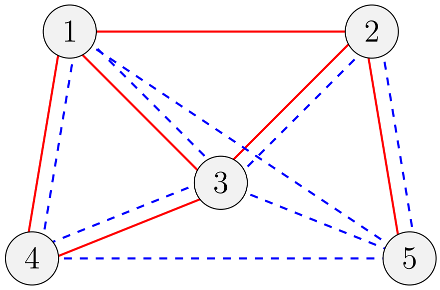

Figure 4-1: Example: undirected graph of the information exchange of the output (solid line) and the dependency of the agent's cost function on neighbouring agents (dashed).

Dynamic Consensus

Since the cost functions can depend on agents that are not directly accessible to the respective agents, a way for these agents to get a certain estimate of these outputs must be introduced. For simplicity of notation we will discuss a system with a scalar output. However, the following findings can be extended to n-dimensional output vectors as well (with all agents having the same output dimensions).

We start by defining the adjacency and Laplacian matrix corresponding to the communication graph $\mathcal{G}_c(\mathcal{V}, \mathcal{E}_c)$. The adjacency matrix is constructed as

$$\{A_{\mathcal{G}_c}\}_{i,j} = a_{ij} \tag{4-3}$$

where a_{ij} is equal to the weight of the edge from node i to node j, where $a_{ij} = 0$ if $\{i, j\} \notin \mathcal{E}_c$. For un-weighted graphs the edge weights are set to 1 and as such $a_{ij} = 1$ if $\{i, j\} \in \mathcal{E}_c$. We can determine the Laplacian matrix of the graph using the adjacency matrix as follows:

$$L_{\mathcal{G}_c} = \text{diag}(A_{\mathcal{G}_c}\mathbb{1}_N) - A_{\mathcal{G}_c} \tag{4-4}$$

The Laplacian matrix plays a key role in continuous-time consensus. However, certain assumptions on the graph topology must hold for the system to reach a consensus.

Assumption 4.1. *The communication graph $\mathcal{G}_c(\mathcal{V}, \mathcal{E}_c)$ is connected and has at most one sink.*

In view of Assumption 4.1, the Laplacian matrix has a unique eigenvalue of $\lambda = 0$ with a corresponding eigenvector of $\mathbb{1}_N$. We first consider a constant output $\mathbf{y}(t) = \mathbf{y}$, where the consensus algorithm

$$\dot{\mathbf{z}}(t) = -L_{\mathcal{G}_c}\mathbf{z}(t) \tag{4-5}$$

ensures that $\mathbf{z}(t) \to \mathbb{1}_N(\mathbf{w}^\top \mathbf{y})$ for $t \to \infty$ under Assumption 4.1 and if $\mathbf{z}(0) = \mathbf{y}$, where $\mathbf{w}$ is the normalized left-eigenvector of $L_{\mathcal{G}_c}$ corresponding to the eigenvalue $\lambda = 0$ (which is equal to $\mathbf{w} = \frac{1}{N}\mathbb{1}_N$ in view of the graph being undirected). As such all agents reach consensus on the average of the system outputs. The algorithm will converge to $\mathbf{z}(t) \to \mathbb{1}_N(\frac{1}{N}\mathbb{1}_N^\top \mathbf{y})$ for $t \to \infty$.

The approach from Equation (4-5) works well for a constant consensus variable. However, in case $\mathbf{y}(t)$ changes over time, the algorithm will converge to the (weighted) average of the initial values $\mathbf{y}(0)$. To compensate for this, the algorithm will be extended by giving the derivative of the estimate $\dot{\mathbf{z}}(t)$ a bias with respect to the derivative of the output $\dot{\mathbf{y}}(t)$:

$$\dot{\mathbf{z}}(t) = -L_{\mathcal{G}_c}\mathbf{z}(t) + \dot{\mathbf{y}}(t), \quad \mathbf{z}(0) = \mathbf{y}(0) \tag{4-6}$$

which, by introducing a change of coordinates $\mathbf{p}(t) = \mathbf{z}(t) - \mathbf{y}(t)$, transforms to

$$\dot{\mathbf{p}}(t) = -L_{\mathcal{G}_c}\mathbf{p}(t) - L_{\mathcal{G}_c}\mathbf{y}(t) \tag{4-7a}$$
$$\mathbf{z}(t) = \mathbf{p}(t) + \mathbf{y}(t) \tag{4-7b}$$

For the algorithm proposed in Equation (4-7) we find

Theorem 4.1. *The consensus algorithm proposed in Equation* (4-7) *yields* $\mathbf{z}(t) \rightarrow \mathbb{1}_N(\mathbf{w}^\top \mathbf{y}(t^\star))$ *for* $t \rightarrow \infty$ *if* $\exists t^\star > 0$ *such that for* $t > t^\star$ *we find* $\mathbf{y}(t) = \mathbf{y}(t^\star)$.

Proof: Since the spectral abscissa of $-L_{\mathcal{G}_c}$ is equal to $\mu(-L_{\mathcal{G}_c}) = 0$, the system is (marginally) stable. We find the steady-state value of the system by setting the derivative of the auxiliary variable $\mathbf{p}_{ss}$ to zero, $\dot{\mathbf{p}}_{ss} = \mathbb{0}_N$. As such we find $L_{\mathcal{G}_c}\mathbf{p}_{ss} = -L_{\mathcal{G}_c}\mathbf{y}(t^\star)$. Hence, in view of $(0, \mathbb{1}_N)$ being an eigenpair of $L_{\mathcal{G}_c}$, we find

$$\mathbf{p}_{ss} = \lim_{t\rightarrow\infty} \mathbf{p}(t) = \left(\mathbb{1}_N\mathbf{k}^\top - I_N\right)\mathbf{y}(t^\star) \tag{4-8}$$

where if $\mathbf{k} = \mathbf{w}$ we find $\mathbf{z}_{ss} = \mathbf{p}_{ss} + \mathbf{y}(t^\star) = \mathbb{1}_N(\mathbf{w}^\top \mathbf{y}(t^\star))$. Hence to prove Theorem 4.1, we need to show that $\mathbf{k} = \mathbf{w}$.

In order to determine $\mathbf{k}$, we introduce the coordinate change $\bar{\mathbf{p}}(t) = \mathbf{p}(t) - \mathbf{p}_{ss}$ and $\bar{\mathbf{y}}(t) = \mathbf{y}(t) - \mathbf{y}(t^\star) = \mathbb{0}_N$ for $t > t^\star$. Which results in the dynamics equal to

$$\dot{\bar{\mathbf{p}}}(t) = -L_{\mathcal{G}_c}\bar{\mathbf{p}}(t), \quad t > t^\star \tag{4-9}$$

Similar to the consensus algorithm from Equation (4-5) we note that $\bar{\mathbf{p}}(t) \rightarrow \mathbb{1}_N(\mathbf{w}^\top \bar{\mathbf{p}}(0))$ for $t \rightarrow \infty$. Since $\mathbf{z}(0) = \mathbf{y}(0)$ we can conclude that $\mathbf{p}(0) = \mathbb{0}_N$ and $\bar{\mathbf{p}}(0) = -\mathbf{p}_{ss}$. With regards to Equation (4-8) we note that $\bar{\mathbf{p}}(t) \rightarrow \mathbb{0}_N$, thus

$$\mathbb{1}_N(\mathbf{w}^\top \bar{\mathbf{p}}(0)) = \mathbb{1}_N\mathbf{w}^\top(I_N - \mathbb{1}_N\mathbf{k}^\top)\mathbf{y}(t^\star) = (\mathbb{1}_N\mathbf{w}^\top - \mathbb{1}_N\mathbf{k}^\top)\mathbf{y}(t^\star) = \mathbb{0}_N \tag{4-10}$$

hence $\mathbf{k} = \mathbf{w}$ and Theorem 4.1 holds.

The consensus algorithm performs quite well in asymptotically reaching the weighted average of $\mathbf{y}(t)$; which is sufficient for a step-signal response. However, if $\mathbf{y}(t)$ has a ramp-like (or higher order) behaviour, the algorithm fails to track the weighted average as shown in Figure 4-2.

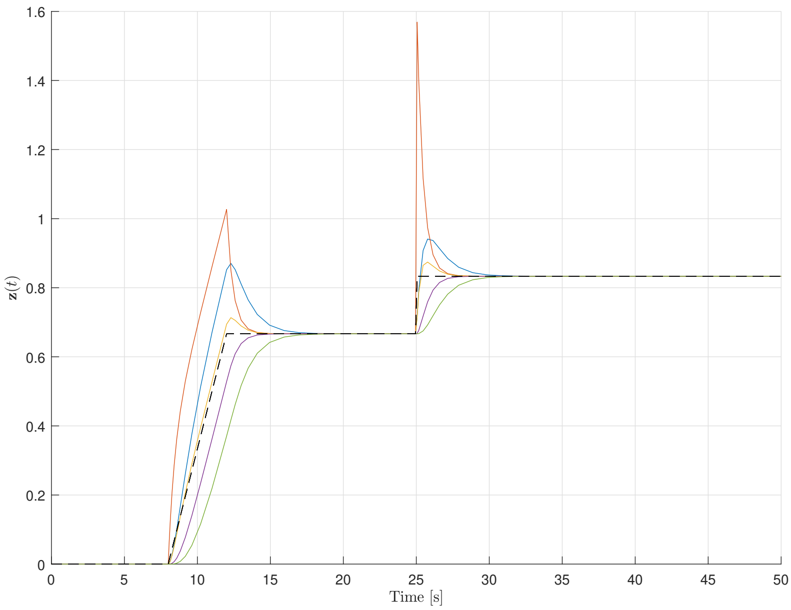

Figure 4-2: Consensus finding of a multi-agent system with $N = 5$ agents using the consensus algorithm defined in Equation (4-7). Both the true average (dotted) and the agents' estimates (solid line) are displayed.

In order to track higher order signals, we introduce an integrator term $\mathbf{q}(t)$ in the consensus algorithm. We then find the new algorithm

$$\dot{\mathbf{q}}(t) = \beta L_{\mathcal{G}_c}\mathbf{p}(t) + \beta L_{\mathcal{G}_c}\mathbf{y}(t) \tag{4-11a}$$
$$\dot{\mathbf{p}}(t) = -\alpha\mathbf{q}(t) - \alpha\mathbf{p}(t) - \beta L_{\mathcal{G}_c}\mathbf{p}(t) - \beta L_{\mathcal{G}_c}\mathbf{y}(t) \tag{4-11b}$$
$$\mathbf{z}(t) = \mathbf{p}(t) + \mathbf{y}(t) \tag{4-11c}$$

which can be rewritten as

$$\begin{bmatrix}\dot{\mathbf{q}}(t)\\ \dot{\mathbf{p}}(t)\end{bmatrix} = \begin{bmatrix}\mathbb{0}_{N\times N} & \beta L_{\mathcal{G}_c}\\ -\alpha I_N & -\alpha I_N - \beta L_{\mathcal{G}_c}\end{bmatrix}\begin{bmatrix}\mathbf{q}(t)\\ \mathbf{p}(t)\end{bmatrix} + \begin{bmatrix}\beta L_{\mathcal{G}_c}\\ -\beta L_{\mathcal{G}_c}\end{bmatrix}\mathbf{y}(t) \tag{4-12a}$$
$$\mathbf{z}(t) = \mathbf{p}(t) + \mathbf{y}(t) \tag{4-12b}$$

with $\mathbf{q}(0) = \mathbb{0}_N$ and $\mathbf{p}(0) = \mathbb{0}_N$. The algorithm introduces two tuning parameters $\alpha \in \mathbb{R}_{>0}$ and $\beta \in \mathbb{R}_{>0}$ which can be adjusted to increase the overall performance.

Theorem 4.2. *The consensus algorithm proposed in Equation* (4-12) *yields* $\mathbf{z}(t) \to \mathbb{1}_N(\mathbf{w}^\top\mathbf{y}(t^\star))$ *for* $t \to \infty$ *if* $\exists t^\star > 0$ *such that for* $t > t^\star$ *we find* $\mathbf{y}(t) = \mathbf{y}(t^\star)$.

Proof: In order to prove Theorem 4.2 we first need to determine the stability of the system in Equation (4-12). Hence we want to find λ such that

$$\begin{bmatrix} \mathbb{0}_{N\times N} & \beta L_{\mathcal{G}_c} \\ -\alpha I_N & -\alpha I_N - \beta L_{\mathcal{G}_c} \end{bmatrix} \begin{bmatrix} \mathbf{v}_1 \\ \mathbf{v}_2 \end{bmatrix} = \lambda \begin{bmatrix} \mathbf{v}_1 \\ \mathbf{v}_2 \end{bmatrix} \tag{4-13}$$

Which leads to the set of equations

$$\beta L_{\mathcal{G}_c}\mathbf{v}_2 = \lambda \mathbf{v}_1 \tag{4-14a}$$

$$-\alpha \mathbf{v}_1 - \alpha \mathbf{v}_2 - \beta L_{\mathcal{G}_c}\mathbf{v}_2 = \lambda \mathbf{v}_2 \tag{4-14b}$$

we can then substitute Equation (4-14a) into Equation (4-14b) and find

$$(\alpha + \lambda)(\mathbf{v}_1 + \mathbf{v}_2) = \mathbb{0}_N \tag{4-15}$$

which is satisfied for $\lambda = -\alpha$ or $\mathbf{v}_1 = -\mathbf{v}_2$. We first consider $\mathbf{v}_1 = -\mathbf{v}_2$ and find Equation (4-14a) equal to

$$\beta L_{\mathcal{G}_c}\mathbf{v}_2 = -\lambda \mathbf{v}_2 \tag{4-16}$$

hence $\lambda = -\beta \text{eig}(L_{\mathcal{G}_c}) \leq 0$. These first N eigenvalues result in a response analogous to that of Equation (4-5). For the other N eigenvalues we take $\lambda = -\alpha$, hence $\lambda = -\alpha$ is an eigenvalue to the system with multiplicity N. Concluding, if $\alpha, \beta > 0$ and the graph topology follows Assumption 4.1 the system is marginally stable and leads to consensus.

We again set the derivative of the auxiliary variables to zero, $\dot{\mathbf{q}}_{ss} = \mathbb{0}_N$ and $\dot{\mathbf{p}}_{ss} = \mathbb{0}_N$, and find

$$\mathbf{q}_{ss} = \lim_{t\to\infty} \mathbf{q}(t) = -\left(\mathbb{1}_N \mathbf{k}^\top - I_N\right) \mathbf{y}(t^\star) \tag{4-17a}$$

$$\mathbf{p}_{ss} = \lim_{t\to\infty} \mathbf{p}(t) = \left(\mathbb{1}_N \mathbf{k}^\top - I_N\right) \mathbf{y}(t^\star) \tag{4-17b}$$

By defining $\bar{\mathbf{q}}(t) = \mathbf{q}(t) - \mathbf{q}_{ss}$, $\bar{\mathbf{p}}(t) = \mathbf{p}(t) - \mathbf{p}_{ss}$ and $\bar{\mathbf{y}}(t) = \mathbf{y}(t) - \mathbf{y}(t^\star) = \mathbb{0}_N$ we obtain the transformed dynamics

$$\begin{bmatrix} \dot{\bar{\mathbf{q}}}(t) \\ \dot{\bar{\mathbf{p}}}(t) \end{bmatrix} = \begin{bmatrix} \mathbb{0}_{N\times N} & \beta L_{\mathcal{G}_c} \\ -\alpha I_N & -\alpha I_N - \beta L_{\mathcal{G}_c} \end{bmatrix} \begin{bmatrix} \bar{\mathbf{q}}(t) \\ \bar{\mathbf{p}}(t) \end{bmatrix} \tag{4-18}$$

with a right-eigenpair of

$$\left(\lambda, \begin{bmatrix} \mathbf{v}_1 \\ \mathbf{v}_2 \end{bmatrix}\right) = \left(0, \begin{bmatrix} \mathbb{1}_N \\ -\mathbb{1}_N \end{bmatrix}\right) \tag{4-19}$$

and a left-eigenpair of

$$\left(\lambda, \begin{bmatrix} \mathbf{w}_1 \\ \mathbf{w}_2 \end{bmatrix}\right) = \left(0, \begin{bmatrix} \mathbf{w} \\ \mathbb{0}_N \end{bmatrix}\right) \tag{4-20}$$

which for $t \to \infty$ then results in

$$\bar{\mathbf{p}}(t) = -\mathbb{1}_N \left(\mathbf{w}^\top \bar{\mathbf{q}}(0) \right) \tag{4-21a}$$
$$= -\mathbb{1}_N \left(\mathbf{w}^\top \left(\mathbb{1}_N \mathbf{k}^\top - I_N \right) \mathbf{y}(t^\star) \right) \tag{4-21b}$$
$$= \mathbb{1}_N \mathbf{w}^\top \left(I_N - \mathbb{1}_N \mathbf{k}^\top \right) \mathbf{y}(t^\star) \tag{4-21c}$$

which again yields $\mathbf{k} = \mathbf{w}$ and accordingly Theorem 4.2 holds.

Due to the introduction of tuning parameters, the algorithm can be adjusted to increase the convergence rate on the consensus value. In Figure 4-3 we depict the response of the system to the same tracking signal $\mathbf{y}(t)$ as in Figure 4-2 with consensus parameters $\alpha = 1$ and $\beta = 10$.

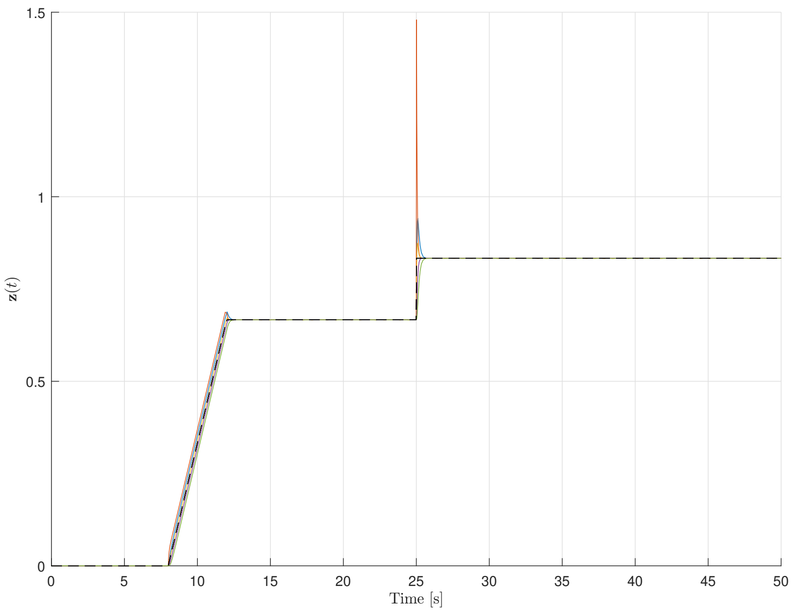

Figure 4-3: Consensus finding of a multi-agent system with $N = 5$ agents using the consensus algorithm defined in Equation (4-12) with $\alpha = 1$ and $\beta = 10$. Both the true average (dotted) and the agents' beliefs (solid line) are displayed.

Note that an increase in β yields a decrease in tracking error and a faster response time at the cost of a sudden spike at $t = 25\ s$. Furthermore throughout this section we considered a system output of dimension 1, however these results can easily be extended to an n-dimensional output vector.

Part II

Control design: steering dynamic multi-agent networks to their Nash equilibrium

Chapter 5

Problem definition: multi-agent games subject to dynamics

This chapter will discuss the main problem of this thesis: steering a multi-agent dynamical system to its Nash equilibrium. We start by describing the multi-agent system with intrinsic dynamics, which is promptly followed by the game theoretic definitions.

5-1 Multi-agent system dynamics

This section will describe the dynamic system considered in this thesis. We define the multi-agent system as a set of N agents where each agent v is subject to local dynamics of the form

$$\dot{x}_v(t) = A_v x_v(t) + B_v u_v(t) \tag{5-1a}$$
$$y_v(t) = C_v x_v(t) \tag{5-1b}$$

where $x_v \in \mathbb{R}^{n_v}$ is the state vector of agent v, $u_v \in \mathbb{R}^{m_v}$ its input vector, $y_v \in \mathbb{R}^{m_v}$ the output vector, and state space matrices $A_v \in \mathbb{R}^{n_v \times n_v}$, $B_v \in \mathbb{R}^{n_v \times m_v}$, $C_v \in \mathbb{R}^{m_v \times n_v}$. Furthermore we define $n_s = \sum_{i=1}^{N} n_i$, $m_s = \sum_{i=1}^{N} m_i$.

Assumption 5.1. *For each agent v, (A_v, B_v) is a controllable pair and the input and output vectors have the same dimensions.*

Due to the possible instability of the system matrices A_v, we introduce a stabilizing control action as $u_v(t) = -K_v x_v(t)$.

In view of Assumption 5.1 there exists a K_v such that $(A_v - B_v K_v)$ is Hurwitz, resulting in a stable closed-loop system. For the design of such a K_v, we introduce the Lyapunov function

$$V(x_v) = x_v^\top P_v x_v > 0 \quad \forall\, x_v \neq \mathbb{0}_{n_v} \tag{5-2}$$

where $P_v \in \mathbb{R}^{n_v \times n_v}$, $P_v > 0$ a symmetric positive-definite matrix.

With the earlier mentioned control action of $u_v(t) = -K_v x_v(t)$, this results in the following time derivative of the Lyapunov function

$$\dot{V}(x_v) = \dot{x}_v^\top P_v x_v + x_v^\top P_v \dot{x}_v \tag{5-3a}$$
$$= x_v^\top \left(A_v^\top P_v + P_v A_v - K_v^\top B_v^\top P_v - P_v B_v K_v \right) x_v < 0 \tag{5-3b}$$

The feedback matrix is set equal to $K_v = \gamma_v B_v^\top P_v$ and we introduce $S_v = P_v^{-1}$, as such we find

$$S_v A_v^\top + A_v S_v - 2\gamma_v B_v B_v^\top < 0 \tag{5-4}$$

Solve for $S_v > 0$, $\gamma_v > 0$ and find K_v. As such, in the following chapters we will discuss control actions of the form $u_v(t) = -K_v x_v(t) + \tilde{u}_v(t)$, where the first addend ensures that the agents are locally stable and the second addend aims to steer the agents to the Nash equilibrium.

5-2 Game theory definitions

The agents additionally take part in a game, where each of them aims to minimize a different cost function $\theta_v(y_v, \mathbf{y}_{-v})$. We define the collection of output vectors y_v as $\mathbf{y} = [y_1^\top, \ldots, y_N^\top]^\top$ and the set of output vectors excluding the output of agent v as $\mathbf{y}_{-v}$. As a result the Nash equilibrium problem can be defined as

$$\forall v : \quad y_v^\star \in \arg\min_{\zeta_v} \theta_v(\zeta_v, \mathbf{y}_{-v}^\star) \tag{5-5}$$

where $\mathbf{y}^\star$ is the Nash Equilibrium of the game. Note that finding the Nash equilibrium of agent v, $y_v^\star$, requires knowledge of the other agents' equilibria, $\mathbf{y}_{-v}^\star$. This is generally not known, as such we redefine the Nash equilibrium problem to an iterative best response approach, which yields

$$\forall v : \quad \bar{y}_v(t) \in \arg\min_{\zeta_v} \theta_v(\zeta_v, \mathbf{y}_{-v}(t)) \tag{5-6}$$

where $\bar{y}_v(t)$ is the best response at time t, given the outputs of the other agents.

In the upcoming chapters we provide control laws that steer the systems to their Nash equilibria, given assumptions on the cost function and system dynamics. We define the error between the agent output y_v and its Nash equilibrium $y_v^\star$ as

$$\varepsilon_v^\star(t) = y_v(t) - y_v^\star \tag{5-7}$$

and our goal is to ensure $\varepsilon_v^\star(t) \to \mathbb{0}_{k_v}$ for $t \to \infty$ for all agents v.

Chapter 6

Reference tracking based controller: steering multi-agent systems to their Nash equilibrium

This chapter will provide more details about the control actions aiming to steer the system to its Nash equilibrium. In this chapter we will assume a system where all agents have access to the output of all other agents, i.e. a fully connected system. In the first section we will propose a first order reference based control action that constantly steers the agents to their best response as mentioned in Equation (5-6). The section thereafter will provide some assumptions on the cost function, leading to stability and convergence proofs. The last section will provide a higher order alternative to the controller.

6-1 First order reference control

Given the optimal output for agent v at time t, $\bar{y}_v(t)$, a controller can be proposed to steer the agent to this state. The error between agent outputs y_v and $\bar{y}_v$ will be defined as

$$\bar{\varepsilon}_v(t) = y_v(t) - \bar{y}_v(t) \tag{6-1}$$

The control goal $\varepsilon_v^\star(t) \to \mathbb{0}_{k_v}$ for $t \to \infty$ is satisfied if $\bar{\varepsilon}_v(t) \to \mathbb{0}_{k_v}$ with $\bar{y}_v(t) \to y_v^\star$ for $t \to \infty$. We will now propose a controller that ensures $\bar{\varepsilon}_v(t) \to \mathbb{0}_{k_v}$ for $t \to \infty$ under given assumptions on the system.

In order to track this reference signal, we introduce a first order reference tracking controller with state-feedback as depicted in Figure 6-1 and described by:

$$\dot{\xi}_v(t) = -k_v \xi_v(t) + k_v \bar{y}_v(t) \tag{6-2a}$$
$$u_v(t) = -K_v x_v(t) + H_v \xi_v(t) \tag{6-2b}$$

where $K_v \in \mathbb{R}^{m_v \times n_v}$ is a state-feedback matrix that stabilizes the system, $k_v \in \mathbb{R}_{>0}$ a control gain parameter, and $H_v \in \mathbb{R}^{m_v \times m_v}$ a gain matrix that compensates for steady-state gain errors.

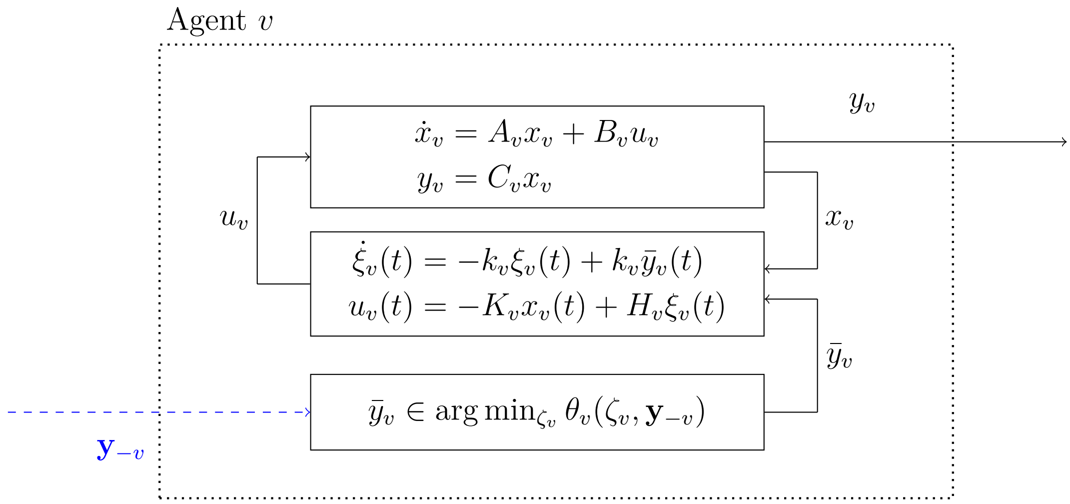

Figure 6-1: Dynamics of agent v with the proposed state-feedback reference control. The blue, dashed line represents the outputs of the other agents on which the cost-function θ_v depends.

This controller can be implemented on the system dynamics from Equation (5-1), which results in

$$\dot{\xi}_v(t) = -k_v \xi_v(t) + k_v \bar{y}_v(t) \tag{6-3a}$$
$$\dot{x}_v(t) = (A_v - B_v K_v) x_v(t) + B_v H_v \xi_v(t) \tag{6-3b}$$
$$y_v(t) = C_v x_v(t) \tag{6-3c}$$

With the closed-loop dynamics of Equation (6-3), the steady-state gain from $\bar{y}_v$ to x_v can be determined. We introduce the subscript $_{ss}$ for the steady-state values. Note that $\dot{\xi}_{v,ss} = \mathbb{0}_{m_v}$, $\dot{x}_{v,ss} = \mathbb{0}_{n_v}$ and $y_{v,ss} = C_v x_{v,ss}$, hence

$$\xi_{v,ss} = \bar{y}_{v,ss} \tag{6-4a}$$
$$(A_v - B_v K_v) x_{v,ss} = -B_v H_v \xi_{v,ss} \tag{6-4b}$$

Since $(A_v - B_v K_v)$ is Hurwitz it is also non-singular hence its inverse exists. We find

$$x_{v,ss} = -(A_v - B_v K_v)^{-1} B_v H_v \bar{y}_{v,ss} \tag{6-5}$$

thus by pre-multiplying both sides with C_v

$$y_{v,ss} = -C_v (A_v - B_v K_v)^{-1} B_v H_v \bar{y}_{v,ss} \tag{6-6}$$

Our goal is to steer the outputs to their best response, hence we want to design H_v such that $y_{v,ss} = \bar{y}_{v,ss}$. In view of the input and output vectors having equal dimensions as in Assumption 5.1, a suitable value for the gain matrix H_v would be

$$H_v = -\left(C_v(A_v - B_vK_v)^{-1}B_v\right)^{-1} \tag{6-7}$$

Theorem 6.1. *The state-space dynamics from Equation* (5-1) *can be stabilized with a control law as in Equation* (6-2) *ensuring* $\bar{\varepsilon}_v(t) \to \mathbb{0}_{k_v}$ *for* $t \to \infty$ *with* $\bar{\varepsilon}_v(t)$ *as defined in Equation* (6-1)*.*

Proof: By rewriting the state-space representation to its transfer function form

$$G_{tf}(s) = C_v\left(sI_{n_v} - A_v + B_vK_v\right)^{-1}B_vH_v \tag{6-8}$$

and as a result finding $Y_v(s) = G_{tf}(s)\bar{Y}_v(s)$, we can apply the Final Value Theorem (FVT), as explained in [16], to find

$$\lim_{t\to\infty}\bar{\varepsilon}_v(t) = \lim_{s\to 0} sI_{m_v}\bar{E}(s) \tag{6-9a}$$

$$= \lim_{s\to 0} sI_{m_v}\left(Y_v(s) - \bar{Y}_v(s)\right) \tag{6-9b}$$

$$= \lim_{s\to 0}\left(G_{tf}(s) - I_{m_v}\right)s\bar{Y}_v(s) \tag{6-9c}$$

Since $(A_v - B_vK_v)$ is Hurwitz, implying $(A_v - B_vK_v)$ is non-singular, $G_{tf}(0)$ exists. If the reference output $\bar{y}_v(t)$ remains constant for a sufficiently long time, it can be considered a step function, i.e., $\bar{Y}_v(s) = \frac{1}{s}\bar{y}_c$ for any constant vector $\bar{y}_c \in \mathbb{R}^{n_v}$. As a result the error $\bar{\varepsilon}_v(t)$ converges to

$$\lim_{t\to\infty}\bar{\varepsilon}_v(t) = \left(G_{tf}(0) - I_{m_v}\right)\bar{y}_c \tag{6-10a}$$

$$= -\left(C_v(A_v - B_vK_v)^{-1}B_vH_v + I_{m_v}\right)\bar{y}_c \tag{6-10b}$$

$$= \mathbb{0}_{n_v} \tag{6-10c}$$

in view of Equation (6-7).

However, this proof applies to a reference output $\bar{y}_v(t)$ that *remains constant for a sufficiently long time*. Note that the reference output is a function of the output of all other agents, as shown in Equation (5-6). Hence the dynamics of agent v will be influenced by that of the other agents. In the following, we will introduce a specific form for the cost-function as a linear-quadratic function, and adapt the control scheme proposed in Equation (6-2) accordingly.

6-2 Linear-quadratic cost function

We now describe the cost function in a linear-quadratic form, yielding

$$\theta_v(y_v, \mathbf{y}_{-v}(t)) = \tfrac{1}{2}y_v^\top Q_{d,v}y_v - y_v^\top b_v - \sum_{j\neq v} y_v^\top Q_{c,v,j}y_j(t) \tag{6-11}$$

where $Q_{d,v} \in \mathbb{R}^{m_v \times m_v}$ is the quadratic-term symmetric matrix with $Q_{d,v} > 0$, $Q_{c,v,j} \in \mathbb{R}^{m_v \times m_j}$ a linear-term matrix relating to a cost from agent j to agent v and $b_v \in \mathbb{R}^{m_v}$ a linear-term vector. The solution $\bar{y}_v$ following Equation (5-6) can be determined by setting the gradient of $\theta_v(y_v, \mathbf{y}_{-v})$ with respect to y_v to zero, i.e.:

$$\bar{y}_v(t) = \{\zeta_v(t) \in \mathbb{R}^{m_v} \mid \nabla_{\zeta_v}\theta_v(\zeta_v, \mathbf{y}_{-v}(t)) = \mathbb{0}_{m_v}\} \tag{6-12}$$

For the cost function defined in Equation (6-11), Equation (6-12) results in

$$\bar{y}_v(t) = Q_{d,v}^{-1}\left(b_v + \sum_{j \neq v} Q_{c,v,j}y_j(t)\right) \tag{6-13}$$

for all agents v.

The result from Equation (6-13) can be combined with the controller from Equation (6-2). To get more insight into the system dynamics we will consider the overall system of all agents. We define the system matrices $A = \text{blockdiag}(A_1, \ldots, A_N)$ and likewise for B, C, K and H. We describe the control parameters k_v by a diagonal matrix $\mathbf{k} = \text{blockdiag}(k_1 I_{m_1}, \ldots, k_N I_{m_N})$. Furthermore we obtain

$$Q_d = \begin{bmatrix} Q_{d,1} & \mathbb{0} & \mathbb{0} & \cdots & \mathbb{0} \\ \mathbb{0} & Q_{d,2} & \mathbb{0} & \cdots & \mathbb{0} \\ \mathbb{0} & \mathbb{0} & Q_{d,3} & \cdots & \mathbb{0} \\ \vdots & \vdots & \vdots & \ddots & \vdots \\ \mathbb{0} & \mathbb{0} & \mathbb{0} & \cdots & Q_{d,N} \end{bmatrix}, \quad Q_c = \begin{bmatrix} \mathbb{0} & Q_{c,1,2} & Q_{c,1,3} & \cdots & Q_{c,1,N} \\ Q_{c,2,1} & \mathbb{0} & Q_{c,2,3} & \cdots & Q_{c,2,N} \\ Q_{c,3,1} & Q_{c,3,2} & \mathbb{0} & \cdots & Q_{c,3,N} \\ \vdots & \vdots & \vdots & \ddots & \vdots \\ Q_{c,N,1} & Q_{c,N,2} & Q_{c,N,3} & \cdots & \mathbb{0} \end{bmatrix} \tag{6-14}$$

with zero blocks of appropriate size. We use these matrices to find the reference state

$$\bar{\mathbf{y}}(t) = Q_d^{-1}\left(\mathbf{b} + Q_c\mathbf{y}(t)\right) \tag{6-15}$$

where $\mathbf{b} = [b_1^\top, \ldots, b_N^\top]^\top$. Recall that $\mathbf{y} = [y_1^\top, \ldots, y_N^\top]^\top$ and similarly for $\mathbf{u}$, $\mathbf{x}$, and $\boldsymbol{\xi}$. Since the goal is to steer $\mathbf{y}(t)$ to $\bar{\mathbf{y}}(t)$, we find that if the gain from $\mathbf{y}(t)$ to $\bar{\mathbf{y}}(t)$ is greater than 1 the system will exponentially converge. Hence we ensure that the gain of $Q_d^{-1}Q_c$ is smaller than 1, as such we introduce the following assumption:

Assumption 6.1. *The spectral radius of $Q_d^{-1}Q_c$ is smaller than 1, i.e. $\rho(Q_d^{-1}Q_c) < 1$.*

These definitions result in the overall system dynamics equal to:

$$\dot{\mathbf{x}}(t) = A\mathbf{x}(t) + B\mathbf{u}(t) \tag{6-16a}$$
$$\dot{\boldsymbol{\xi}}(t) = -\mathbf{k}\boldsymbol{\xi}(t) + \mathbf{k}Q_d^{-1}Q_c\mathbf{y}(t) \tag{6-16b}$$
$$\mathbf{y}(t) = C\mathbf{x}(t) \tag{6-16c}$$
$$\mathbf{u}(t) = -K\mathbf{x}(t) + H\left(\boldsymbol{\xi}(t) + Q_d^{-1}\mathbf{b}\right) \tag{6-16d}$$

thus

$$\begin{bmatrix} \dot{\mathbf{x}} \\ \dot{\boldsymbol{\xi}} \end{bmatrix} = \begin{bmatrix} A - BK & BH \\ \mathbf{k}Q_d^{-1}Q_c C & -\mathbf{k} \end{bmatrix} \begin{bmatrix} \mathbf{x} \\ \boldsymbol{\xi} \end{bmatrix} + \begin{bmatrix} BHQ_d^{-1}\mathbf{b} \\ \mathbb{0}_{m_s \times m_s} \end{bmatrix} \tag{6-17}$$

To analyse the stability of the resulting system, the eigenvalues of the closed-loop system matrix must be considered, which are a function of the diagonal control parameter matrix $\mathbf{k}$.

Theorem 6.2. *Given Assumption 6.1 and* $\mathbf{k} = \text{blockdiag}(k_1 I_{m_1}, \ldots, k_N I_{m_N})$ *with* $\forall v\ k_v > 0$ *there exists a set of parameters* $k_1, \ldots, k_N$ *small enough such that the system defined in Equation* (6-17) *is stable.*

Proof: The system in Equation (6-17) is stable if the state matrix is Hurwitz. This means that the spectral abscissa of the state matrix is smaller than zero:

$$\mu \left(\begin{bmatrix} A - BK & BH \\ \mathbf{k}Q_d^{-1}Q_c C & -\mathbf{k} \end{bmatrix} \right) < 0 \tag{6-18}$$

We will first discuss the case when $\mathbf{k}$ is equal to zero.

With $\mathbf{k} = \mathbb{0}_{m_s \times m_s}$, the system matrix simplifies to

$$\begin{bmatrix} A - BK & BH \\ \mathbb{0}_{m_s \times n_s} & \mathbb{0}_{m_s \times m_s} \end{bmatrix} \tag{6-19}$$

as such we can define the right-eigenvector as $\mathbf{v} = [v_1^\top, v_2^\top]^\top$ and write

$$\begin{bmatrix} A - BK & BH \\ \mathbb{0}_{m_s \times n_s} & \mathbb{0}_{m_s \times m_s} \end{bmatrix} \begin{bmatrix} v_1 \\ v_2 \end{bmatrix} = \lambda_i \begin{bmatrix} v_1 \\ v_2 \end{bmatrix} \tag{6-20}$$

or

$$(A - BK)v_1 + BHv_2 = \lambda_i v_1 \tag{6-21a}$$

$$\mathbb{0}_{m_s} = \lambda_i v_2 \tag{6-21b}$$

$$\tag{6-21c}$$

We find the first set of eigenvalues equal to $\lambda_i = 0$ with multiplicity m_s and eigenvectors

$$v_{1,i} = v_a \tag{6-22a}$$

$$v_{2,i} = Cv_a \tag{6-22b}$$

for arbitrary eigenvector $v_a \in \mathbb{R}^{n_s}$; and a second set of eigenvalues equal to the eigenvalues of $A - BK$, with eigenvectors

$$v_{1,i} = v_{sys,i} \tag{6-23a}$$

$$v_{2,i} = \mathbb{0}_{m_s} \tag{6-23b}$$

where $(\lambda_i, v_{sys,i})$ are eigenpairs of $A - BK$. Note that due to the first set of eigenvectors equal to $\lambda_i = 0$, the system is marginally stable. As a result we will discuss non-zero but very small values for $\mathbf{k}$. Due to the continuity of the eigenvalues with respect to $\mathbf{k}$ we find that $\mathbf{k} \to \mathbb{0}_{m_s \times m_s}$ yields $\lambda_i \to 0$. We aim to determine whether the eigenvalues reach this asymptotic value from the positive right half-plane or the negative left half-plane (with the latter yielding stability). With $\mathbf{k}$ being non-zero, we consider the following equation:

$$\begin{bmatrix} A - BK & BH \\ \mathbf{k}Q_d^{-1}Q_cC & -\mathbf{k} \end{bmatrix} \begin{bmatrix} v_1 \\ v_2 \end{bmatrix} = \lambda_i \begin{bmatrix} v_1 \\ v_2 \end{bmatrix} \tag{6-24}$$

This then leads to the following set of equations

$$(A - BK - \lambda_i I_{n_s})v_1 = -BHv_2 \tag{6-25a}$$

$$\mathbf{k}Q_d^{-1}Q_cCv_1 - \mathbf{k}v_2 = \lambda_i v_2 \tag{6-25b}$$

with the first equation leading to

$$Cv_1 = -C(A - BK - \lambda_i I_{n_s})^{-1}BHv_2 \tag{6-26}$$

According to the Neumann series [17], for a matrix X with $\rho(X) < 1$ we find

$$(I - X)^{-1} = \sum_{k=0}^{\infty} X^k \tag{6-27}$$

as such with $X = I - (A - BK)^{-1}(A - BK - \lambda_i I_{n_s})$, which leads to $X = \lambda_i(A - BK)^{-1}$ hence $\exists \mathbf{k} \neq \mathbb{0}_{m_s \times m_s}$ such that $\rho(X) < 1$ for $\lambda_i \to 0$, we find

$$\Big((A - BK)^{-1}(A - BK - \lambda_i I_{n_s})\Big)^{-1} = \sum_{k=0}^{\infty} \Big(\lambda_i (A - BK)^{-1}\Big)^k \tag{6-28}$$

which, by reworking the inverse as $(YZ)^{-1} = Z^{-1}Y^{-1}$ and post-multiplying both sides with $(A - BK)^{-1}$, then gives us

$$(A - BK - \lambda_i I_{n_s})^{-1} = \sum_{k=0}^{\infty} \lambda_i^k (A - BK)^{-k-1} \tag{6-29}$$

or

$$(A - BK - \lambda_i I_{n_s})^{-1} = (A - BK)^{-1} + \lambda_i (A - BK)^{-2} + \mathcal{O}(\lambda_i^2) \tag{6-30}$$

We can substitute these results in Equation (6-26) after neglecting the higher order terms $\mathcal{O}(\lambda_i^2)$. Along with $H = -\left(C(A - BK)^{-1}B\right)^{-1}$ from Equation (6-7), this will result in

$$Cv_1 = -C(A - BK - \lambda_i I_{n_s})^{-1}BHv_2 \tag{6-31a}$$

$$= -C\left((A - BK)^{-1} + \lambda_i (A - BK)^{-2}\right)BHv_2 \tag{6-31b}$$

$$= v_2 - \lambda_i C(A - BK)^{-2}BHv_2 \tag{6-31c}$$

Substituting this into Equation (6-25b) then gives us

$$\mathbf{k}(Q_d^{-1}Q_c - I_{m_s})v_2 + \lambda_i \mathbf{k} Q_d^{-1}Q_c C(A-BK)^{-2}BHv_2 = \lambda_i v_2 \tag{6-32}$$

With both λ_i and $\mathbf{k}$ going to zero, $\lambda_i \mathbf{k}$ can be considered a higher order term as well. As such we can neglect it and find

$$\mathbf{k}(Q_d^{-1}Q_c - I_{m_s})v_2 = \lambda_i v_2 \tag{6-33}$$

which implies that λ_i are the eigenvalues of $\mathbf{k}(Q_d^{-1}Q_c - I_{m_s})$, which in view of Assumption 6.1 have strictly negative real part for positive $\mathbf{k}$. As such the system matrix is Hurwitz.

In view of the system matrix being Hurwitz, i.e. the system from Equation (6-17) is stable, we can discuss its convergence to the Nash equilibrium.

Theorem 6.3. *The control law as proposed in Equation* (6-2) *with the control matrix* $\mathbf{k} = \text{blockdiag}(k_1 I_{m_1}, \ldots, k_N I_{m_N})$ *ensures that* $\mathbf{y}(t) \to \mathbf{y}^\star$ *for* $t \to \infty$ *for the system in Equation* (6-17) *with a set of parameters* $k_1, \ldots, k_N$ *small enough.*

Proof: For the steady state response of the system, we find that $\dot{\mathbf{x}}_{ss} = \mathbb{0}_{n_s}$, $\dot{\boldsymbol{\xi}}_{ss} = \mathbb{0}_{m_s}$, and we again denote the steady state values with subscript $_{ss}$. We find

$$(A-BK)\mathbf{x}_{ss} + BH\boldsymbol{\xi}_{ss} + BHQ_d^{-1}\mathbf{b} = \mathbb{0}_{n_s} \tag{6-34a}$$
$$\mathbf{k}Q_d^{-1}Q_c C\mathbf{x}_{ss} - \mathbf{k}\boldsymbol{\xi}_{ss} = \mathbb{0}_{m_s} \tag{6-34b}$$

thus, with $\mathbf{y}_{ss} = C\mathbf{x}_{ss}$

$$\boldsymbol{\xi}_{ss} = Q_d^{-1}Q_c C\mathbf{x}_{ss} = Q_d^{-1}Q_c \mathbf{y}_{ss} \tag{6-35}$$

and

$$\mathbf{y}_{ss} = C\mathbf{x}_{ss} \tag{6-36a}$$
$$= C(A-BK)^{-1}BH\left(\boldsymbol{\xi}_{ss} + Q_d^{-1}\mathbf{b}\right) \tag{6-36b}$$
$$= Q_d^{-1}\left(Q_c\mathbf{y}_{ss} + \mathbf{b}\right) \tag{6-36c}$$

Which after some rewriting leads to $\mathbf{y}_{ss} = (Q_d - Q_c)^{-1}\mathbf{b} = \mathbf{y}^\star$. As such $\mathbf{y}(t) \to \mathbf{y}^\star$ for $t \to \infty$.

6-3 Higher order reference control

To introduce more control design flexibility, we can extend the first order controller from Equation (6-2) to higher order controllers. As such we propose the following second order controller

$$\ddot{\xi}_v(t) = -d_v\dot{\xi}_v(t) - k_v\xi(t) + k_v \sum_{j\neq v} Q_{d,v}^{-1}Q_{c,v,j}y_j(t) \tag{6-37a}$$

$$u_v(t) = -K_v x_v(t) + H_v\left(\xi(t) + Q_{d,v}^{-1}b_v\right) \tag{6-37b}$$

with $k_v, d_v \in \mathbb{R}_{>0}$. Note again that if the system reaches its steady state, implying $\ddot{\xi}_{v,ss} = \dot{\xi}_{v,ss} = \mathbb{0}_{m_v}$, the controller state is equal to $\xi_{v,ss} = \sum_{j\neq v} Q_{d,v}^{-1}Q_{c,v,j}y_{j,ss}$. This leads to a steady state control of

$$u_{v,ss} = -K_v x_{v,ss} + H_v\left(\sum_{j\neq v} Q_{d,v}^{-1}Q_{c,v,j}y_{j,ss} + Q_{d,v}^{-1}b_v\right) \tag{6-38a}$$

$$= -K_v x_{v,ss} + H_v\bar{y}_{v,ss} \tag{6-38b}$$

which for a stable system implies that the system once more reaches the Nash equilibrium, following a similar proof as in Section 6-1.

To analyse the stability of the system, we introduce $\mathbf{k} = \text{blockdiag}(k_1 I_{m_1}, \ldots, k_N I_{m_N})$, $\mathbf{d} = \text{blockdiag}(d_1 I_{m_1}, \ldots, d_N I_{m_N})$, and $\boldsymbol{\xi} = [\xi_1^\top, \ldots, \xi_N^\top]^\top$, and by introducing the controller to the system dynamics from Equation (5-1), we find the overall system equal to

$$\begin{bmatrix}\dot{\mathbf{x}}\\ \dot{\boldsymbol{\xi}}\\ \ddot{\boldsymbol{\xi}}\end{bmatrix} = \begin{bmatrix} A-BK & BH & \mathbb{0}_{n_s\times m_s}\\ \mathbb{0}_{m_s\times n_s} & \mathbb{0}_{m_s\times m_s} & I_{m_s}\\ \mathbf{k}Q_d^{-1}Q_cC & -\mathbf{k} & -\mathbf{d}\end{bmatrix}\begin{bmatrix}\mathbf{x}\\ \boldsymbol{\xi}\\ \dot{\boldsymbol{\xi}}\end{bmatrix} + \begin{bmatrix}BHQ_d^{-1}\mathbf{b}\\ \mathbb{0}_{m_s\times m_s}\\ \mathbb{0}_{m_s\times m_s}\end{bmatrix} \tag{6-39a}$$

$$\mathbf{y} = \begin{bmatrix} C & \mathbb{0}_{m_s\times m_s} & \mathbb{0}_{m_s\times m_s}\end{bmatrix}\begin{bmatrix}\mathbf{x}\\ \boldsymbol{\xi}\\ \dot{\boldsymbol{\xi}}\end{bmatrix} \tag{6-39b}$$

This leads to the following theorem:

Theorem 6.4. *Given Assumption 6.1 and* $\mathbf{k} = \text{blockdiag}(k_1 I_{m_1}, \ldots, k_N I_{m_N})$ *with* $\forall v\ k_v > 0$ *there exists a set of parameters* $k_1, \ldots, k_N$ *small enough such that the system defined in Equation* (6-39) *is stable.*

Proof: The proof for stability is analogous to that of Theorem 6.2. We will first discuss the case when $\mathbf{k}$ is equal to zero.

With $\mathbf{k} = \mathbb{0}_{m_s\times m_s}$, the system matrix simplifies to

$$\begin{bmatrix} A-BK & BH & \mathbb{0}_{n_s\times m_s}\\ \mathbb{0}_{m_s\times n_s} & \mathbb{0}_{m_s\times m_s} & I_{m_s}\\ \mathbb{0}_{m_s\times n_s} & \mathbb{0}_{m_s\times m_s} & -\mathbf{d}\end{bmatrix} \tag{6-40}$$

as such we can define the right-eigenvector as $\mathbf{v} = [v_1^\top, v_2^\top, v_3^\top]^\top$ and write

$$\begin{bmatrix} A-BK & BH & \mathbb{0}_{n_s\times m_s}\\ \mathbb{0}_{m_s\times n_s} & \mathbb{0}_{m_s\times m_s} & I_{m_s}\\ \mathbb{0}_{m_s\times n_s} & \mathbb{0}_{m_s\times m_s} & -\mathbf{d}\end{bmatrix}\begin{bmatrix}v_1\\ v_2\\ v_3\end{bmatrix} = \lambda_i\begin{bmatrix}v_1\\ v_2\\ v_3\end{bmatrix} \tag{6-41}$$

or

$$(A - BK)v_1 + BHv_2 = \lambda_i v_1 \tag{6-42a}$$
$$v_3 = \lambda_i v_2 \tag{6-42b}$$
$$-\mathbf{d}v_3 = \lambda_i v_3 \tag{6-42c}$$
$$\tag{6-42d}$$

We find the first set of eigenvalues equal to $\lambda_i = -d_{ii}$, with eigenvectors equal to

$$v_{1,i} = a \cdot (A - BK + d_{ii} I_{n_s})^{-1} BH \mathbb{e}_i \tag{6-43a}$$
$$v_{2,i} = a \cdot \mathbb{e}_i \tag{6-43b}$$
$$v_{3,i} = -a \cdot d_{ii} \mathbb{e}_i \tag{6-43c}$$

for arbitrary $a \in \mathbb{R}$; a second set of eigenvectors equal to $\lambda_i = 0$ with multiplicity m_s and eigenvectors

$$v_{1,i} = v_a \tag{6-44a}$$
$$v_{2,i} = Cv_a \tag{6-44b}$$
$$v_{3,i} = \mathbb{0}_{m_s} \tag{6-44c}$$

for arbitrary eigenvector $v_a \in \mathbb{R}^{n_s}$; and a last set of eigenvalues equal to the eigenvalues of $A - BK$, with eigenvectors

$$v_{1,i} = v_{sys,i} \tag{6-45a}$$
$$v_{2,i} = \mathbb{0}_{m_s} \tag{6-45b}$$
$$v_{3,i} = \mathbb{0}_{m_s} \tag{6-45c}$$

where $(\lambda_i, v_{sys,i})$ are eigenpairs of $A - BK$. Note that we again find a set of eigenvectors equal to $\lambda_i = 0$, leading to a marginally stable system. Following the same reasoning as in Theorem 6.2 we find:

$$\begin{bmatrix} A - BK & BH & \mathbb{0}_{n_s \times m_s} \\ \mathbb{0}_{m_s \times n_s} & \mathbb{0}_{m_s \times m_s} & I_{m_s} \\ \mathbf{k} Q_d^{-1} Q_c C & -\mathbf{k} & -\mathbf{d} \end{bmatrix} \begin{bmatrix} v_1 \\ v_2 \\ v_3 \end{bmatrix} = \lambda_i \begin{bmatrix} v_1 \\ v_2 \\ v_3 \end{bmatrix} \tag{6-46}$$

or

$$(A - BK - \lambda_i I_{n_s})v_1 = -BHv_2 \tag{6-47a}$$
$$v_3 = \lambda_i v_2 \tag{6-47b}$$
$$\mathbf{k} Q_d^{-1} Q_c C v_1 - \mathbf{k} v_2 - \mathbf{d} v_3 = \lambda_i v_3 \tag{6-47c}$$
$$\tag{6-47d}$$

This once more yields $Cv_1 = v_2 - \lambda_i C(A - BK)^{-2} BHv_2$. This result along with $v_3 = \lambda_i v_2$ then leads us to

$$\mathbf{k}\left(Q_d^{-1}Q_c - I_{m_s}\right)v_2 + \lambda_i \mathbf{k}C(A-BK)^{-2}BHv_2 = \lambda_i \mathbf{d}v_2 + \lambda_i^2 v_2 \tag{6-48}$$

again neglecting higher order terms λ_i^2 and $\lambda_i\mathbf{k}$ we find

$$\mathbf{d}^{-1}\mathbf{k}\left(Q_d^{-1}Q_c - I_{m_s}\right)v_2 = \lambda_i v_2 \tag{6-49}$$

Hence λ_i represent the eigenvalues of $\mathbf{d}^{-1}\mathbf{k}\left(Q_d^{-1}Q_c - I_{m_s}\right)$, which are strictly negative for $\rho(Q_d^{-1}Q_c) < 1$ with positive $\mathbf{k}$, $\mathbf{d}$. In view of Assumption 6.1 the eigenvalues of the state matrix are all negative and as such the state matrix is Hurwitz.

In view of the state matrix being Hurwitz, i.e. the system from Equation (6-39) is stable, we can discuss its convergence to the Nash equilibrium.

Theorem 6.5. *The control law as proposed in Equation* (6-37) *with the control matrix* $\mathbf{k} = \text{blockdiag}(k_1 I_{m_1}, \ldots, k_N I_{m_N})$ *ensures that* $\mathbf{y}(t) \to \mathbf{y}^\star$ *for* $t \to \infty$ *for the system in Equation* (6-39) *with a set of parameters* $k_1, \ldots, k_N$ *small enough.*

Proof: For the steady-state response of the system, we find that $\dot{\mathbf{x}}_{ss} = \mathbb{0}_{n_s}$, $\ddot{\boldsymbol{\xi}}_{ss} = \dot{\boldsymbol{\xi}}_{ss} = \mathbb{0}_{m_s}$, and we again denote the steady-state values with subscript $_{ss}$. We find

$$(A - BK)\mathbf{x}_{ss} + BH\boldsymbol{\xi}_{ss} + BHQ_d^{-1}\mathbf{b} = \mathbb{0}_{n_s} \tag{6-50a}$$
$$\mathbf{k}Q_d^{-1}Q_cC\mathbf{x}_{ss} - \mathbf{k}\boldsymbol{\xi}_{ss} = \mathbb{0}_{m_s} \tag{6-50b}$$

thus, with $\mathbf{y}_{ss} = C\mathbf{x}_{ss}$

$$\boldsymbol{\xi}_{ss} = Q_d^{-1}Q_cC\mathbf{x}_{ss} = Q_d^{-1}Q_c\mathbf{y}_{ss} \tag{6-51}$$

and

$$\mathbf{y}_{ss} = C\mathbf{x}_{ss} \tag{6-52a}$$
$$= C(A-BK)^{-1}BH\left(\boldsymbol{\xi}_{ss} + Q_d^{-1}\mathbf{b}\right) \tag{6-52b}$$
$$= Q_d^{-1}\left(Q_c\mathbf{y}_{ss} + \mathbf{b}\right) \tag{6-52c}$$

Which after some rewriting leads to $\mathbf{y}_{ss} = (Q_d - Q_c)^{-1}\mathbf{b} = \mathbf{y}^\star$. As such $\mathbf{y}(t) \to \mathbf{y}^\star$ for $t \to \infty$.

6-4 Numerical example

To illustrate the findings in this chapter, we introduce a numerical example in which a networked system will be described. We assume a system of $N = 10$ agents, homogeneous with respect to their internal dynamics, and each having access to all other agent outputs. Each of these agents are subject to the following state-space dynamics:

$$\dot{x}_v(t) = \begin{bmatrix} 1 & 0 \\ -1 & 1 \end{bmatrix} x_v(t) + \begin{bmatrix} 1 \\ 0 \end{bmatrix} u_v(t) \tag{6-53a}$$

$$y_v(t) = \begin{bmatrix} 0.8 & -0.2 \end{bmatrix} x_v(t) \tag{6-53b}$$

Note that the eigenvalues of A_v are equal to $\lambda = \frac{1}{2} \pm \frac{1}{2}\sqrt{3}\ i$ and as such the system is unstable. We find that $K_v = [5, -6]$ stabilizes the system resulting in closed-loop eigenvalues of $\lambda \in \{-2, -1\}$. Furthermore we set the other control parameters equal to $k_v = 1$, $\forall v \in \{1, \dots, N\}$. With the system matrices defined, we refer to Equation (6-7) and find a gain of

$$H_v = -\tfrac{10}{3} \tag{6-54}$$

We take the adjacency matrix as $A_{\mathcal{G}_c} = A_{\mathcal{G}_\theta} = (\mathbb{1}_N \mathbb{1}_N^\top - I_N)$ and set the cost function parameters Q_c, Q_d, $\mathbf{b}$ as introduced in Equation (6-14) equal to

$$Q_d = 5I_N \tag{6-55a}$$

$$Q_c = 2\text{diag}(A_{\mathcal{G}_\theta}\mathbb{1}_N)^{-1}A_{\mathcal{G}_\theta} \tag{6-55b}$$

$$\mathbf{b} = 5\mathbb{1}_N \tag{6-55c}$$

which yields a spectral radius of $\rho(Q_d^{-1}Q_c) = 0.4$ and a Nash equilibrium of $\mathbf{y}^\star = \frac{5}{3}\mathbb{1}_N$.

As a benchmark to the controller proposed in Equation (6-2), we introduce a controller that has full access to the information of the other agents. With full information on the overall system, the agents can use the Nash equilibrium $\mathbf{y}^\star$ as control input, i.e.

$$\dot{\boldsymbol{\xi}}(t) = -\mathbf{k}\boldsymbol{\xi}(t) + \mathbf{k}\mathbf{y}^\star \tag{6-56a}$$

$$\mathbf{u}(t) = -K\mathbf{x}(t) + H\boldsymbol{\xi}(t) \tag{6-56b}$$

This assumption is unrealistic but provides a useful comparison. We refer to this control action as *full information control* with output y_{fi}.

For agents 1 through 5 we take an initial state of $x_v(0) = [0.8, -0.2]^\top$ and for agents 6 through 10 we take $x_v(0) = [0.8, 0.2]^\top$. The transient response of the systems subject to the reference control from Equation (6-2) is depicted in Figure 6-2. We also define a root-mean-square error term to discuss the performance of the controller with respect to the full information control. This term is equal to

$$\varepsilon_{RMS} = \sqrt{\frac{1}{N}\sum_{v=1}^{N}(x_v(t) - x_v^\star)^2} \tag{6-57}$$

This error response is shown in Figure 6-2 as well. Note that the system consists of homogenous agents which only differ in initial state. As such we choose to only depict the output response of one of the agents, agent 1.

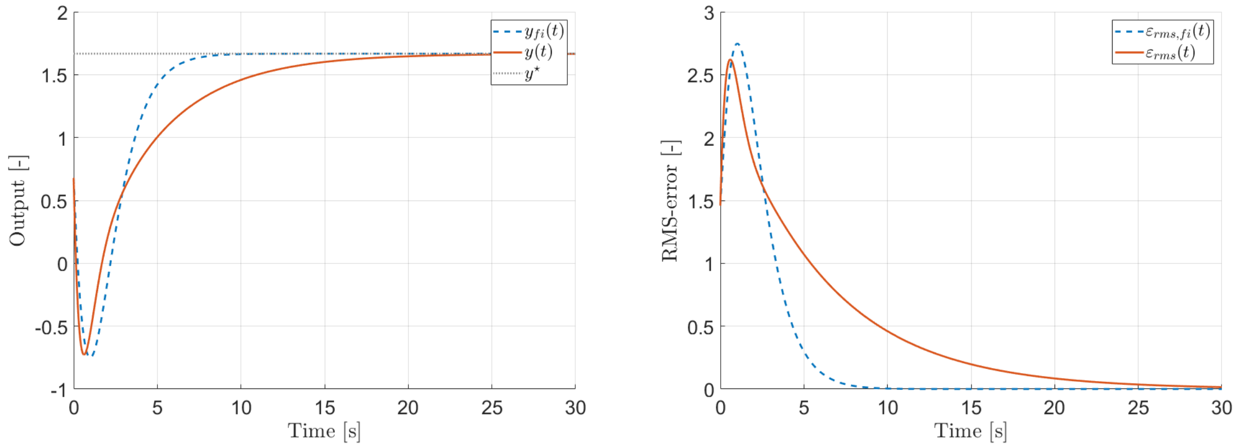

Figure 6-2: Response of a networked game of $N = 10$ agents, subject to linear state-space dynamics whilst aiming to minimize a linear-quadratic cost function by means of a local first order reference control law with state feedback. The left panel shows the transient response of the agents (red solid line), as well as the Nash equilibrium (black dotted), and the full information control (blue dashed). The right panel depicts the sum of the errors of all agents with respect to the Nash equilibrium (red solid line) as well as the error in case of full information control (blue dashed).

Chapter 7

Extension to Aggregate games: steering multi-agent systems to an aggregate game Nash equilibrium

This chapter will extend the results from Chapter 6. In Chapter 6 it is assumed that the agents are connected to all agents that influence their cost function, which is not always the case. Therefore this chapter will introduce methods to deal with cost functions that depend on agents not in the neighbour set. The first section introduces a cost function that is based on the average output of all agents. Following that, we extend the results further to additionally include costs on agents within the neighbour sets. The results in this chapter rely on the findings in Chapter 4.

7-1 Aggregate cost function and controller design

In this section we define the aggregate cost function, which adds a cost term depending on the average of the agent outputs. The consensus algorithm found in Equation (4-12) provides a way for the individual agents to find the weighted average state values of the system in a decentralized way. As such we can redefine the cost function and control actions as:

$$\theta_v = \theta_v(y_v, \mathrm{avg_w}\mathbf{y}) \tag{7-1}$$

and

$$u_v = u_v(y_v, z_v) \tag{7-2}$$

where we define $\mathrm{avg_w}$ as the weighted average such that $\mathrm{avg_w}\mathbf{y} = \sum_j w_j y_j$.

Assumption 7.1. *The communication graph $\mathcal{G}_c(\mathcal{V}, \mathcal{E}_c)$ is undirected, i.e. the Laplacian matrix $L_{\mathcal{G}_c}$ is symmetric.*

In view of Assumption 4.1 and Assumption 7.1 we find that the left-eigenvector of the Laplacian matrix corresponding to an eigenvalue of $\lambda = 0$ is equal to $\mathbf{w} = \frac{1}{N}\mathbb{1}_N$.

As a result we get $\text{avg}_\text{w}\mathbf{y} = \text{avg}\mathbf{y} = \frac{1}{N}\sum_j y_j$. By implementing the consensus algorithm from Chapter 4 we find the following model depicted in Figure 7-1.

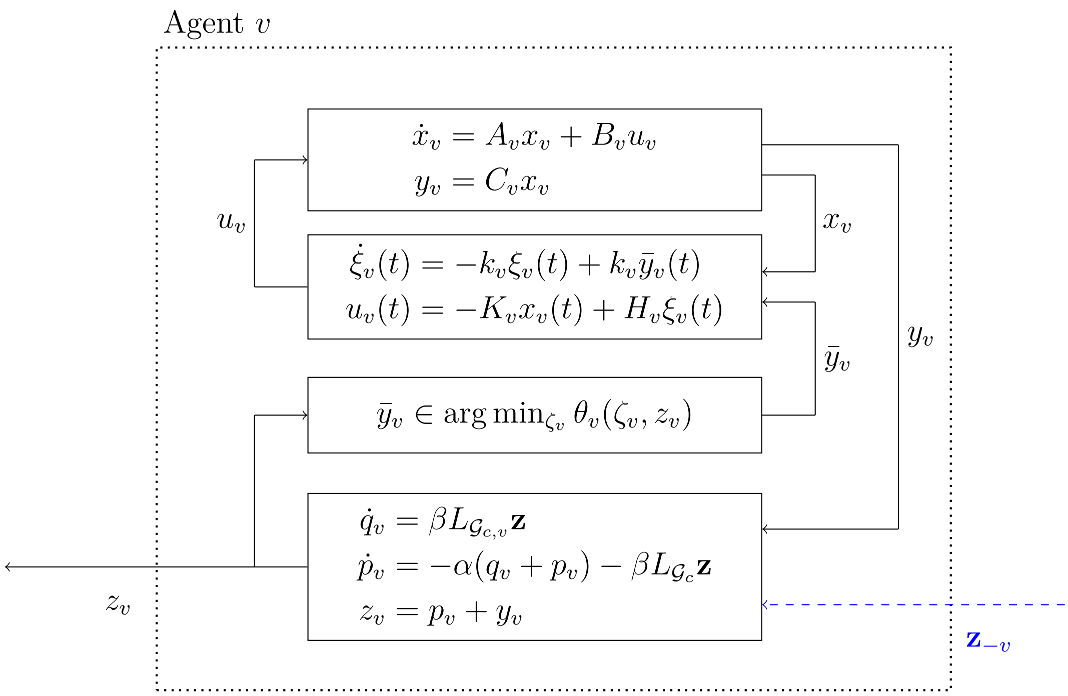

Figure 7-1: Dynamics of agent v with proposed state-feedback reference control and consensus algorithm. The blue, dashed line represents the estimate of the average output computed by the other agents in the neighbour set $\mathcal{N}_v$.

We now redefine the linear-quadratic cost function from Equation (6-11) as a function of the average instead. This results in

$$\theta_v(y_v, \text{avg}\mathbf{y}(t)) = \tfrac{1}{2}y_v^\top Q_{d,v} y_v - y_v^\top b_v - y_v^\top Q_{a,v}\text{avg}\mathbf{y}(t) \tag{7-3}$$

where $Q_{d,v} \in \mathbb{R}^{m\times m}$ is the quadratic-term symmetric matrix with $Q_{d,v} > 0$, $Q_{a,v} \in \mathbb{R}^{m\times m}$ a symmetric linear-term matrix relating to a cost due to the average of the agents affecting agent v and $b_v \in \mathbb{R}^m$ a linear-term vector. Note that we define $m := m_v = m_1 = \cdots = m_N$, in view of the required homogeneous system dimension for consensus. We once more find the solution $\bar{y}_v$ to this system by setting to zero the gradient of $\theta_v(y_v, \text{avg}\mathbf{y}(t))$ with respect to y_v. We find

$$\nabla_{y_v}\theta_v(y_v, \text{avg}\mathbf{y}(t)) = Q_{d,v}y_v - b_v - \tfrac{1}{N}Q_{a,v}y_v - Q_{a,v}\text{avg}\mathbf{y}(t) \tag{7-4}$$

$$= \left(Q_{d,v} - \tfrac{1}{N}Q_{a,v}\right) y_v - b_v - Q_{a,v}\text{avg}\mathbf{y}(t) \tag{7-5}$$

$$= 0 \tag{7-6}$$

which results in

$$\bar{y}_v = \left(Q_{d,v} - \tfrac{1}{N}Q_{a,v}\right)^{-1}(b_v + Q_{a,v}\text{avg}\mathbf{y}(t)) \tag{7-7}$$

Since the control actions do not have access to the other agent's outputs, we can rewrite Equation (7-7) as a function of z_v and implement the resulting $\bar{y}_v$ with the controller from Equation (6-2).

$$\bar{y}_v = \left(Q_{d,v} - \tfrac{1}{N}Q_{a,v}\right)^{-1}(b_v + Q_{a,v}z_v) \tag{7-8}$$

for all agents v. We once more discuss the overall system dynamics by introducing

$$Q_d = \text{blockdiag}(Q_{d,1}, \dots, Q_{d,N}) \tag{7-9}$$
$$Q_a = \text{blockdiag}(Q_{a,1}, \dots, Q_{a,N}) \tag{7-10}$$
$$L = L_{\mathcal{G}_c} \otimes I_m \tag{7-11}$$
$$\text{b} = [b_1^\top, \dots, b_N^\top]^\top \tag{7-12}$$

which then results in an overall optimum $\bar{\mathbf{y}}$ of

$$\bar{\mathbf{y}}(t) = \left(Q_d - \tfrac{1}{N}Q_a\right)^{-1}(\mathbf{b} + Q_a\mathbf{z}(t)) \tag{7-13}$$

and system dynamics equal to

$$\dot{\mathbf{x}}(t) = A\mathbf{x}(t) + B\mathbf{u}(t) \tag{7-14a}$$
$$\dot{\boldsymbol{\xi}}(t) = -\mathbf{k}\boldsymbol{\xi}(t) + \mathbf{k}\left(Q_d - \tfrac{1}{N}Q_a\right)^{-1}Q_a\mathbf{z}(t) \tag{7-14b}$$
$$\dot{\mathbf{q}}(t) = \beta L\mathbf{p}(t) + \beta L\mathbf{y}(t) \tag{7-14c}$$
$$\dot{\mathbf{p}}(t) = -\alpha\mathbf{q}(t) - \alpha\mathbf{p}(t) - \beta L\mathbf{p}(t) - \beta L\mathbf{y}(t) \tag{7-14d}$$
$$\mathbf{y}(t) = C\mathbf{x}(t) \tag{7-14e}$$
$$\mathbf{z}(t) = \mathbf{p}(t) + \mathbf{y}(t) \tag{7-14f}$$
$$\mathbf{u}(t) = -K\mathbf{x}(t) + H\left(\boldsymbol{\xi}(t) + \left(Q_d - \tfrac{1}{N}Q_a\right)^{-1}\mathbf{b}\right) \tag{7-14g}$$

thus

$$\begin{bmatrix}\dot{\mathbf{x}}\\ \dot{\boldsymbol{\xi}}\\ \dot{\mathbf{q}}\\ \dot{\mathbf{p}}\end{bmatrix} = \begin{bmatrix} A - BK & BH & \mathbb{0}_{n_s\times m_s} & \mathbb{0}_{n_s\times m_s} \\ \mathbf{k}(Q_d - \frac{1}{N}Q_a)^{-1}Q_aC & -\mathbf{k} & \mathbb{0}_{m_s\times m_s} & \mathbf{k}(Q_d - \frac{1}{N}Q_a)^{-1}Q_a \\ \beta LC & \mathbb{0}_{m_s\times m_s} & \mathbb{0}_{m_s\times m_s} & \beta L \\ -\beta LC & \mathbb{0}_{m_s\times m_s} & -\alpha I_{m_s} & -\alpha I_{m_s} - \beta L \end{bmatrix}\begin{bmatrix}\mathbf{x}\\ \boldsymbol{\xi}\\ \mathbf{q}\\ \mathbf{p}\end{bmatrix} + \begin{bmatrix} BH(Q_d - \frac{1}{N}Q_a)^{-1} \\ \mathbb{0}_{m_s\times m_s} \\ \mathbb{0}_{m_s\times m_s} \\ \mathbb{0}_{m_s\times m_s}\end{bmatrix}\mathbf{b} \tag{7-15}$$

Theorem 7.1. *Given* $\mathbf{k} = \text{blockdiag}(k_1 I_{m_1}, \dots, k_N I_{m_N})$ *with* $\forall v\ k_v > 0$ *there exists a set of parameters* $k_1, \dots, k_N$ *small enough such that the system defined in Equation* (7-15) *is stable.*

Proof: For the stability proof we follow a similar approach to Theorem 6.2; we take $\mathbf{k}$ equal to zero. Doing so leads us to the following equalities for the eigenvalues of the system matrix.

$$(A - BK)v_1 + BHv_2 = \lambda v_1 \tag{7-16a}$$
$$\mathbb{0}_{m_s} = \lambda v_2 \tag{7-16b}$$
$$\beta L(Cv_1 + v_4) = \lambda v_3 \tag{7-16c}$$
$$-(\lambda + \alpha)v_3 = (\lambda + \alpha)v_4 \tag{7-16d}$$

This again leads to the eigenvalues $\lambda_i = \text{eig}(A - BK)$, $\lambda_i = 0$, $\lambda_i = -a$, and $\lambda_i = -\beta\text{eig}(L)$. We again consider $\mathbf{k} \to \mathbb{0}_{m_s \times m_s}$, $\lambda_i \to 0$ and the Neumann series and find

$$v_2 - \lambda_i C(A - BK)^{-2}BHv_2 = Cv_1 \tag{7-17a}$$
$$\mathbf{k}(Q_d - \tfrac{1}{N}Q_a)^{-1}Q_a(Cv_1 + v_4) - \mathbf{k}v_2 = \lambda_i v_2 \tag{7-17b}$$
$$\beta L(Cv_1 + v_4) = \lambda_i v_3 \tag{7-17c}$$
$$v_3 + v_4 = \mathbb{0}_{m_s} \tag{7-17d}$$

with $\lambda_i v_3 \to \mathbb{0}_{m_s}$ we find $v_4 = -Cv_1$ and accordingly

$$-\mathbf{k}v_2 = \lambda_i v_2 \tag{7-18}$$

thus $\lambda_i = -k_{ii}$, in view of $\mathbf{k}$ being a diagonal matrix, resulting in all eigenvalues being negative and as such the system matrix is Hurwitz.

With the stability of the system in mind, we can discuss the resulting steady-state response. In fact we find that the following theorem holds:

Theorem 7.2. *The system as described in Equation* (7-14) *with the control matrix* $\mathbf{k} = \text{blockdiag}(k_1 I_{m_1}, \ldots, k_N I_{m_N})$ *ensures that* $\mathbf{y}(t) \to \mathbf{y}^\star$ *for* $t \to \infty$ *with a set of parameters* $k_1, \ldots, k_N$ *small enough.*

Proof: We begin by finding the Nash equilibrium associated with the game where the agents minimize the cost function described in Equation (7-3). We again define the Nash equilibrium as $\mathbf{y}^\star$ and find $\mathbf{z}^\star = \text{avg}\mathbf{y}^\star = \frac{1}{N}(\mathbb{1}_{N\times N} \otimes I_m)\mathbf{y}^\star$. With $\bar{\mathbf{y}} = \mathbf{y}^\star$ and $\mathbf{z} = \mathbf{z}^\star$, Equation (7-13) results in

$$\mathbf{y}^\star = \left(Q_d - \tfrac{1}{N}Q_a\right)^{-1}\left(\mathbf{b} + \tfrac{1}{N}Q_a(\mathbb{1}_{N\times N} \otimes I_m)\mathbf{y}^\star\right) \tag{7-19}$$

thus

$$\mathbf{y}^\star = \left(Q_d - \tfrac{1}{N}Q_a\left((\mathbb{1}_{N\times N} + I_N) \otimes I_m\right)\right)^{-1}\mathbf{b} \tag{7-20}$$

In view of the system being at steady state, we note that $\dot{\mathbf{x}}_{ss} = \mathbb{0}_{nN}$ and $\dot{\boldsymbol{\xi}}_{ss} = \dot{\mathbf{q}}_{ss} = \dot{\mathbf{p}}_{ss} = \mathbb{0}_{mN}$. This leads to the set of equalities

$$(A - BK)\mathbf{x}_{ss} + BH\left(\boldsymbol{\xi}_{ss} + \left(Q_d - \tfrac{1}{N}Q_a\right)^{-1}\mathbf{b}\right) = \mathbb{0}_{n_s} \tag{7-21a}$$

$$\mathbf{k}(Q_d - \tfrac{1}{N}Q_a)^{-1}Q_a(C\mathbf{x}_{ss} + \mathbf{p}_{ss}) - \mathbf{k}\boldsymbol{\xi}_{ss} = \mathbb{0}_{m_s} \tag{7-21b}$$

$$\beta L(C\mathbf{x}_{ss} + \mathbf{p}_{ss}) = \mathbb{0}_{m_s} \tag{7-21c}$$

$$-\beta L(C\mathbf{x}_{ss} + \mathbf{p}_{ss}) - \alpha(\mathbf{q}_{ss} + \mathbf{p}_{ss}) = \mathbb{0}_{m_s} \tag{7-21d}$$

With $\mathbf{y}_{ss} = C\mathbf{x}_{ss}$, the latter two equations yield

$$\mathbf{q}_{ss} = -\left((\mathbb{1}_N\mathbf{w}^\top - I_N) \otimes I_m\right)\mathbf{y}_{ss} \tag{7-22a}$$

$$\mathbf{p}_{ss} = \left((\mathbb{1}_N\mathbf{w}^\top - I_N) \otimes I_m\right)\mathbf{y}_{ss} \tag{7-22b}$$

and following the same approach as in Chapter 4, specifically the proof following Theorem 4.2, this results in

$$\mathbf{q}_{ss} = -\left((\tfrac{1}{N}\mathbb{1}_{N\times N} - I_N) \otimes I_m\right)\mathbf{y}_{ss} \tag{7-23a}$$

$$\mathbf{p}_{ss} = \left((\tfrac{1}{N}\mathbb{1}_{N\times N} - I_N) \otimes I_m\right)\mathbf{y}_{ss} \tag{7-23b}$$

We now consider Equation (7-21b), which we can rewrite to

$$\boldsymbol{\xi}_{ss} = (Q_d - \tfrac{1}{N}Q_a)^{-1}Q_a\left(\tfrac{1}{N}\mathbb{1}_{N\times N} \otimes I_m\right)\mathbf{y}_{ss} \tag{7-24}$$

and substituting this in Equation (7-21a) then yields

$$(A - BK)\mathbf{x}_{ss} = -BH(Q_d - \tfrac{1}{N}Q_a)^{-1}\left(Q_a\left(\tfrac{1}{N}\mathbb{1}_{N\times N} \otimes I_m\right)\mathbf{y}_{ss} + \mathbf{b}\right) \tag{7-25}$$

Pre-multiplying both sides with $C(A - BK)^{-1}$ then leads to

$$\mathbf{y}_{ss} = \left(Q_d - \tfrac{1}{N}Q_a\right)^{-1}\left(\tfrac{1}{N}Q_a\left(\mathbb{1}_{N\times N} \otimes I_m\right)\mathbf{y}_{ss} + \mathbf{b}\right) \tag{7-26}$$

which, after some rewriting, leads to

$$\mathbf{y}_{ss} = \left(Q_d - \tfrac{1}{N}Q_a\Big((\mathbb{1}_{N\times N} + I_N) \otimes I_m\Big)\right)^{-1}\mathbf{b} = \mathbf{y}^\star \tag{7-27}$$

and as such $\mathbf{y}_{ss} = \mathbf{y}^\star$ implying $\mathbf{y}(t) \to \mathbf{y}^\star$ for $t \to \infty$.

7-2 Aggregate games with local costs

To get a more general result, this section extends the cost function defined in Equation (7-1) with a cost dependent on the neighbours of agent v.

$$\theta_v = \theta_v(y_v, \{y_j\}_{j\in\mathcal{N}_v}, \text{avg}\mathbf{y}) \tag{7-28}$$

Which, in linear-quadratic form, leads to

$$\theta_v(y_v, \{y_j\}_{j\in\mathcal{N}_v}, \text{avg}\mathbf{y}) = \tfrac{1}{2} y_v^\top Q_{d,v} y_v - y_v^\top b_v - \sum_{j\in\mathcal{N}_v} y_v^\top Q_{c,v,j} y_j(t) - y_v^\top Q_{a,v}\text{avg}\mathbf{y}(t) \quad (7\text{-}29)$$

Taking the derivative with respect to y_v and setting it to zero then leads to a best response similar to those found before.

$$\bar{y}_v = \left(Q_{d,v} - \tfrac{1}{N} Q_{a,v}\right)^{-1} \left(b_v + \sum_{j\in\mathcal{N}_v} Q_{c,v,j} y_j(t) + Q_{a,v}\text{avg}\mathbf{y}(t)\right) \quad (7\text{-}30)$$

or in overall terms

$$\bar{\mathbf{y}} = \left(Q_d - \tfrac{1}{N} Q_a\right)^{-1} (\mathbf{b} + Q_c\mathbf{y}(t) + Q_a\text{avg}\mathbf{y}(t)) \quad (7\text{-}31)$$

Assumption 7.2. *The spectral radius of* $(Q_d - \frac{1}{N}Q_a)^{-1}Q_c$ *is smaller than 1, i.e.* $\rho((Q_d - \frac{1}{N}Q_a)^{-1}Q_c) < 1$.

If we then implement this updating scheme in the system dynamics from Equation (7-14), we find

$$\dot{\mathbf{x}}(t) = A\mathbf{x}(t) + B\mathbf{u}(t) \quad (7\text{-}32a)$$
$$\dot{\boldsymbol{\xi}}(t) = -\mathbf{k}\boldsymbol{\xi}(t) + \mathbf{k}\left(Q_d - \tfrac{1}{N}Q_a\right)^{-1} (Q_c\mathbf{y}(t) + Q_a\mathbf{z}(t)) \quad (7\text{-}32b)$$
$$\dot{\mathbf{q}}(t) = \beta L\mathbf{p}(t) + \beta L\mathbf{y}(t) \quad (7\text{-}32c)$$
$$\dot{\mathbf{p}}(t) = -\alpha\mathbf{q}(t) - \alpha\mathbf{p}(t) - \beta L\mathbf{p}(t) - \beta L\mathbf{y}(t) \quad (7\text{-}32d)$$
$$\mathbf{y}(t) = C\mathbf{x}(t) \quad (7\text{-}32e)$$
$$\mathbf{z}(t) = \mathbf{p}(t) + \mathbf{y}(t) \quad (7\text{-}32f)$$
$$\mathbf{u}(t) = -K\mathbf{x}(t) + H\left(\boldsymbol{\xi}(t) + \left(Q_d - \tfrac{1}{N}Q_a\right)^{-1}\mathbf{b}\right) \quad (7\text{-}32g)$$

Additionally we can rewrite the first order controller approach and find the overall system dynamics equal to

$$\begin{bmatrix}\dot{\mathbf{x}}\\ \dot{\boldsymbol{\xi}}\\ \dot{\mathbf{q}}\\ \dot{\mathbf{p}}\end{bmatrix} = \begin{bmatrix} A - BK & BH & \mathbb{0}_{n_s\times m_s} & \mathbb{0}_{n_s\times m_s}\\ \mathbf{k}(Q_d - \frac{1}{N}Q_a)^{-1}(Q_c + Q_a)C & -\mathbf{k} & \mathbb{0}_{m_s\times m_s} & \mathbf{k}(Q_d - \frac{1}{N}Q_a)^{-1}Q_a\\ \beta LC & \mathbb{0}_{m_s\times m_s} & \mathbb{0}_{m_s\times m_s} & \beta L\\ -\beta LC & \mathbb{0}_{m_s\times m_s} & -\alpha I_{m_s} & -\alpha I_{m_s} - \beta L\end{bmatrix}\begin{bmatrix}\mathbf{x}\\ \boldsymbol{\xi}\\ \mathbf{q}\\ \mathbf{p}\end{bmatrix} + \begin{bmatrix} BH(Q_d - \frac{1}{N}Q_a)^{-1}\\ \mathbb{0}_{m_s\times m_s}\\ \mathbb{0}_{m_s\times m_s}\\ \mathbb{0}_{m_s\times m_s}\end{bmatrix}\mathbf{b} \quad (7\text{-}33)$$

Theorem 7.3. *Given Assumption 7.2 and* $\mathbf{k} = \text{blockdiag}(k_1 I_{m_1}, \ldots, k_N I_{m_N})$ *with* $\forall v\ k_v > 0$ *there exists a set of parameters* $k_1, \ldots, k_N$ *small enough such that the system defined in Equation* (7-33) *is stable.*

Proof: When analysing the eigenvalues of the system, we follow the exact approach as in the proof of Theorem 7.3. Consider $\mathbf{k} \to \mathbb{0}_{m_s \times m_s}$, $\lambda_i \to 0$ and the Neumann series and find

$$v_2 - \lambda_i C(A - BK)^{-2} BH v_2 = Cv_1 \tag{7-34}$$

$$\mathbf{k}(Q_d - \tfrac{1}{N}Q_a)^{-1} Q_a (Cv_1 + v_4) + \mathbf{k}(Q_d - \tfrac{1}{N}Q_a)^{-1} Q_c C v_1 - \mathbf{k} v_2 = \lambda_i v_2 \tag{7-35}$$

$$\beta L (Cv_1 + v_4) = \lambda_i v_3 \tag{7-36}$$

$$v_3 + v_4 = \mathbb{0}_{m_s} \tag{7-37}$$

With the first and third equation we find $Cv_1 = v_2 - \lambda_i C(A - BK)^{-2} BH v_2 = -v_4$ and as such the second equation leads to

$$\mathbf{k}(Q_d - \tfrac{1}{N}Q_a)^{-1} Q_c v_2 - \mathbf{k} v_2 - \lambda_i \mathbf{k}(Q_d - \tfrac{1}{N}Q_a)^{-1} Q_c C(A - BK)^{-2} BH v_2 = \lambda_i v_2 \tag{7-38}$$

thus, by neglecting the term $\lambda_i \mathbf{k}$,

$$\mathbf{k}\left((Q_d - \tfrac{1}{N}Q_a)^{-1} Q_c - I_{m_s}\right) v_2 = \lambda_i v_2 \tag{7-39}$$

Which in view of Assumption 7.2 leads to strictly negative eigenvalues.

7-3 Numerical example

Again we introduce a numerical example to showcase the results found in this chapter. We take a system of $N = 10$ agents, similar to that of Section 6-4, but instead with a graph topology as depicted in Figure 7-2.

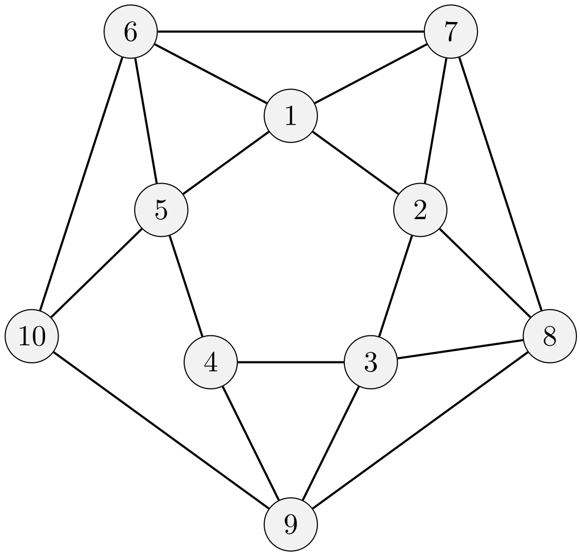

Figure 7-2: The undirected graph of the network system with $N = 10$ agents used in the numerical example for the aggregate cost function controller.

The resulting adjacency matrix is equal to

$$A_{\mathcal{G}_c} = \begin{bmatrix} 0 & 1 & 0 & 0 & 1 & 1 & 1 & 0 & 0 & 0 \\ 1 & 0 & 1 & 0 & 0 & 0 & 1 & 1 & 0 & 0 \\ 0 & 1 & 0 & 1 & 0 & 0 & 0 & 1 & 1 & 0 \\ 0 & 0 & 1 & 0 & 1 & 0 & 0 & 0 & 1 & 0 \\ 1 & 0 & 0 & 1 & 0 & 1 & 0 & 0 & 0 & 1 \\ 1 & 0 & 0 & 0 & 1 & 0 & 1 & 0 & 0 & 1 \\ 1 & 1 & 0 & 0 & 0 & 1 & 0 & 1 & 0 & 0 \\ 0 & 1 & 1 & 0 & 0 & 0 & 1 & 0 & 1 & 0 \\ 0 & 0 & 1 & 1 & 0 & 0 & 0 & 1 & 0 & 1 \\ 0 & 0 & 0 & 0 & 1 & 1 & 0 & 0 & 1 & 0 \end{bmatrix} \tag{7-40}$$

We let the agents follow the same dynamics as in Section 6-4, specifically Equation (6-53). This results in the same control matrix $K_v = [5, -6]$, control parameter $k_v = 1$, and gain matrix $H_v = -\frac{10}{3}$. For the cost matrices we take a similar approach with

$$Q_d = 5I_N \tag{7-41a}$$
$$Q_c = 2\text{diag}(A_{\mathcal{G}_c}\mathbb{1}_N)^{-1}A_{\mathcal{G}_c} \tag{7-41b}$$
$$Q_a = \frac{1}{N}\text{diag}(1, 2, \ldots, N) \tag{7-41c}$$
$$\mathbf{b} = 5\mathbb{1}_N \tag{7-41d}$$

This results in a Nash equilibrium of

$$\mathbf{y}^\star = \begin{bmatrix} 1.8670 \\ 1.9084 \\ 1.9770 \\ 2.0243 \\ 2.0622 \\ 2.1142 \\ 2.1308 \\ 2.1976 \\ 2.2688 \\ 2.3233 \end{bmatrix}$$

We again introduce the reference *full information control* y_{fi} by means of the control action from Equation (6-56). With the same initial states of $x_v(0) = [0.8, -0.2]^\top$ for agents 1 through 5, and $x_v(0) = [0.8, 0.2]^\top$ for agents 6 through 10. For the consensus parameters we take $\alpha = 1$ and $\beta = 1$.

In Figure 7-3 we find the resulting transient response of agent 1, and the rms-error of all agents.

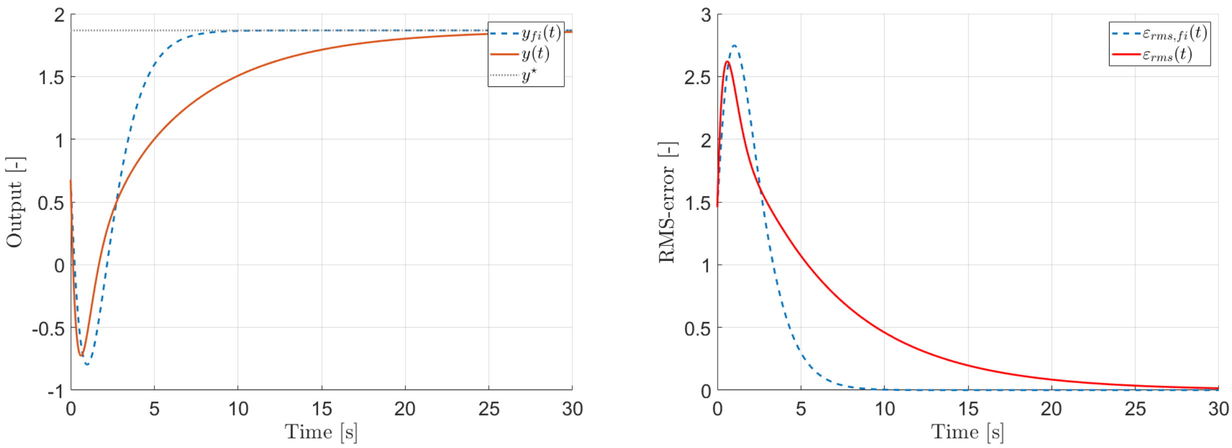

Figure 7-3: Response of a networked game of $N = 10$ agents, subject to linear state-space dynamics whilst aiming to minimize a linear-quadratic aggregate cost function by means of a local first order reference control law with state feedback. The left panel shows the transient response of agent 1 (red solid line), as well as its Nash equilibrium (black dotted), and the full information control (blue dashed). The right panel depicts the sum of the errors of all agents with respect to the Nash equilibrium (red solid line) as well as the error in case of full information control (blue dashed).

Chapter 8

Full output estimation: steering to the Nash equilibrium by means of output estimation

This chapter will discuss a situation where the individual agents don't have full information about the system, but their cost function does depend on the individual agent states. This differs from the system of Chapter 7 where we merely discussed aggregate games with the optional addition of neighbour state dependencies.

In order to obtain information on all individual states, we propose a decentralized estimation approach where each agent aims to estimate all agent outputs. Since the agents aim to estimate the true outputs, a proper estimation algorithm leads to a common estimate of the system outputs. Hence the decentralized estimation can also be referred to as a full-system consensus where all agents reach a consensus on the overall output vector.

8-1 Decentralized Estimation

For the decentralized estimation approach we introduce in this chapter, it is assumed that all agents construct a certain vector containing the overall system outputs. For this to work across all individual agents there must be a certain agreement on the agent numbering. This means that if the agents discuss for example the fourth entry of the estimation vector, they all talk about the same output of the same agent. However, this is the only global information required for this approach and can be agreed upon beforehand.

The goal of the decentralized estimation approach is for each agent to reach an accurate estimation of all agent outputs $\mathbf{y}$. With the estimation of agent v defined as $\mathbf{z}_v$ this leads to $\mathbf{z}_v(t) \to \mathbf{y}(t^\star)$ for $t \to \infty$ similar to Theorem 4.2.

We once more define an undirected communication graph $\mathcal{G}_c(\mathcal{V}, \mathcal{E}_c)$ following Assumption 4.1. Again the Laplacian matrix $L_{\mathcal{G}_c}$ is defined as in Equation (4-4). If we followed the same approach as in general consensus methods we would find an estimation approach for agent v equal to:

$$\dot{\mathbf{z}}_v(t) = -\sum_j l_{v,j}\mathbf{z}_j(t) \tag{8-1}$$

However this approach implies that agent v updates his belief on output y_v. Since agent v has full access to his own output this output should not be part of his estimation algorithm. Therefore we extend the algorithm such that the v-th entry of $\dot{\mathbf{z}}_v$ remains zero, i.e.:

$$\dot{\mathbf{z}}_v(t) = -(I_N - \mathbb{e}_v\mathbb{e}_v^\top)\sum_j l_{v,j}\mathbf{z}_j(t) \tag{8-2}$$

We now define the vector containing all agent beliefs as $\mathbf{z} = [\mathbf{z}_1^\top, \ldots, \mathbf{z}_N^\top]^\top$ and find the overall estimation algorithm as

$$\dot{\mathbf{z}}(t) = -L_{\mathcal{G}_c,est}\mathbf{z}(t) \tag{8-3}$$

where

$$L_{\mathcal{G}_c,est} = \begin{bmatrix} (I_N - \mathbb{e}_1\mathbb{e}_1^\top)l_{1,1} & (I_N - \mathbb{e}_1\mathbb{e}_1^\top)l_{1,2} & \cdots & (I_N - \mathbb{e}_1\mathbb{e}_1^\top)l_{1,N} \\ (I_N - \mathbb{e}_2\mathbb{e}_2^\top)l_{2,1} & (I_N - \mathbb{e}_2\mathbb{e}_2^\top)l_{2,2} & \cdots & (I_N - \mathbb{e}_2\mathbb{e}_2^\top)l_{2,N} \\ \vdots & \vdots & \ddots & \vdots \\ (I_N - \mathbb{e}_N\mathbb{e}_N^\top)l_{N,1} & (I_N - \mathbb{e}_N\mathbb{e}_N^\top)l_{N,2} & \cdots & (I_N - \mathbb{e}_N\mathbb{e}_N^\top)l_{N,N} \end{bmatrix} \tag{8-4}$$

We note that $L_{\mathcal{G}_c,est}$ is simply a reordering of N separate consensus algorithms where in each of the algorithms one of the agents acts as a sink node. For a Laplacian matrix with one sink node, e.g. node v, we find that there exists a right eigenpair $(0, \mathbb{1}_N)$ and a corresponding left eigenpair $(0, \mathbb{e}_v)$. Hence after reordering for $L_{\mathcal{G}_c,est}$ we find N unique eigenpairs equal to right eigenpairs $(0, \mathbb{1}_N \otimes \mathbb{e}_i)$ and left eigenpairs $(0, \mathbb{e}_i \otimes \mathbb{e}_i)$ for $i \in \{1, \ldots, N\}$. As such we find

$$\lim_{t\to\infty} e^{-L_{\mathcal{G}_c,est}t} = \mathbb{1}_N \otimes [\mathbb{e}_1\mathbb{e}_1^\top, \ldots, \mathbb{e}_N\mathbb{e}_N^\top] \tag{8-5}$$

thus $\mathbf{z}(t) \to \mathbb{1}_N \otimes \mathbf{y}(0)$ for $t \to \infty$ with $\mathbf{z}_v(0) = \mathbb{e}_v \otimes \mathbf{y}(0)$.

With this newly constructed Laplacian matrix we can follow the same procedures as in Chapter 4, ultimately resulting in

$$\begin{bmatrix}\dot{\mathbf{q}}(t) \\ \dot{\mathbf{p}}(t)\end{bmatrix} = \begin{bmatrix} \mathbb{0}_{N^2\times N^2} & \beta L_{\mathcal{G}_c,est} \\ -\alpha I_{N^2} & -\alpha I_{N^2} - \beta L_{\mathcal{G}_c,est}\end{bmatrix}\begin{bmatrix}\mathbf{q}(t) \\ \mathbf{p}(t)\end{bmatrix} + \begin{bmatrix}\beta L_{\mathcal{G}_c,est} \\ -\beta L_{\mathcal{G}_c,est}\end{bmatrix} G\mathbf{y}(t) \tag{8-6a}$$

$$\mathbf{z}(t) = \mathbf{p}(t) + G\mathbf{y}(t) \tag{8-6b}$$

with $G = \text{blockdiag}(\mathbb{e}_1, \ldots, \mathbb{e}_N)$.

Theorem 8.1. *The decentralized estimation algorithm proposed in Equation* (8-6) *yields* $\mathbf{z}(t) \to \mathbb{1}_N \otimes \mathbf{y}(t^\star)$ *for* $t \to \infty$ *if* $\exists t^\star > 0$ *such that for* $t > t^\star$ *we find* $\mathbf{y}(t) = \mathbf{y}(t^\star)$.

Proof: In view of $L_{\mathcal{G}_c}$ and $L_{\mathcal{G}_c,est}$ having similar properties, the proof for Theorem 8.1 follows the same reasoning as Theorem 4.2. Hence by setting the steady-state derivatives to zero, $\dot{\mathbf{q}}_{ss} = \dot{\mathbf{p}}_{ss} = \mathbb{0}_{N^2}$, we find $\mathbf{q}_{ss} = -\mathbf{p}_{ss}$ and $L_{\mathcal{G}_c,est}\mathbf{p}_{ss} = -L_{\mathcal{G}_c,est}G\mathbf{y}(t^\star)$, as such

$$\mathbf{q}_{ss} = -\left(\sum_{j=1}^{N}(\mathbb{1}_N \otimes \mathbb{e}_j)\mathbf{a}_j^\top - I_{N^2}\right) G\mathbf{y}(t^\star) \tag{8-7a}$$

$$\mathbf{p}_{ss} = \left(\sum_{j=1}^{N}(\mathbb{1}_N \otimes \mathbb{e}_j)\mathbf{a}_j^\top - I_{N^2}\right) G\mathbf{y}(t^\star) \tag{8-7b}$$

$$\mathbf{z}_{ss} = \sum_{j=1}^{N}(\mathbb{1}_N \otimes \mathbb{e}_j)\mathbf{a}_j^\top G\mathbf{y}(t^\star) \tag{8-7c}$$

with arbitrary vector $\mathbf{a}_j$.

Additionally, by defining $\bar{\mathbf{q}}(t) = \mathbf{q}(t) - \mathbf{q}_{ss}$, $\bar{\mathbf{p}}(t) = \mathbf{p}(t) - \mathbf{p}_{ss}$ and $\bar{\mathbf{y}}(t) = \mathbf{y}(t) - \mathbf{y}(t^\star) = \mathbb{0}_N$ we again obtain the transformed dynamics

$$\begin{bmatrix}\dot{\bar{\mathbf{q}}}(t) \\ \dot{\bar{\mathbf{p}}}(t)\end{bmatrix} = \begin{bmatrix}\mathbb{0}_{N^2\times N^2} & \beta L_{\mathcal{G}_c} \\ -\alpha I_N & -\alpha I_N - \beta L_{\mathcal{G}_c}\end{bmatrix}\begin{bmatrix}\bar{\mathbf{q}}(t) \\ \bar{\mathbf{p}}(t)\end{bmatrix} \tag{8-8}$$

with N right-eigenpairs equal to

$$\left(\lambda_i, \begin{bmatrix}\mathbf{v}_{1,i} \\ \mathbf{v}_{2,i}\end{bmatrix}\right) = \left(0, \begin{bmatrix}\mathbb{1}_N \otimes \mathbb{e}_i \\ -\mathbb{1}_N \otimes \mathbb{e}_i\end{bmatrix}\right) \tag{8-9}$$

and N left-eigenpairs of

$$\left(\lambda_i, \begin{bmatrix}\mathbf{w}_{1,i} \\ \mathbf{w}_{2,i}\end{bmatrix}\right) = \left(0, \begin{bmatrix}\mathbb{e}_i \otimes \mathbb{e}_i \\ \mathbb{0}_N\end{bmatrix}\right) \tag{8-10}$$

which for $t \to \infty$ then results in

$$\bar{\mathbf{p}}(t) = -\sum_{i=1}^{N}\left((\mathbb{1}_N \otimes \mathbb{e}_i)(\mathbb{e}_i \otimes \mathbb{e}_i)^\top \bar{\mathbf{q}}(0)\right) \tag{8-11a}$$

$$= -\sum_{i=1}^{N}\left((\mathbb{1}_N \otimes \mathbb{e}_i)(\mathbb{e}_i \otimes \mathbb{e}_i)^\top \left(\sum_{j=1}^{N}(\mathbb{1}_N \otimes \mathbb{e}_j)\mathbf{a}_j^\top - I_{N^2}\right) G\mathbf{y}(t^\star)\right) \tag{8-11b}$$

$$= -\sum_{i=1}^{N}\left((\mathbb{1}_N \otimes \mathbb{e}_i)(\mathbb{e}_i \otimes \mathbb{e}_i)^\top(\mathbb{1}_N \otimes \mathbb{e}_i)\mathbf{a}_i^\top - (\mathbb{1}_N \otimes \mathbb{e}_i)(\mathbb{e}_i \otimes \mathbb{e}_i)^\top\right) G\mathbf{y}(t^\star) \tag{8-11c}$$

$$= -\sum_{i=1}^{N}\left((\mathbb{1}_N \otimes \mathbb{e}_i)\mathbf{a}_i^\top - (\mathbb{1}_N \otimes \mathbb{e}_i)(\mathbb{e}_i \otimes \mathbb{e}_i)^\top\right) G\mathbf{y}(t^\star) \tag{8-11d}$$

It is known that $\bar{\mathbf{p}}(t) \to \mathbb{0}_{N^2}$ for $t \to \infty$, hence we find $\mathbf{a}_i = \mathbb{e}_i \otimes \mathbb{e}_i$. Going back to the set of steady state equalities, we find that

$$\mathbf{z}_{ss} = \sum_{j=1}^{N} (\mathbb{1}_N \otimes \mathbb{e}_j)(\mathbb{e}_j \otimes \mathbb{e}_j)^\top G\mathbf{y}(t^\star) \tag{8-12}$$
$$= \sum_{j=1}^{N} (\mathbb{1}_N \otimes \mathbb{e}_j)\mathbb{e}_j^\top \mathbf{y}(t^\star) \tag{8-13}$$
$$= (\mathbb{1}_N \otimes I_N)\mathbf{y}(t^\star) \tag{8-14}$$
$$= \mathbb{1}_N \otimes \mathbf{y}(t^\star) \tag{8-15}$$

The notions of convergence and stability are analogous to those of Chapter 7, where we replace $L_{\mathcal{G}_c}$ with $L_{\mathcal{G}_c,est}$.

With this estimation method we have access to all outputs, even if the game graphs is not fully encompassed by the communication graph, i.e. $\mathcal{E}_\theta \not\subseteq \mathcal{E}_c$. Therefore we can still consider games where the cost function has the form

$$\theta_v(y_v, \mathbf{y}_{-v}(t)) = \tfrac{1}{2} y_v^\top Q_{d,v} y_v - y_v^\top b_v - \sum_{j \neq v} y_v^\top Q_{c,v,j} y_j(t) \tag{8-16}$$

We construct Q_d as in Equation (6-14) but follow a different structure for Q_c. Since Q_c is not related to $\mathbf{y}$ but instead to $\mathbf{z}$ from Equation (8-6), we find

$$Q_c = \operatorname{blockdiag}(Q_{c,1}, Q_{c,2}, \dots, Q_{c,N}) \tag{8-17}$$

where

$$Q_{c,v} = \begin{bmatrix} Q_{c,v,1} & Q_{c,v,2} & \cdots & Q_{c,v,v-1} & \mathbb{0} & Q_{c,v,v+1} & \cdots & Q_{c,v,N} \end{bmatrix} \tag{8-18}$$

Following a similar approach to the one in Chapter 6, this ultimately results in the best responses equal to

$$\bar{\mathbf{y}}(t) = Q_d^{-1}\left(\mathbf{b} + Q_c \mathbf{z}(t)\right) \tag{8-19}$$

We combine the results from Equation (8-6) and Equation (7-15), with $L = L_{\mathcal{G}_c,est} \otimes I_m$ and find

$$\begin{bmatrix} \dot{\mathbf{x}} \\ \dot{\boldsymbol{\xi}} \\ \dot{\mathbf{q}} \\ \dot{\mathbf{p}} \end{bmatrix} = \begin{bmatrix} A - BK & BH & \mathbb{0}_{n_s \times m_s^2} & \mathbb{0}_{n_s \times m_s^2} \\ \mathbf{k}Q_d^{-1}Q_c GC & -\mathbf{k} & \mathbb{0}_{m_s \times m_s^2} & \mathbf{k}Q_d^{-1}Q_c \\ \beta LGC & \mathbb{0}_{m_s^2 \times m_s} & \mathbb{0}_{m_s^2 \times m_s^2} & \beta L \\ -\beta LGC & \mathbb{0}_{m_s^2 \times m_s} & -\alpha I_{m_s^2} & -\alpha I_{m_s^2} - \beta L \end{bmatrix} \begin{bmatrix} \mathbf{x} \\ \boldsymbol{\xi} \\ \mathbf{q} \\ \mathbf{p} \end{bmatrix} + \begin{bmatrix} BHQ_d^{-1} \\ \mathbb{0}_{m_s \times m_s} \\ \mathbb{0}_{m_s^2 \times m_s} \\ \mathbb{0}_{m_s^2 \times m_s} \end{bmatrix} \mathbf{b} \tag{8-20}$$

8-2 Numerical example

To conclude this section we revisit the numerical example from Section 6-4 and Section 7-3. Where we take the game graph topology as $A_{\mathcal{G}_\theta} = (\mathbb{1}_N \mathbb{1}_N^\top - I_N)$ and the communication topology equal to that of Equation (7-40). We once more set

$$Q_d = 5I_N \quad (8\text{-}21a)$$
$$Q_c = 2\text{diag}(A_{\mathcal{G}_\theta}\mathbb{1}_N)^{-1}A_{\mathcal{G}_\theta} \quad (8\text{-}21b)$$
$$\mathbf{b} = 5\mathbb{1}_N \quad (8\text{-}21c)$$

and take the same initial state values. For the consensus parameters we take $\alpha = 1$ and $\beta = 2$. With the system being equal to that of Section 6-4 (with the exception of $A_{\mathcal{G}_c}$), we find the same Nash equilibrium, being $\mathbf{y}^\star = \frac{5}{3}\mathbb{1}_N$. Also due to this similarity we will include the results shown in Figure 6-2, referred to as y_{ref}. This leads to the following figure, Figure 8-1:

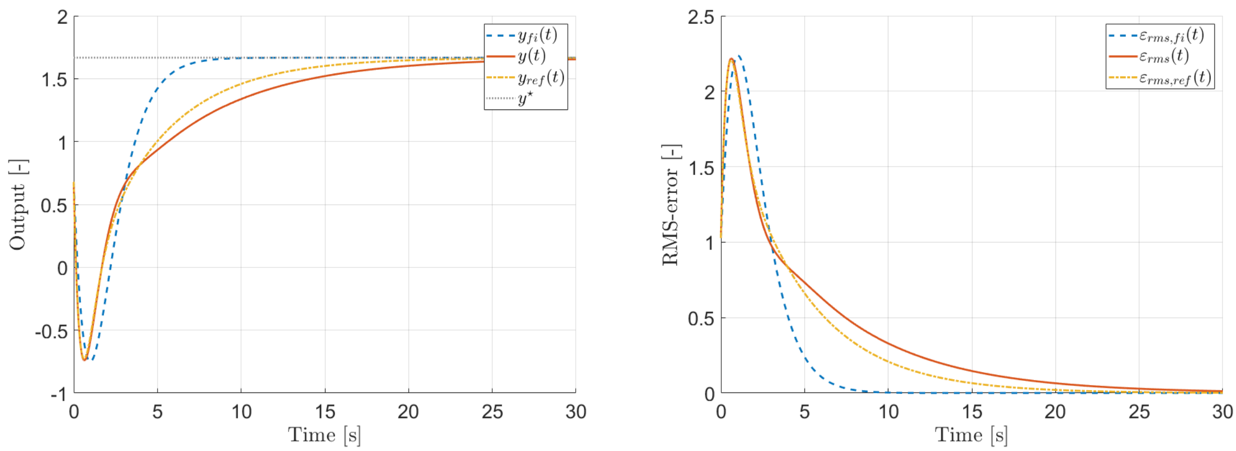

Figure 8-1: Response of a networked game of $N = 10$ agents, subject to linear state-space dynamics whilst aiming to minimize a linear-quadratic cost function with limited communication by means of a local first order reference control law with state feedback. The left panel shows the transient response of agent 1 (red solid line), as well as its Nash equilibrium (black dotted), and the full information control (blue dashed). The right panel depicts the sum of the errors of all agents with respect to the Nash equilibrium (red solid line) as well as the error in case of full information control (blue dashed).

Part III

Case study: applying the main results on an illustrative wind farm model

Chapter 9

Wind farm case study: implementing the main results on an illustrative example

As an illustrative case study to demonstrate the results found in this research, we will discuss the dynamics and power generation of a wind turbine farm. The wind farm consists of multiple pitch controlled turbines [18], [19], of which the power generated depends on the wind speed and pitch angle of the turbine blades [20], [21]. This chapter will go into details of power generated and the dynamics of the individual turbines. A desired operating state will be defined by determining the power generated and the stresses on the system. The model will be linearised around this operating point, and the system dynamics will be modelled accordingly. In the last section of this chapter we provide a few design goals and propose multiple cost functions that aim to fulfil these goals.

9-1 Power model: finding the desired turbine operating state

This section will provide insights into the power model of the wind turbines. We do so by introducing a certain power coefficient dependent on the blade pitch and angular velocity of the turbine blades, $C_p(\psi, \omega)$. We find the generated power as

$$P_{wt} = \tfrac{1}{2}\rho A v^3 C_p(\psi, \omega) \tag{9-1}$$

where ρ is the air density, $A = \pi R^2$ the area swept by the turbine blades with blade length R, and v is the incoming wind speed.

Using the coefficient equation from [20], [22] as a basis, we find values for $C_p(\psi, \omega)$ calculated as

$$C_p(\psi, \omega) = 0.5176\,(116\Omega(\omega) - 0.4\psi - 5)\,e^{-21\Omega(\omega)} + 6.8 \cdot 10^{-3}\frac{\omega R}{v} \tag{9-2}$$

with

$$\Omega(\omega) = \frac{v}{\omega R + 0.08\psi v} - \frac{0.035}{\psi^3 + 1} \tag{9-3}$$

With an incoming wind speed of $v = 15m/s$, blade length $R = 55m$, and air density $\rho = 1.225kg/m^3$, this results in the surface plot shown in Figure 9-1.

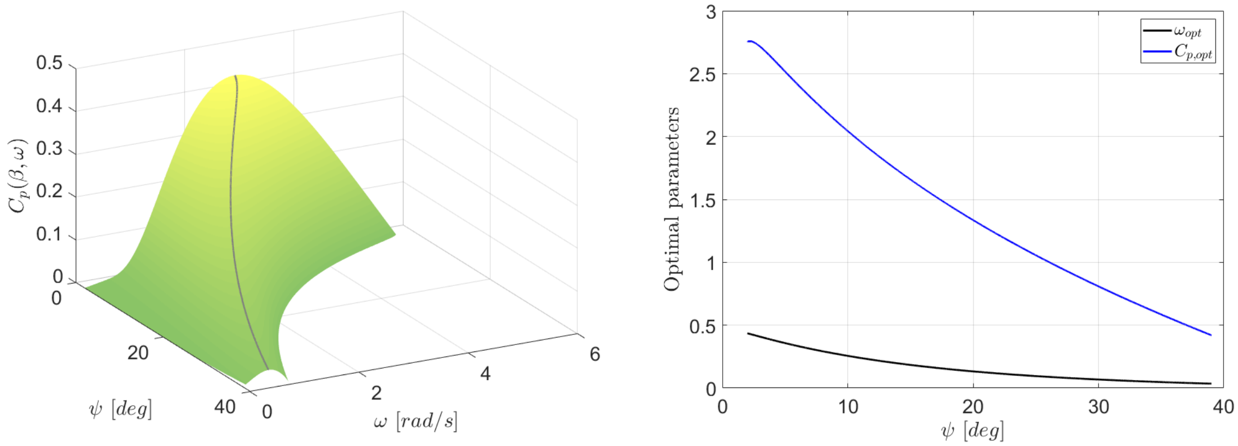

Figure 9-1: Left: Power coefficient $C_p(\psi, \omega)$ as a function of pitch angle ψ and angular velocity ω. The solid grey line denotes the angular velocity that maximizes the power coefficient given a certain blade pitch. Right: Maximizing angular velocity ω and power coefficient $C_p(\psi, \omega)$ as a function of pitch angle ψ.

Given a certain blade pitch ψ, we find an angular velocity that maximizes the power coefficient as depicted in Figure 9-1 (left). The resulting angular velocities and power coefficients are shown in Figure 9-1 (right).

Each of the turbines has a certain trade-off between maximizing the generated power and minimizing the stress on the system. Seeing how the incoming power is proportional to the the wind speed cubed, $\propto v^3$, we base the mechanical strain of the system on the angular velocity cubed, ω_{opt}^3. Furthermore the power generated is of interest, $C_{p,opt}$, as well as the ratio between angular velocity and power generated $\frac{C_{p,opt}}{\omega_{opt}}$. We normalize the angular velocity and power coefficient by dividing them with their maximum values, $\bar{C}_{p,opt} = \frac{C_{p,opt}}{C_{p,opt,max}}$, $\bar{\omega}_{opt} = \frac{\omega_{opt}}{\omega_{opt,max}}$ and find the trade-off function:

$$tradeoff = w_1 \frac{\bar{C}_{p,opt}}{\bar{\omega}_{opt}} + w_2 \bar{C}_{p,opt} - w_3 \bar{\omega}_{opt}^3 \tag{9-4}$$

We take arbitrary values for the trade-off weights; $w_1 = 1.5$, $w_2 = 0.5$, $w_3 = 1.2$. As a result the desired pitch angle, angular velocity and power coefficient are equal to

$$\psi_{des} = 12.78^\circ \tag{9-5a}$$

$$\omega_{des} = 1.82\ rad/s \tag{9-5b}$$

$$C_{p,des} = 0.213 \tag{9-5c}$$

Ultimately we possibly want to control the turbines by providing a reference power, where the blade pitch and angular velocity change according to Figure 9-1 (right). We linearise around the desired states and find

$$\omega(\psi) = \omega_{des} - 0.076(\psi - \psi_{des}) \tag{9-6a}$$
$$C_p(\psi) = C_{p,des} - 0.014(\psi - \psi_{des}) \tag{9-6b}$$

In view of Equation (9-1), the given values for the parameters, and by introducing $P_{wt,des} = \frac{1}{2}\rho A v^3 C_{p,des} = 4.185 \cdot 10^6 W$ we find

$$P_{wt}(\psi) = 1.965 \cdot 10^7 C_p(\psi) = P_{wt,des} - 2.75 \cdot 10^5(\psi - \psi_{des}) \tag{9-7}$$

Hence, given a reference power $\bar{P}_{wt}$ we find the reference blade pitch and angular velocities:

$$\bar{\psi}(\bar{P}_{wt}) = \psi_{des} - 15.218 \frac{\bar{P}_{wt} - P_{wt,des}}{P_{wt,des}} \tag{9-8a}$$
$$\bar{\omega}(\bar{P}_{wt}) = \omega_{des} + 1.157 \frac{\bar{P}_{wt} - P_{wt,des}}{P_{wt,des}} \tag{9-8b}$$

And given a turbine state (ψ, ω) we find the ideal power by again linearising around the desired state:

$$P_{wt}(\psi, \omega) = \frac{1}{2}\rho A v^3 C_p(\bar{\psi}, \bar{\omega}) \tag{9-9a}$$
$$= \frac{1}{2}\rho A v^3 \left(C_{p,des} - 0.014(\psi - \psi_{des}) + 4.15 \cdot 10^{-4}(\omega - \omega_{des})\right) \tag{9-9b}$$
$$= P_{wt,des} - 2.75 \cdot 10^5(\psi - \psi_{des}) + 8.15 \cdot 10^3(\omega - \omega_{des}) \tag{9-9c}$$

9-2 Turbine dynamics: defining the turbine state-space model

With the desired operating point of the turbine defined, we can discuss the turbine dynamics around this point. We view the pitch dynamics and angular dynamics as two separate systems, defined as

$$J_\omega \dot{\omega} + c_\omega \omega = c_\omega \omega_{des} + T_\omega \tag{9-10a}$$
$$J_\psi \ddot{\psi} + c_\psi \dot{\psi} = T_\psi \tag{9-10b}$$

where T_ψ and T_ω are the control torques that aim to steer the turbine to its desired state, where $c_\omega \omega_{des}$ accounts for the steady state offset of T_ω. We define $\delta\psi = \psi - \psi_{des}$,

$\delta\omega = \omega - \omega_{des}$, and find

$$\begin{bmatrix}\dot{\omega}\\ \dot{\psi}\\ \ddot{\psi}\end{bmatrix} = \begin{bmatrix}-\frac{c_\omega}{J_\omega} & 0 & 0\\ 0 & 0 & 1\\ 0 & 0 & -\frac{c_\psi}{J_\psi}\end{bmatrix}\begin{bmatrix}\delta\omega\\ \delta\psi\\ \dot{\psi}\end{bmatrix} + \begin{bmatrix}\frac{1}{J_\omega} & 0\\ 0 & 0\\ 0 & \frac{1}{J_\psi}\end{bmatrix}\begin{bmatrix}T_\omega\\ T_\psi\end{bmatrix} \tag{9-11a}$$

$$P_{wt} = \begin{bmatrix}8.15\cdot 10^3 & -2.75\cdot 10^5 & 0\end{bmatrix}\begin{bmatrix}\delta\omega\\ \delta\psi\\ \dot{\psi}\end{bmatrix} + P_{wt,des} \tag{9-11b}$$

where we additionally take $J_\omega = 6.3{\cdot}10^6 kgm^2$ ([21]), $J_\psi = .01 J_\omega$, and $c_\omega = 1{\cdot}10^3 kgm^2/s$, $c_\psi = 100 kgm^2/s$. This leads to the following dynamics:

$$\begin{bmatrix}\dot{\omega}\\ \dot{\psi}\\ \ddot{\psi}\end{bmatrix} = \begin{bmatrix}-1.587\cdot 10^{-4} & 0 & 0\\ 0 & 0 & 1\\ 0 & 0 & -1.587\cdot 10^{-3}\end{bmatrix}\begin{bmatrix}\delta\omega\\ \delta\psi\\ \dot{\psi}\end{bmatrix} + \begin{bmatrix}1.587\cdot 10^{-7} & 0\\ 0 & 0\\ 0 & 1.587\cdot 10^{-5}\end{bmatrix}\begin{bmatrix}T_\omega\\ T_\psi\end{bmatrix} \tag{9-12a}$$

$$P_{wt} = \begin{bmatrix}8.15\cdot 10^3 & -2.75\cdot 10^5 & 0\end{bmatrix}\begin{bmatrix}\delta\omega\\ \delta\psi\\ \dot{\psi}\end{bmatrix} + 4.185\cdot 10^6 \tag{9-12b}$$

which can be represented with the following state-space system:

$$\dot{x} = Ax + Bu \tag{9-13a}$$

$$y = Cx \tag{9-13b}$$

$$P = Dy + d \tag{9-13c}$$

with $x = [\delta\omega, \delta\psi, \dot{\psi}]^\top$, $y = [\delta\omega, \delta\psi]^\top$, and $u(y, P) = [T_\omega, T_\psi]^\top$. And with:

$$A = \begin{bmatrix}-1.587\cdot 10^{-4} & 0 & 0\\ 0 & 0 & 1\\ 0 & 0 & -1.587\cdot 10^{-3}\end{bmatrix} \tag{9-14a}$$

$$B = \begin{bmatrix}1.587\cdot 10^{-7} & 0\\ 0 & 0\\ 0 & 1.587\cdot 10^{-5}\end{bmatrix} \tag{9-14b}$$

$$C = \begin{bmatrix}1 & 0 & 0\\ 0 & 1 & 0\end{bmatrix} \tag{9-14c}$$

$$D = \begin{bmatrix}8.15\cdot 10^3 & -2.75\cdot 10^5\end{bmatrix} \tag{9-14d}$$

$$d = 4.185\cdot 10^6 \tag{9-14e}$$

9-3 Turbine wake: power losses due to wind disturbances

The model from Equation (9-12) describes a singular, isolated wind turbine. However when discussing the power output of a wind farm, the turbines have a certain influence on the aerodynamics. In fact, each turbine generates a wake in which the wind properties are less favourable (reduced wind speed, increased turbulence). As an illustration, a depiction of such a wake and the resulting loss of potential power can be seen in Figure 9-4.

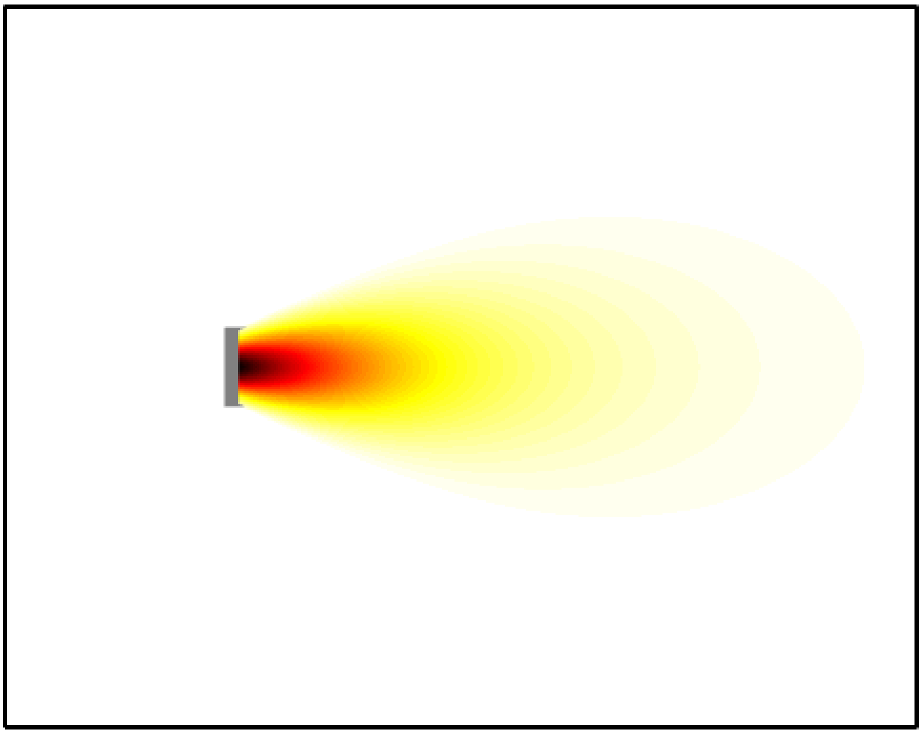

Figure 9-2: The wake generated by a wind turbine. The wind direction is from left to right, the turbine (grey line) disturbs the air flow and results in a decrease of potential power.

To model this loss of power we define an efficiency factor $\eta \in \mathbb{R}$ with $0 < \eta < 1$. In practice this term is a function of the power generated by the turbine, where an increase in power generated results in an increase of wind disturbance [23], [24]. However we discuss this as a fixed parameter in view of the otherwise high complexity. As such the dynamics of an individual turbine v will be

$$\dot{x}_v = A_v x_v + B_v u_v \tag{9-15a}$$

$$y_v = C_v x_v \tag{9-15b}$$

$$P_v = \eta_v \left(D_v y_v + d_v \right) \tag{9-15c}$$

Due to this loss of efficiency, we note that the turbines can no longer operate at their desired state with $\psi = \psi_{des}$, $\omega = \omega_{des}$, and $P_{wt} = P_{wt,des}$.

As stated, the efficiency factor is a function of the power generated by the turbine. The more power the turbine generates, the higher the influence of the turbine on the wind flow. This causes more turbulence and as a result decreases the potential of the neighbouring turbines in its wake. In the following section we introduce cross-turbine cost functions to compensate for this behaviour, without the need for explicit information about the aerodynamics around the turbine.

9-4 Cross-turbine interactions: defining cost functions to reach global wind farm goals

The overarching goal of the wind farm is to have each of the N turbines operate under favourable conditions whilst still reaching a desirable power output. We first define a cost function that aims to even out all power generated by the individual wind turbines. This ensures that the turbines do not operate selfishly and as a result stubbornly stay at their desired angular velocity and pitch angle, $y_v = y_{v,des}$. The idea is for the turbines with most favourable conditions to lower their power output such that the neighbouring turbines have more power potential (in practice; not modelled here).

Equalizing individual power outputs

With the goal of having each of the turbines operate under similar conditions, we propose local cost functions that steer the powers generated to a global average. These functions are dependent on the neighbours of the turbines, and keep the local desired state in mind. We propose the following cost function:

$$\theta_v(y_v, P_v, P_{-v}) = \theta_{1,v}(y_v) + \theta_{2,v}(y_v, P_v, P_{-v}) \tag{9-16}$$

where the first function $\theta_{1,v}(y_v)$ aims to minimize the local cost of operating around the desired sate. The second cost function $\theta_{2,v}(y_v, P_v, P_{-v})$ ensures that the individual turbines cooperate in their power generation. If one of the turbines generates most of the power compared to the other turbines, this function aims to reduce its output.

We define a linear-quadratic form of the cost function from Equation (9-16) as:

$$\theta_v(y_v, P_v, P_{-v}) = \tfrac{1}{2} y_v^\top Q_{d,v} y_v - \sum_{j \in \mathcal{N}_v} (D_v y_v)^\top F_{c,v,j}(P_j - P_v) \tag{9-17}$$

Since the value for η_v is not explicitly known we do not know the relation between y_v and P_v. As such we will take P_v as a given value and determine the derivative of the cost-function with respect to y_v alone. This leads to a best response of:

$$\bar{y}_v = Q_{d,v}^{-1} \sum_{j \in \mathcal{N}_v} D_v^\top F_{c,v,j}(P_j - P_v) \tag{9-18}$$

We take $D = \text{blockdiag}(D_1, \cdots, D_N)$ and define

$$Q_d = \begin{bmatrix} Q_{d,1} & \mathbb{0} & \mathbb{0} & \cdots & \mathbb{0} \\ \mathbb{0} & Q_{d,2} & \mathbb{0} & \cdots & \mathbb{0} \\ \mathbb{0} & \mathbb{0} & Q_{d,3} & \cdots & \mathbb{0} \\ \vdots & \vdots & \vdots & \ddots & \vdots \\ \mathbb{0} & \mathbb{0} & \mathbb{0} & \cdots & Q_{d,N} \end{bmatrix}, \quad F_c = \begin{bmatrix} \mathbb{0} & F_{c,1,2} & F_{c,1,3} & \cdots & F_{c,1,N} \\ F_{c,2,1} & \mathbb{0} & F_{c,2,3} & \cdots & F_{c,2,N} \\ F_{c,3,1} & F_{c,3,2} & \mathbb{0} & \cdots & F_{c,3,N} \\ \vdots & \vdots & \vdots & \ddots & \vdots \\ F_{c,N,1} & F_{c,N,2} & F_{c,N,3} & \cdots & \mathbb{0} \end{bmatrix} \tag{9-19}$$

and find the best overall response with $P = [P_1, \dots, P_N]^\top$ of

$$\bar{\mathbf{y}} = Q_d^{-1} D^\top F_c P - Q_d^{-1} D^\top \mathrm{diag}(F_c \mathbb{1}_N) P \tag{9-20a}$$
$$= Q_d^{-1} D^\top \left(F_c - \mathrm{diag}(F_c \mathbb{1}_N)\right) P \tag{9-20b}$$
$$= Q_d^{-1} Q_c P \tag{9-20c}$$

With $Q_c = D^\top \left(F_c - \mathrm{diag}(F_c \mathbb{1}_N)\right)$. Furthermore we find the Nash equilibrium of the cost function by taking the optimum power as $P^\star = \boldsymbol{\eta}\left(D\mathbf{y}^\star + \mathbf{d}\right)$ with $\boldsymbol{\eta} = \mathrm{diag}(\eta_1, \dots, \eta_N)$ and $\mathbf{d} = [d_1, \dots, d_N]^\top$. Thus we find

$$\mathbf{y}^\star = Q_d^{-1} Q_c \boldsymbol{\eta}\left(D\mathbf{y}^\star + \mathbf{d}\right) \tag{9-21}$$

By isolating the $\mathbf{y}^\star$ terms we find:

$$\mathbf{y}^\star = \left(Q_d - Q_c \boldsymbol{\eta} D\right)^{-1} Q_c \boldsymbol{\eta} \mathbf{d} \tag{9-22}$$

Reaching a global power goal

The function from Equation (9-16) causes the turbines to operate under similar power outputs whilst not diverging too far from their own desired state. However, the outcome of the cost function does not consider the total power generated. Instead the focus is on the power differences between turbines. When the wind farm has a certain desired amount of total power, say $\sum_{i \in \{1,\dots,N\}} P_i = P_{net}$, the previous cost function will not provide guarantees that this goal is met. This leads us to the following aggregate cost function:

$$\theta_v(y_v, P_v, \mathrm{avg}P) = \tfrac{1}{2} y_v^\top Q_{d,v} y_v - (D_v y_v)^\top F_{a,v} \left(\tfrac{1}{N} P_{net} - \mathrm{avg}P\right) \tag{9-23}$$

With this cost function the turbines still consider their own desired operating point whilst also aiming to reach the overarching power goal. Again, we consider the relation between output power P_v and state output y_v to be unknown. As such we take the derivative with respect to y_v and set it to zero. Doing so will yield us the following overall best response:

$$\bar{\mathbf{y}} = Q_d^{-1} D^\top F_a \mathbb{1}_N \left(\tfrac{1}{N} P_{net} - \mathrm{avg}P\right) \tag{9-24a}$$
$$= Q_d^{-1} Q_a \mathbb{1}_N \left(\tfrac{1}{N} P_{net} - \mathrm{avg}P\right) \tag{9-24b}$$

with $F_a = \text{diag}(F_1, \dots, F_N)$ and $Q_a = D^\top F_a$. We take the optimum power as $P^\star = \boldsymbol{\eta}\left(D\mathbf{y}^\star + \mathbf{d}\right)$ and find the Nash equilibrium as:

$$\mathbf{y}^\star = Q_d^{-1} Q_a \mathbb{1}_N \left(\tfrac{1}{N} P_{net} - \text{avg}\left(\boldsymbol{\eta}\left(D\mathbf{y}^\star + \mathbf{d}\right)\right)\right) \tag{9-25a}$$

$$= Q_d^{-1} Q_a \mathbb{1}_N \left(\tfrac{1}{N} P_{net} - \tfrac{1}{N}\mathbb{1}_N^\top \boldsymbol{\eta}\left(D\mathbf{y}^\star + \mathbf{d}\right)\right) \tag{9-25b}$$

$$\tag{9-25c}$$

By isolating the $\mathbf{y}^\star$ terms we get:

$$\mathbf{y}^\star = \left(NQ_d + Q_a \mathbb{1}_N \mathbb{1}_N^\top \boldsymbol{\eta} D\right)^{-1} Q_a \mathbb{1}_N \left(P_{net} - \mathbb{1}_N^\top \boldsymbol{\eta}\mathbf{d}\right) \tag{9-26}$$

We note that this cost function will simply distort all turbines from their desired state by equal amounts. As a result the most efficient turbine accounts for most of the power demand, which is undesirable. This motivates the following aggregate cost function with local cost:

$$\begin{aligned}\theta_v(y_v, P_v, P_{-v}, \text{avg}P) = \tfrac{1}{2} y_v^\top Q_{d,v} y_v - (D_v y_v)^\top F_{a,v}\left(\tfrac{1}{N} P_{net} - \text{avg}P\right) \\ - \sum_{j \in \mathcal{N}_v} (D_v y_v)^\top F_{c,v,j}(P_j - P_v)\end{aligned} \tag{9-27}$$

With a best response of:

$$\bar{\mathbf{y}} = Q_d^{-1} Q_a \left(\tfrac{1}{N}\mathbb{1}_N P_{net} - \text{avg}P\right) + Q_d^{-1} Q_c P \tag{9-28}$$

and a Nash equilibrium of:

$$\mathbf{y}^\star = \left(NQ_d - NQ_c \boldsymbol{\eta} D + Q_a \mathbb{1}_N \mathbb{1}_N^\top \boldsymbol{\eta} D\right)^{-1} \left(NQ_c \boldsymbol{\eta}\mathbf{d} + Q_a \mathbb{1}_N \left(P_{net} - \mathbb{1}_N^\top \boldsymbol{\eta}\mathbf{d}\right)\right) \tag{9-29}$$

Combining both approaches from Equation (9-17) and Equation (9-23), this function considers the selfish goal to operate at the desired state, the cost on generating a disproportionate amount of power compared to the turbine's neighbours, as well as the global power demand.

9-5 Results: turbine performances in a static case

This section will discuss the results given values for the cost functions. Specifically we need to set values for the efficiencies η_v, local costs $Q_{d,v}$, the cross-agent costs $F_{c,v,j}$ and the cost on the total power output $F_{a,v}$. To do so we will first define the wind farm topology. We take $N = 10$ homogenous turbines which are subject to the following communication graph:

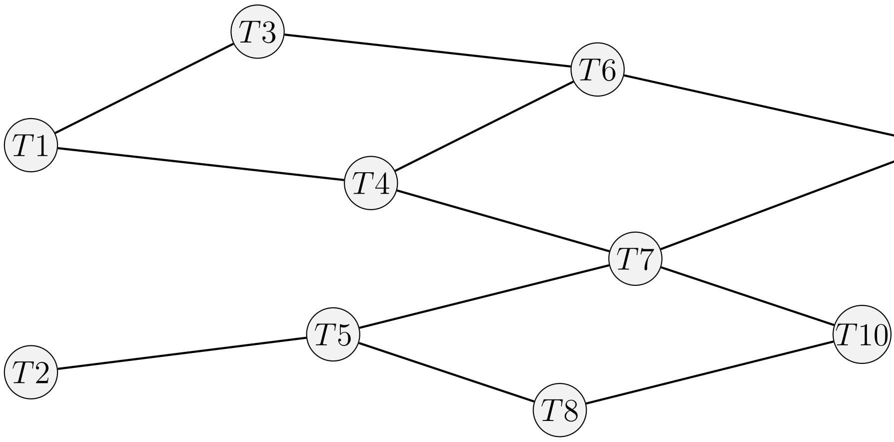

Figure 9-3: Communication graph topology of the wind farm with $N = 10$ turbines (nodes T1 to T10) and communication links (edges).

We take the wind direction in Figure 9-3 from left to right. This results in the graphical representation of the collective wind wake depicted in Figure 9-4.

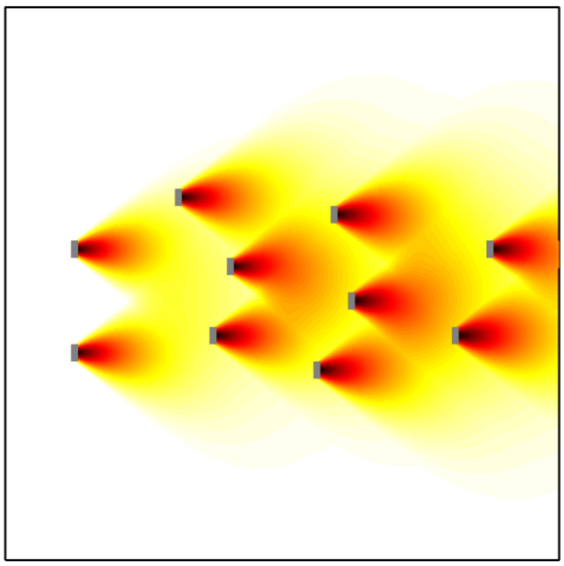

Figure 9-4: The wake generated by the wind farm. The wind direction is from left to right, the turbines (grey lines) disturb the air flow and result in a decrease of potential power.

We use this resulting wake and find a set of efficiency factors η_v equal to:

$\eta_{T1} = 1$	$\eta_{T5} = 0.8339$	$\eta_{T9} = 0.7741$
$\eta_{T2} = 1$	$\eta_{T6} = 0.7721$	$\eta_{T10} = 0.6820$
$\eta_{T3} = 0.8906$	$\eta_{T7} = 0.7177$	
$\eta_{T4} = 0.8609$	$\eta_{T8} = 0.7965$	

From the communication graph we also obtain the row-stochastic adjacency matrix, equal to

$$A_{\mathcal{G}_c} = \begin{bmatrix} 0 & 0 & 1 & 1 & 0 & 0 & 0 & 0 & 0 & 0 \\ 0 & 0 & 0 & 0 & 1 & 0 & 0 & 0 & 0 & 0 \\ 1 & 0 & 0 & 0 & 0 & 1 & 0 & 0 & 0 & 0 \\ 1 & 0 & 0 & 0 & 0 & 1 & 1 & 0 & 0 & 0 \\ 0 & 1 & 0 & 0 & 0 & 0 & 1 & 1 & 0 & 0 \\ 0 & 0 & 1 & 1 & 0 & 0 & 0 & 0 & 1 & 0 \\ 0 & 0 & 0 & 1 & 1 & 0 & 0 & 0 & 1 & 1 \\ 0 & 0 & 0 & 0 & 1 & 0 & 0 & 0 & 0 & 1 \\ 0 & 0 & 0 & 0 & 0 & 1 & 1 & 0 & 0 & 0 \\ 0 & 0 & 0 & 0 & 0 & 0 & 1 & 1 & 0 & 0 \end{bmatrix} \tag{9-30}$$

For the cost matrices we take $Q_{d,1} = \cdots = Q_{d,N} = \text{diag}(50, 100)$, $F_{c,v,j} = 0.01 d_v^{-1}$ for all $j \in \mathcal{N}_v$ and zero otherwise, $F_{a,v} = d_v^{-1}$, and $P_{net} = 1.1 \cdot \mathbb{1}_N^\top \mathbf{d}$. Note that with $d_1 = \cdots = d_N$ it holds that $F_c = 0.01 d_v^{-1} A_{\mathcal{G}_c}$. We define the following four cost functions as introduced in the previous section:

$$\theta_1 = \tfrac{1}{2} y_v^\top Q_{d,v} y_v \tag{9-31a}$$

$$\theta_2 = \tfrac{1}{2} y_v^\top Q_{d,v} y_v - \sum_{j \in N} (D_v y_v)^\top F_{c,v,j} (P_j - P_v) \tag{9-31b}$$

$$\theta_3 = \tfrac{1}{2} y_v^\top Q_{d,v} y_v - (D_v y_v)^\top F_{a,v} \left(\tfrac{1}{N} P_{net} - \text{avg} P \right) \tag{9-31c}$$

$$\theta_4 = \tfrac{1}{2} y_v^\top Q_{d,v} y_v - (D_v y_v)^\top F_{a,v} \left(\tfrac{1}{N} P_{net} - \text{avg} P \right) - \sum_{j \in \mathcal{N}_v} (D_v y_v)^\top F_{c,v,j} (P_j - P_v) \tag{9-31d}$$

With the Nash equilibria as defined in Equation (9-22), Equation (9-26), and Equation (9-29) for θ_2, θ_3 and θ_4 respectively. As a result we obtain the output powers as depicted in Figure 9-5.

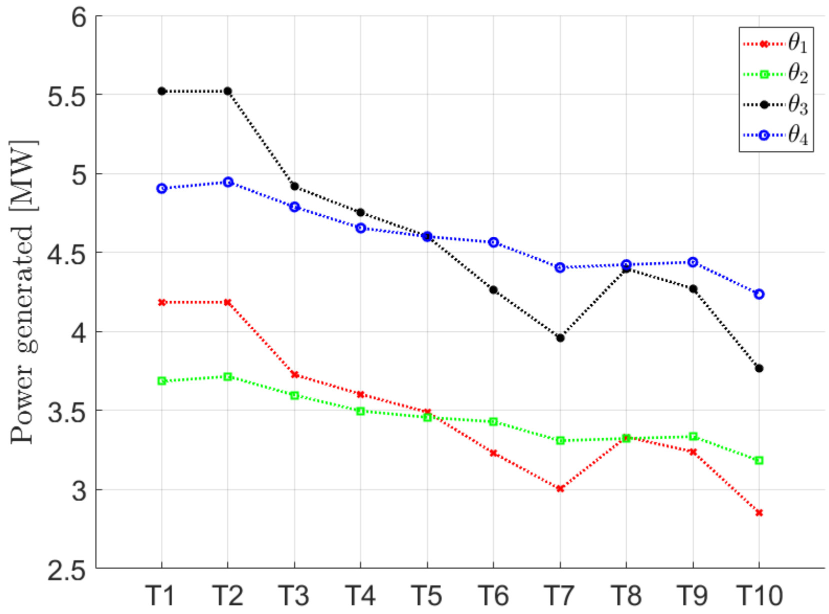

Figure 9-5: Output powers for the wind farm as a result of the Nash equilibria solving Equation (9-31), for θ_1 (red cross), θ_2 (green square), θ_3 (black dot), θ_4 (blue circle).

From Figure 9-5 we note that indeed introducing the cross terms by means of F_c (green square) results in the output powers tending more to the average powers compared to a selfish approach (red cross). Furthermore the system indeed increases the overall power generated to reach the global power goal P_{net}. We find the divergence of the sum of output powers for cost functions θ_3 and θ_4 equal to:

$$\frac{\mathbb{1}_N^\top P_{\theta_3} - P_{net}}{P_{net}} = -1.6008 \cdot 10^{-3}$$
$$\frac{\mathbb{1}_N^\top P_{\theta_4} - P_{net}}{P_{net}} = -1.6614 \cdot 10^{-3}$$

This error in power is sufficiently small, but can be decreased even further by increasing the values of $F_{a,v}$. We keep the earlier mentioned values in view of the already low error rate. With the Nash equilibria having desired values, we can introduce the dynamics to the system and discuss the convergence rates of the different cost functions.

9-6 Results: convergence to the equilibrium in a dynamic case

In this section we add the system dynamics to the model and aim to steer the turbines to the Nash equilibria. First we will define the state-feedback matrices K_v that aim to stabilize the individual turbine dynamics. As defined in Section 9-2, the state-space matrices are equal to:

$$A_v = \begin{bmatrix} -1.587 \cdot 10^{-4} & 0 & 0 \\ 0 & 0 & 1 \\ 0 & 0 & -1.587 \cdot 10^{-3} \end{bmatrix} \tag{9-32a}$$

$$B_v = \begin{bmatrix} 1.587 \cdot 10^{-7} & 0 \\ 0 & 0 \\ 0 & 1.587 \cdot 10^{-5} \end{bmatrix} \tag{9-32b}$$

By taking

$$K_v = \begin{bmatrix} 5 \cdot 10^6 & 0 & 0 \\ 0 & 5 \cdot 10^4 & 2 \cdot 10^5 \end{bmatrix} \tag{9-33}$$

the system will be stabilized with $\text{eig}(A_v - B_v K_v) \in (-2.9022, -0.2734, -0.7937)$. We take the efficiency coefficients and cost functions as defined in Section 9-5. We note that for the cost function in Equation (9-31a) the input torques are set to zero; $\bar{\mathbf{y}} = \mathbb{0}_{2N}$. Furthermore, for Equation (9-31b) we use the model in Figure 6-1 with Equation (9-20), for Equation (9-31c) we use Figure 7-1 with Equation (9-20). Lastly for Equation (9-31d) we use a combination of Figure 6-1 and Figure 7-1 as mentioned in Section 7-2.

For the control parameters k_v we use $k_{1,v} = 2 \cdot 10^{-2}$ for Equation (9-31a), $k_{2,v} = 2 \cdot 10^{-2}$ for Equation (9-31b), $k_{3,v} = 3 \cdot 10^{-3}$ for Equation (9-31c), and $k_{4,v} = 2 \cdot 10^{-3}$ for Equation (9-31d). Furthermore we set the consensus parameters $\alpha = 200$ and $\beta = 100$. This yields the following transient responses of the powers generated by the individual turbines:

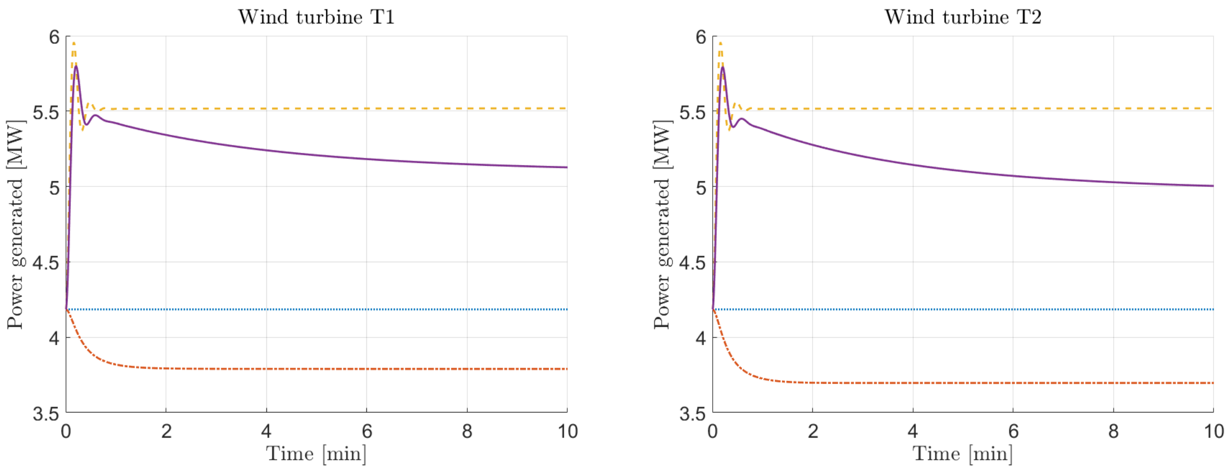

Figure 9-6: Powers generated by wind turbines $T1$ and $T2$ as labelled in Figure 9-3 with the cost functions as defined in Equation (9-31), specifically θ_1 (blue dotted), θ_2 (red dash-dotted), θ_3 (yellow dashed), and θ_4 (purple solid).

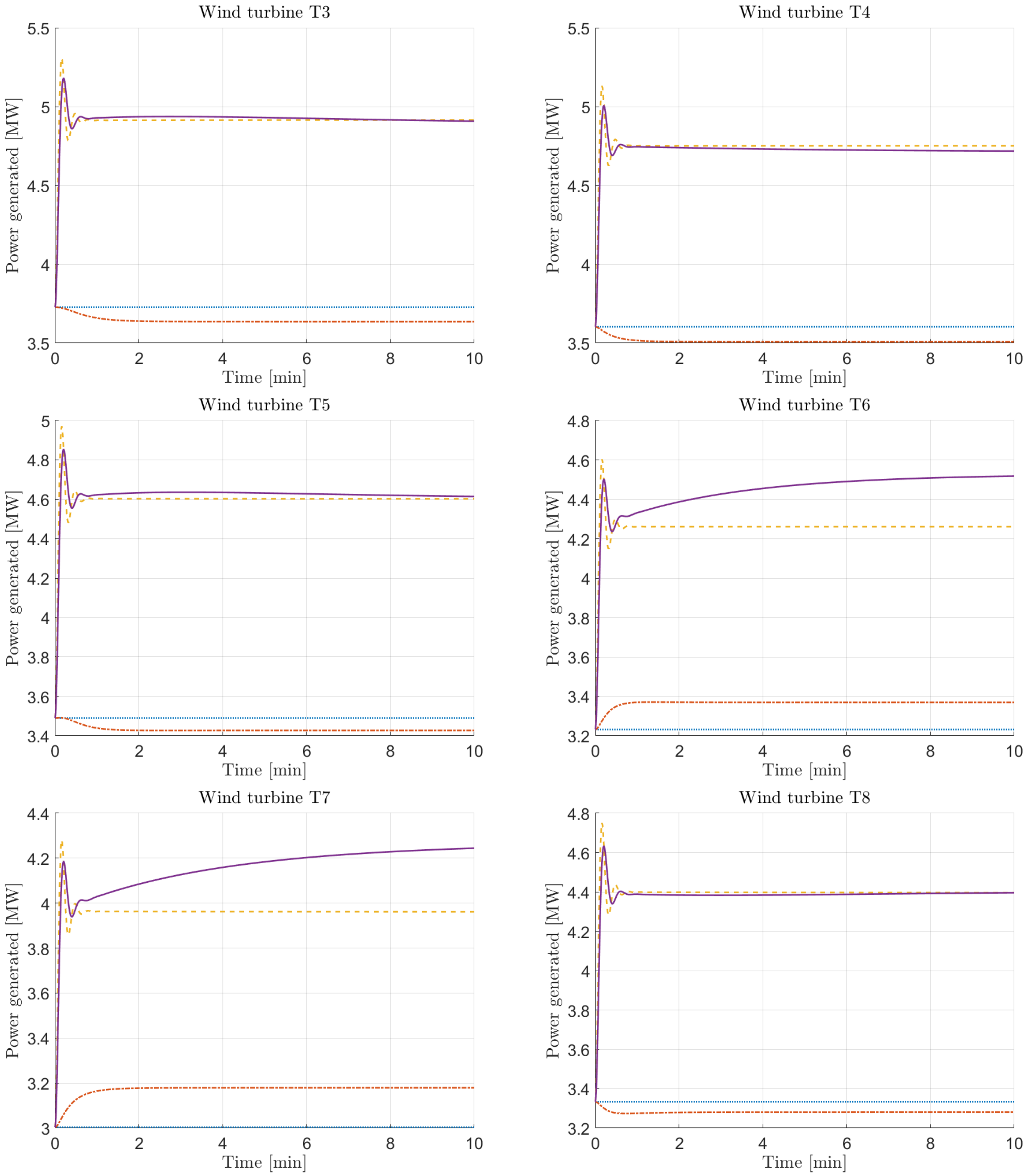

Figure 9-7: Powers generated by wind turbines $T3$ through $T8$ as labelled in Figure 9-3 with the cost functions as defined in Equation (9-31), specifically θ_1 (blue dotted), θ_2 (red dash-dotted), θ_3 (yellow dashed), and θ_4 (purple solid).

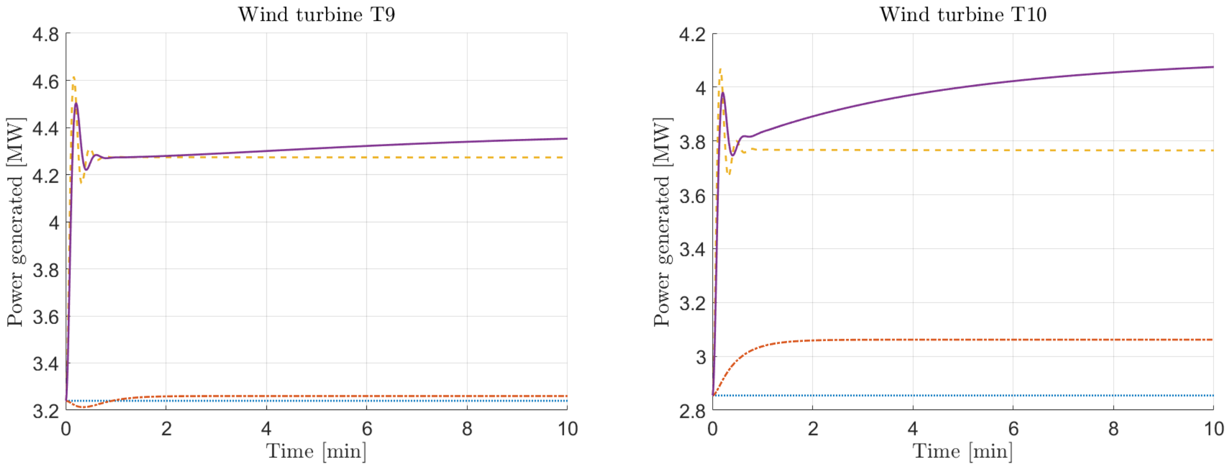

Figure 9-8: Powers generated by wind turbines $T9$ through $T10$ as labelled in Figure 9-3 with the cost functions as defined in Equation (9-31), specifically θ_1 (blue dotted), θ_2 (red dash-dotted), θ_3 (yellow dashed), and θ_4 (purple solid).

As another metric to represent the results, we introduce the RMS error of the turbines. With $P(t)$ as the power vector at a given time t, and $P^\star$ as the power resulting from the Nash equilibrium of the cost functions from Equation (9-31), the RMS error is given by:

$$\varepsilon_{RMS} = \sqrt{\frac{1}{N}(P(t) - P^\star)^\top (P(t) - P^\star)} \tag{9-34}$$

We apply this error function on the transient power responses as a result of cost functions from Equation (9-31). These results are shown in Figure 9-9.

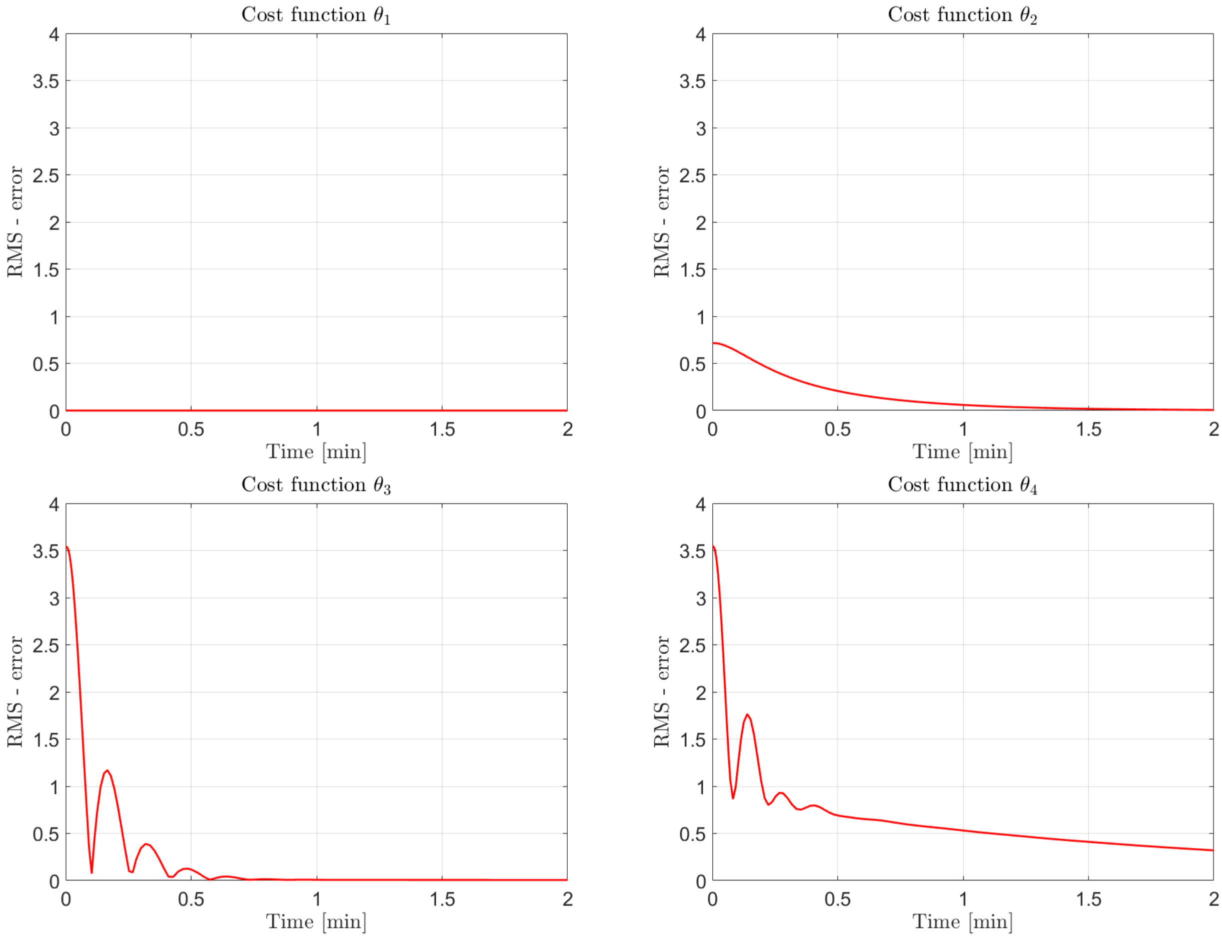

Figure 9-9: RMS error as defined in Equation (9-34) of the turbines from Figure 9-3 subject to the cost functions from Equation (9-31). With the optimal powers $P^\star$ as shown in Figure 9-5.

As can be seen from Figures 9-6 to 9-9, the turbines asymptotically reach the Nash equilibrium. As such the trade-off between generating power and reducing stresses on the turbines is down to the tuning of the cost function parameters. The initially complex system of the wind farm is reduced to the design of interpretable cost function matrices for the individual turbines.

Part IV

Conclusion and recommendations

Chapter 10

Discussion

This chapter will briefly discuss the findings from this research. In the previous chapter we provided numerical results for the proposed controllers. These results are quite promising when compared to the ideal cases, seeing how the controllers have only a slightly slower convergence rate. With these findings complex problems can be solved simply by tuning insightful cost function parameters. This can be observed in the wind farm case study from Chapter 9, where an increase of $Q_{d,v}$ leads to a more selfish approach whereas a decrease leads to a cooperative networked system.

The results from Part II also are as expected, where the systems subject to more general assumptions (hence systems with less ideal circumstances) have a higher settling time.

However, proofs for the convergence rate are left as a future study. Without these proofs there might be certain system dynamics or cost function models in which the controllers function poorly. This problem arises specifically when it comes to the design of control parameter $\mathbf{k}$, seeing how merely the existence of an appropriate $\mathbf{k}$ is discussed and not how to design $\mathbf{k}$.

Furthermore the results are not tested in practice, where the addition of noise or information distribution limitations might pose difficulties. We left these topics out of the scope of this research, seeing how it mostly applies to decentralized consensus and estimation methods.

Chapter 11

Conclusion

In this thesis we discussed the problem of steering a multi-agent game to its Nash equilibrium given that the individual agents are subject to intrinsic dynamics; we defined this problem in Chapter 5. Given the problem definition, in Chapter 6 we started with the initial assumption that all agents have access to the outputs of the agents directly influencing its cost function. We provided a first order reference controller that, using the outputs from the relevant agents, steers all agents to their Nash equilibrium. Stability and convergence proofs were given and a numerical example was done. From the numerical example, Section 6-4 Figure 6-2, we can conclude that the reference controller performs quite well compared to a direct steering to the Nash equilibrium. However, due to each subsystem reacting on the (non-optimal) output of the other systems, the system is subject to a higher overshoot and settling time. It is expected that the system performs worse than a direct steering to the Nash equilibrium, seeing how the latter is an ideal but unrealistic approach.

Chapter 7 dropped the assumption that all agents have access to the outputs that influence their cost function. Instead an aggregate game was introduced, this game consists of cost functions that are based on the average of all outputs. For this we needed to include a continuous time consensus algorithm, as introduced in Chapter 4. We introduced a controller for this problem and provided stability and convergence proofs. We did not include a numerical example for this case, instead we extended the problem by adding local costs to the neighbouring agents. As a result we find a cost function that is dependent directly on the agent output, the neighbouring outputs, and the average of all outputs. We again proved the stabilizability of this new system, and due to the system being analogous to the two preceding systems its convergence is implied. For this extended aggregate game we added a numerical example. Reviewing Section 7-3 Figure 7-3 we can compare the controller from to the full information control. We see that both converge to the Nash equilibrium given enough time. The transient response of the proposed controller is slower than that of the full information control, which is to be expected due to the delays introduced by the consensus algorithm as well as the convergence speed of the best response to the Nash equilibrium.

To extend these findings even further in Chapter 8, we revisit the cost function from

Chapter 6 but instead we let the cost function also be a function of agents which are not direct neighbours. For this we introduced a decentralized estimation algorithm. We provided a convergence proof and found an approach that is similar to that of Chapter 4 as used in Chapter 7. We again included a numerical example Section 8-2, which also contains the results from Section 6-4 due to the analogous cost function. As can be seen from Figure 8-1 the convergence rate of the decentralized estimation is slower than that of the previously found results from Section 6-4. This is to be expected seeing how the system from Chapter 8 is subject to more limiting assumptions.

Concluding the main results, in Part III Chapter 9 we introduced a case study of a wind farm with individual wind turbines as agents. After preliminary system definitions, consisting of power generation models, dynamical models, and cost function definitions, we end up with a model that can be applied to the main results from Part II. As can be seen from Figures 9-6 to 9-9, the network reaches its Nash equilibrium. In other words, applying the relevant controllers from Chapters 6 to 8 the wind farm can be designed to reach a global power output whilst still aiming to minimize turbine strains merely by tuning the cost function parameters $Q_{d,v}$, $F_{c,v,j}$ and $F_{a,v}$.

Chapter 12

Future Challenges

The main results are quite promising, however there are still enough possibilities for future research. In this chapter we will list some of these future recommendations.

Both the dynamics and cost functions were considered to be linear(-quadratic). Although a system can often be linearised around its operating point, extending these findings to non-linear systems and games will make the results more generally applicable. Furthermore we did not include constraints on the inputs, states, or outputs. For both non-linear games and games with constraints, approaches exist to reach the Nash equilibrium. These approaches could provide beneficial results when aiming to extend this research to the non-linear/constrained case.

Furthermore it was assumed that all agents had their own local dynamics, and the only cross-agent interactions exist in the cost functions. This assumption is not too limiting, and having each agent influence the other agents' dynamics can lead to rather complicated systems. However, we still point this one out as a possible follow up study.

A more interesting future research, possibly, is the study of the convergence rates of these approaches. Mainly the influence of the consensus parameters and the definition of the upper-bound of the controller parameter $\mathbf{k}$ can provide useful results.

In view of the controllers being applied to individual agents, the computation limits or controller complexity is also an interesting topic; seeing how the full state estimation from Chapter 8 scales quadratically with the amount of agents.

Lastly, the systems and results are all done for a continuous time case. Hence an interesting follow up study is that of a discrete time approach, where both the system and controllers/estimators are represented by a discrete time model.

Appendix A

Literature review

A-1 Network systems

In this section the concept of network systems will be discussed. Network systems are distributed systems in which a set of participants (agents) interact with each other [1]. An agent in this system only interacts with a set of other agents, called the neighbour set. Water distribution systems are an example of network systems, in which the agents represent the reservoirs and the interaction between agents is done via water flow through pipes between reservoirs. The set of agents and interaction links can be described using a graph, and as such the system can be analysed using findings in the field of graph theory.

Graphs

Graphs are a tool to describe (the interaction within) multi-agent systems; an example of a graph is depicted in Figure A-1. A graph $\mathcal{G}(\mathcal{V}, \mathcal{E})$ consists of a set of n nodes $\mathcal{V} = \{1, 2, \ldots, n\}$ and edges $\mathcal{E} \subseteq \mathcal{V} \times \mathcal{V}$. Furthermore two nodes i and j are neighbours if $\{i, j\} \in \mathcal{E}$, the set of neighbours of node i will be denoted as $\mathcal{N}_i$.

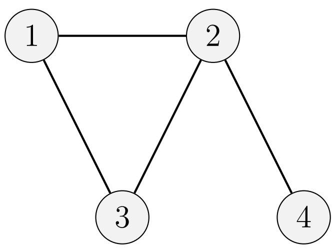

Figure A-1: A graph with 4 nodes and 4 undirected edges.

The graph depicted in Figure A-1 is an example of an undirected graph, in which the edges have no specific direction. In essence if a graph $\mathcal{G}(\mathcal{V}, \mathcal{E})$ is undirected, for all nodes i and j with $i, j \in \mathcal{V}$ it holds that $(i, j) \in \mathcal{E}$ if $(j, i) \in \mathcal{E}$; this is denoted as $\{i, j\} \in \mathcal{E}$ where $\{\cdot, \cdot\}$ relates to an unordered pair. An example of a directed graph (or digraph for short) is shown in Figure A-2. In this example it is clear that an edge from node 2 to node 4 exists, but not vice versa. Note that undirected graphs can be considered a subset of directed graphs.

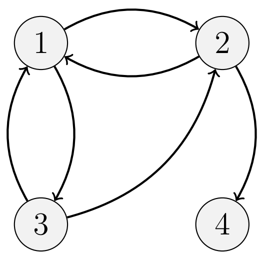

Figure A-2: A directed graph with 4 nodes and 6 directed edges.

Connectivity and periodicity

Two important properties of a graph are its connectivity and periodicity. An undirected graph is connected if for all nodes i and j with $i, j \in \mathcal{V}$ there exists a path from node i to node j, as stated in [25]. Meaning that there is a way to traverse any number of edges to end up on node j, starting from node i. A digraph is strongly connected if for all nodes i and j with $i, j \in \mathcal{V}$ there exists a directed path from node i to node j. It is weakly connected if the undirected version of the digraph is connected. Furthermore, a node i is called a globally reachable node if there exists a path from any other node to node i. Note that for a strongly connected digraph all nodes are globally reachable nodes.

A strongly connected digraph is said to be periodic if the lengths of all cycles (a path starting and ending on the same node) have a common divisor greater than 1. For example, a graph containing only one cycle of any length (larger than 1) is considered periodic. Furthermore a graph containing cycles of, for example, length 6 and 9 is considered periodic since their common divisor is equal to 3. Self-loops are a special type of cycle with length 1. Therefore if any self-loop is present, the resulting graph is aperiodic.

In- and out-degree

The in-degree (out-degree) of a node is equal to the number of ingoing (outgoing) edges of that node [1] [25]. For an undirected graph, the in- and out-degree of the nodes are equal (since every ingoing edge is also an outgoing edge). A weighted graph is a graph where the edges have a set weight, in this case the in- and out-degree are equal to the sum of ingoing and outgoing edge weights respectively. If the out-degree of a node is equal to zero (and the in-degree is non-zero), then the node is called a sink. Similarly, if the in-degree of a node is zero (and its out-degree is non-zero), then the node is called a source. Any graph containing either sinks or sources is not strongly connected.

Condensation digraphs

The subgraph of a graph $\mathcal{G}(\mathcal{V},\mathcal{E})$ is a graph $\mathcal{G}'(\mathcal{V}',\mathcal{E}')$ for which it holds that $\mathcal{V}' \subseteq \mathcal{V}$ and $\mathcal{E}' \subseteq \mathcal{E}$. In essence, the subgraph of a graph $\mathcal{G}$ is a selection of nodes and edges from $\mathcal{G}$. A strongly connected component of graph $\mathcal{G}$ is the subgraph $\mathcal{H}$ which is strongly connected and any other subgraph of $\mathcal{G}$ which strictly contains $\mathcal{H}$ is not strongly connected.
For a weekly connected digraph $\mathcal{G}(\mathcal{V},\mathcal{E})$, a condensation graph $\mathcal{C}(\mathcal{G})$ can be defined. This condensation graph is a graph which replaces all strongly connected subgraphs of $\mathcal{G}$ with a single node. An example of a condensation graph and the original digraph is depicted in Figure A-3.

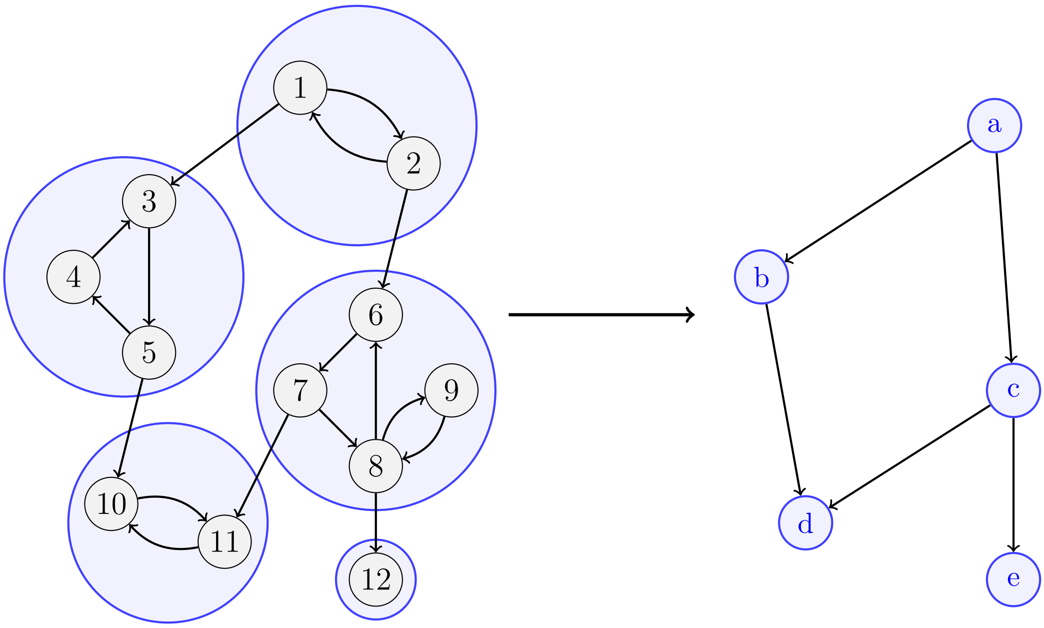

Figure A-3: Example of a condensation digraph with 5 strongly connected components.

Adjacency matrix

A way to algebraically represent the connections between nodes and edges of a (di)graph is by means of the adjacency matrix. For a graph $\mathcal{G}(\mathcal{V},\mathcal{E})$ with n nodes, the adjacency matrix $A \in \mathbb{R}^{n\times n}_{\geq 0}$ is zero-valued at index (i,j) if edge $(i,j) \notin \mathcal{E}$. Otherwise the value at index a_{ij} is equal to the weight of the relevant edge (with unweighted graphs having edge weights of 1). For undirected graphs, the adjacency matrix is symmetric.

The adjacency matrix can also be used to determine the two important graph properties; the connectivity and periodicity. The in-degree of a node is equal to $d_{in,i} = \mathbb{e}_i^\top A^\top \mathbb{1}_n$, with $\mathbb{1}_n$ denoting the one-valued vector of size n and $\mathbb{e}_i$ the vector of size n which is equal to one at index i and zero otherwise. If the in-degree of a node equals one for every node i, the adjacency matrix is said to be column-stochastic. Likewise, the out-degree is equal to $d_{out,i} = \mathbb{e}_i^\top A\mathbb{1}_n$ with the matrix being row-stochastic if $d_{out,i} = 1,\ \forall i \in \mathcal{V}$.

To determine whether a path of length k between nodes i and j exists, again the adjacency matrix can be used. In fact, if a path of lenght 2 from node i to node j through node h exists, it holds that $(i,h) \in \mathcal{E}$ and $(h,j) \in \mathcal{E}$, thus $a_{ih} > 0$ and $a_{hj} > 0$, resulting in $\mathbb{e}_i^\top A^2 \mathbb{e}_j > 0$. This can be extended to paths of length k. Concluding, there exists at least one path of length k between nodes i and j if and only if A^k at index (i,j) is greater than zero.

Also the connectivity of a graph can be discussed using the adjacency matrix. Since a digraph is strongly connected if and only if all nodes of the graph are globally reachable, it suffices to check whether there exists a path of any length from all nodes i to nodes j. If $\exists k$ such that A^k at index $(i,j) \in \mathcal{V}$ is greater than zero, then $\mathbb{e}_i^\top \left(\sum_{k=0}^{n-1} A^k\right) \mathbb{e}_j > 0$ is true as well. Therefore, using $\succ$ and $\prec$ for component-wise inequalities, a graph is strongly connected if $\sum_{k=0}^{n-1} A^k \succ \mathbb{0}_{n \times n}$. A matrix fulfilling this condition is called an irreducible matrix.

An equivalent condition for the irreducibility of a matrix A is that there exists no permutation matrix P such that

$$PAP^\top = \begin{bmatrix} \tilde{A}_{11} & \tilde{A}_{12} \\ \mathbb{0} & \tilde{A}_{22} \end{bmatrix} \tag{A-1}$$

hence the irreducible matrix A cannot be reduced to a block-triangular form.

Now consider a graph $\mathcal{G}(\mathcal{V}, \mathcal{E})$ which is strongly connected and aperiodic. Due to the aperiodicity the cycles in the graph do not have a common divisor greater than one. For high enough k there exists a path from node i to node j of length k, as well as a path-length of $k+1$ and so on. Concluding, $\exists k^* \in \{1, \ldots, n\}$ such that $A^k \succ \mathbb{0}_{n \times n}$, $\forall k \geq k^*$. Matrix A is called a primitive matrix, also note that a primitive matrix is by definition irreducible.

The Perron-Frobenius Theorem for non-negative matrices provides some useful results on the spectral properties of primitive matrices.

Theorem A.1 (Non-negative matrices). *Let A be a matrix such that $A \in \mathbb{R}_{\geq 0}^{n \times n}$ with $n > 2$ then*

(i) there exists a $\lambda \in \mathbb{R}$ such that $\lambda \geq |\mu| \geq 0$ for all other eigenvalues μ,

(ii) the right and left eigenvectors v and w corresponding to λ can be chosen such that $v, w \in \mathbb{R}_{\geq 0}^n$,

Theorem A.2 (Irreducible matrices). *Let A be a matrix such that $A \in \mathbb{R}_{\geq 0}^{n \times n}$ with $n > 2$ and $\sum_k^{n-1} A^k \succ \mathbb{0}_{n \times n}$ then*

(i) $\lambda = \rho(A)$ and $m_a(\lambda) = 1$, thus λ is strictly positive and simple,

(ii) the left and right eigenvectors v and w are additionally unique,

Theorem A.3 (Primitive matrices)**.** *Let A be a matrix such that $A \in \mathbb{R}^{n \times n}_{\geq 0}$ with $n > 2$ and there exists a $k^\star \in \{0, \ldots, n\}$ where $A^k \succ \mathbb{0}_{n \times n}$, $\forall k \geq k^*$ then $\lambda > |\mu|$ for all other eigenvalues μ.*

Proof: see Appendix B and [26].

The adjacency matrix along with its spectral properties prove to be a useful tool in analysis of discrete-time consensus problems, as discussed in Chapter A-2-1.

Laplacian matrix

The adjacency matrix is a useful tool in the field of discrete time consensus, as will be discussed in a later chapter. However, for the continuous time consensus another matrix will be used, the Laplacian matrix. This matrix is constructed from the adjacency matrix, more specifically $L = \text{diag}(A\mathbb{1}_n) - A$. In essence, the Laplacian matrix has the following structure:

$$l_{ij} = \begin{cases} -a_{ij} & \text{if } i \neq j \\ d_{out,i} & \text{if } i = j \end{cases} \tag{A-2}$$

By design, at least one of the eigenvalues of the Laplacian matrix is equal to zero, with the corresponding eigenvector being a one-vector, i.e., $L\mathbb{1}_n = \mathbb{0}_n$.

Analogously to the adjacency matrix, the Laplacian matrix provides useful insights for continuous-time consensus problems as found in Chapter A-2-2.

Incidence matrix

Another way to represent the topology of the interconnections between nodes and edges of an undirected graph $\mathcal{G}(\mathcal{V}, \mathcal{E})$ is by means of the incidence matrix. For a graph with n nodes and m edges, the incidence matrix $B \in \{-1, 0, 1\}^{n \times m}$ can be constructed in the following manner. First number the edges from 1 to m, then set an arbitrary direction for the edges. If edge k is an out-going edge of node i set $b_{ik} = 1$, likewise if the edge is an in-going edge of node j set $b_{jk} = -1$. Do this for all edges and set the other values of the incidence matrix B to zero. In the example depicted in Figure A-1, the edges first need to be numbered and given an arbitrary direction. The resulting graph is depicted in Figure A-4.
From there the incidence matrix can be constructed, which is equal to

$$B = \begin{bmatrix} 1 & 1 & 0 & 0 \\ -1 & 0 & 1 & 1 \\ 0 & -1 & -1 & 0 \\ 0 & 0 & 0 & -1 \end{bmatrix}. \tag{A-3}$$

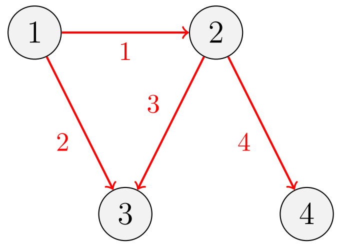

Figure A-4: An undirected graph example, with arbitrary edge numbering and directions.

Digraphs already have a certain edge direction, therefore the incidence matrix will seem less arbitrary. For the digraph mentioned in Figure A-2, dependent on edge numbering, the incidence matrix results in

$$B = \begin{bmatrix} 1 & -1 & 1 & -1 & 0 & 0 \\ -1 & 1 & 0 & 0 & -1 & 1 \\ 0 & 0 & -1 & 1 & 1 & 0 \\ 0 & 0 & 0 & 0 & 0 & -1 \end{bmatrix}. \tag{A-4}$$

Since the incidence matrix describes the set of edges of a graph, it will be used abundantly in network-decentralized problems such as those found in Chapter A-3.

A-2 Consensus theory

In this section the field of consensus will be discussed based on findings from [1]. In multi-agent systems consensus on a variable is said to be reached once all participants reach an agreement on that variable [5]. For example if a grid of sensor nodes measure the temperature of a city, they're initially bound to have some differences. In this system a consensus is reached if all of the nodes reach an equal belief of the temperature. To reach this consensus, a state update of the form

$$T_i^+ = \sum_{j=1}^{n} a_{ij} T_j, \quad \text{s.t.} \sum_{j=1}^{n} a_{ij} = 1 \tag{A-5}$$

will be introduced as in [1]. In this equation the weight coefficients a_{ij} denote the importance of temperature T_j to the updated temperature T_i^+. Note that if node i has no information about node j, i.e. there is no edge from node i to node j, the weight a_{ij} equals zero. From this updating scheme a graph can be constructed, with its adjacency matrix being equal to $A = [a_{ij}]$.

A-2-1 Discrete-time consensus

The previously mentioned state update equation results in a discrete-time consensus problem. If we consider the state of node i at time k to be $x_i(k)$ and we define the vector containing all node states as $\mathbf{x}(k) = \begin{bmatrix} x_1(k) & x_2(k) & \dots & x_n(k) \end{bmatrix}^\top$, the previously mentioned equation results in

$$\mathbf{x}(k+1) = A\mathbf{x}(k) \tag{A-6}$$

with matrix A being a row-stochastic adjacency matrix, as introduced in Chapter A-1. Consensus is reached if $\lim_{k\to\infty} \mathbf{x}(k) = \mathbb{1}_n \bar{x}$, with $\bar{x}$ being the value all nodes converge to. Whether the state converges to this value depends on the adjacency matrix, since $\lim_{k\to\infty} \mathbf{x}(k) = \lim_{k\to\infty} A^k \mathbf{x}(0)$. This converges to $\mathbb{1}_n \bar{x}$ only if $\lim_{k\to\infty} A^k = \mathbb{1}_n \mathbf{w}^\top$, with $\mathbf{w}$ being a vector of size n; which is not always the case. In the following sections the spectral properties of the adjacency matrix, along with conclusions based on the structure of the graph (periodicity and connectivity), will be discussed.

Strongly connected and aperiodic

In case of a strongly connected and aperiodic directed graph, the row-stochastic adjacency matrix A is primitive, i.e. $\exists k^* > 0$ such that $A^k \succ 0$ for $k > k^*$. Since the matrix is row-stochastic, it holds that

$$A\mathbb{1}_n = \mathbb{1}_n \tag{A-7}$$

Thus $(1, \mathbb{1}_n)$ is an eigenpair of the matrix A. Furthermore, because the matrix is primitive its dominant eigenvalue $\lambda = 1$ is simple [26]. As a result the Jordan normal form of A can be written as

$$A = T \begin{bmatrix} 1 & \mathbb{0}_{1\times(n-1)} \\ \mathbb{0}_{(n-1)\times 1} & \tilde{A} \end{bmatrix} T^{-1}, \tag{A-8}$$

with $\rho(\tilde{A}) < 1$.Therefore this implies that $\lim_{k\to\infty} \tilde{A}^k = \mathbb{0}_{(n-1)\times(n-1)}$, and as such

$$\lim_{k\to\infty} A^k = T\left(\lim_{k\to\infty} \begin{bmatrix} 1^k & \mathbb{0}_{1\times(n-1)} \\ \mathbb{0}_{(n-1)\times 1} & \tilde{A}^k \end{bmatrix}\right) T^{-1} = T \begin{bmatrix} 1 & \mathbb{0} \\ \mathbb{0} & \mathbb{0} \end{bmatrix} T^{-1}. \tag{A-9}$$

Furthermore defining $T = [v_1, v_2, \ldots, v_n]$ and $T^{-1} = [w_1, w_2, \ldots, w_n]^\top$ it can be seen from Equation (A-8) that $Av_1 = v_1$ and $w_1^\top A = w_1^\top$, thus v_1 and w_1 are the right and left dominant eigenvectors. Additionally, since $T^{-1}T = I_n$, it must hold that $w_1^\top v_1 = 1$. Hence, the adjacency matrix converges to

$$\lim_{k\to\infty} A^k = \mathbb{1}_n w_1^\top \tag{A-10}$$

and also

$$\lim_{k\to\infty} \mathbf{x}(k) = \lim_{k\to\infty} A^k \mathbf{x}(0) = \mathbb{1}_n \left(w_1^\top \mathbf{x}(0)\right). \tag{A-11}$$

Thus a strongly connected and aperiodic row-stochastic graph leads to a consensus equal to the weighted average of the initial node-states [1]. If on top of that the adjacency matrix is also column-stochastic (i.e. $A^\top \mathbb{1}_n = \mathbb{1}_n$) Equation (A-6) leads to an averaging consensus with $x_i(k) \to \mathbb{1}_n^\top \mathbf{x}(0)$.

Weakly connected and aperiodic

Since not all graphs are strongly connected, in this section a weakly connected graph $\mathcal{G}(\mathcal{V}, \mathcal{E})$ will be considered. These graphs will be divided in two classes, those containing one sink and those containing multiple.

One sink

Consider graph $\mathcal{G}(\mathcal{V}, \mathcal{E})$ containing one sink. Although the graph is by definition weakly connected, it can still have strongly connected components and as a result there exists a condensation graph $\mathcal{C}(\mathcal{G})$. An example of an aperiodic, weakly connected graph with strongly connected components can be seen in Figure A-5.

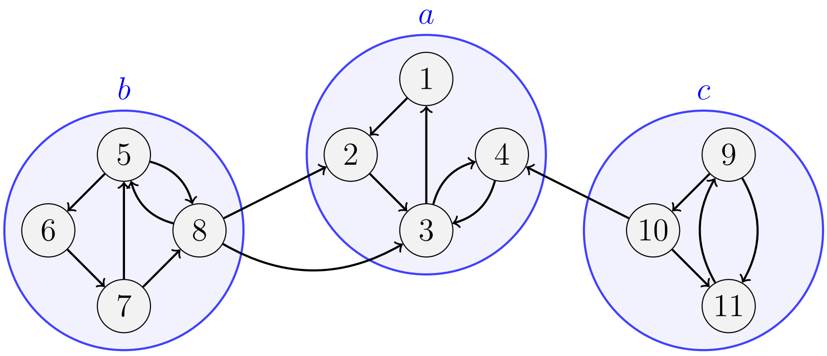

Figure A-5: Example of a digraph with a strongly connected and aperiodic sink. The edge weights are chosen such that the out-degree of every node equals one, i.e. the adjacency matrix is row-stochastic.

Constructing the adjacency matrix for the graph in Figure A-5 yields

$$A = \begin{bmatrix} A_{aa} & \mathbb{0}_{4\times4} & \mathbb{0}_{4\times3} \\ A_{ba} & A_{bb} & \mathbb{0}_{4\times3} \\ A_{ca} & \mathbb{0}_{3\times4} & A_{cc} \end{bmatrix} \tag{A-12}$$

with the adjacency matrices for the strongly connected components equal to

$$A_{aa} = \begin{bmatrix} 0 & 1 & 0 & 0 \\ 0 & 0 & 1 & 0 \\ \frac{1}{2} & 0 & 0 & \frac{1}{2} \\ 0 & 0 & 1 & 0 \end{bmatrix}, \quad A_{bb} = \begin{bmatrix} 0 & \frac{1}{2} & 0 & \frac{1}{2} \\ 0 & 0 & 1 & 0 \\ \frac{1}{2} & 0 & 0 & \frac{1}{2} \\ \frac{1}{3} & 0 & 0 & 0 \end{bmatrix}, \quad A_{cc} = \begin{bmatrix} 0 & \frac{1}{2} & \frac{1}{2} \\ 0 & 0 & \frac{1}{2} \\ 1 & 0 & 0 \end{bmatrix} \tag{A-13}$$

and the edges connecting the strongly connected components with the sink component

$$A_{ba} = \begin{bmatrix} 0 & 0 & 0 & 0 \\ 0 & 0 & 0 & 0 \\ 0 & 0 & 0 & 0 \\ 0 & \frac{1}{3} & \frac{1}{3} & 0 \end{bmatrix}, \quad A_{ca} = \begin{bmatrix} 0 & 0 & 0 & 0 \\ 0 & 0 & 0 & \frac{1}{2} \\ 0 & 0 & 0 & 0 \end{bmatrix} \tag{A-14}$$

A more general row-stochastic adjacency matrix $A \in \mathbb{R}^{n\times n}_{\geq 0}$ for the weakly connected, aperiodic graph $\mathcal{G}(\mathcal{V}, \mathcal{E})$ with n nodes, m strongly connected components and one sink (which will be labelled as the first component), has the following structure

$$A = \begin{bmatrix} A_{11} & \mathbb{0}_{n_1 \times n_2} & \cdots & \mathbb{0}_{n_1 \times n_m} \\ A_{21} & A_{22} & \cdots & \mathbb{0}_{n_2 \times n_m} \\ \vdots & \vdots & \ddots & \vdots \\ A_{m1} & A_{m2} & \cdots & A_{mm} \end{bmatrix} \tag{A-15}$$

with n_i being the amount of nodes in strongly connected component i and $\sum_i n_i = n$. Since the adjacency matrix is row-stochastic, the sum of the rows still equals one i.e. $A\mathbb{1}_n = \mathbb{1}_n$. Due to the graph being weakly connected, the first component must have an in-going edge (since it is a sink and therefore has no out-going edges), thus

$$\exists j \in \{2, 3, \ldots, m\} \quad s.t.\ A_{j1} \neq \mathbb{0}_{n_j \times n_1} \tag{A-16}$$

Furthermore, since the graph contains only one sink, the other components must have at least one out-going edge. This results in the statement

$$\forall k \in \{2, 3, \ldots, m\},\ \exists j \in \{1, 2, \ldots, k\}, \quad s.t.\ A_{kj} \neq \mathbb{0}_{n_k \times n_j}. \tag{A-17}$$

Since the graph is aperiodic, the adjacency matrix of the first strongly connected component is primitive, i.e. $\exists k^* > 0$ such that $A_{11}^k \succ \mathbb{0}_{n_1 \times n_1}$. Also, following statement (A-17), the other diagonal entries A_{kk} with $k \in \{2, 3, \ldots, m\}$ must be row-substochastic. This results in a spectral radius of $\rho(A_{kk}) < 1$, as proven in Appendix C. As a result $I_{n_i} - A_{ii}$ is invertible and $\mathbf{x}_i(k)$ converges. Using the fact that $\sum_{i=1}^{j} A_{ji}\mathbb{1}_{n_i} = \mathbb{1}_{n_j}$ (i.e. $\left(I_{n_j} - A_{jj}\right)^{-1} \sum_{i=1}^{j-1} A_{ji}\mathbb{1}_{n_i} = \mathbb{1}_{n_j}$) then results in the following findings

$$\begin{aligned}
\mathbf{x}_1(k+1) &= A_{11}\mathbf{x}_1(k) && \rightarrow \lim_{k\to\infty} \mathbf{x}_1(k) = \mathbb{1}_{n_1} w_1^\top \mathbf{x}_1(0) \\
\mathbf{x}_2(k+1) &= A_{21}\mathbf{x}_1(k) + A_{22}\mathbf{x}_2(k) && \rightarrow \lim_{k\to\infty} \mathbf{x}_2(k) = \left(I_{n_2} - A_{22}\right)^{-1} A_{21}\mathbb{1}_{n_1}(w_1^\top \mathbf{x}_1(0)) \\
& && \qquad\qquad\qquad = \mathbb{1}_{n_2} w_1^\top \mathbf{x}_1(0) \\
&\vdots \\
\mathbf{x}_j(k+1) &= \sum_{i=1}^{j} A_{ji}\mathbf{x}_i(k) && \rightarrow \lim_{k\to\infty} \mathbf{x}_j(k) = \left(I_{n_j} - A_{jj}\right)^{-1} \sum_{i=1}^{j-1} A_{ji}\mathbb{1}_{n_i}(w_1^\top \mathbf{x}_1(0)) \\
& && \qquad\qquad\qquad = \mathbb{1}_{n_j} w_1^\top \mathbf{x}_1(0).
\end{aligned}$$

This results in a consensus based only on the initial states of the nodes within the sink component. The adjacency matrix converges to

$$\lim_{k\to\infty} A^k = \mathbb{1}_n \begin{bmatrix} w_1^\top & \mathbb{0}_{1\times(n-n_1)} \end{bmatrix} \tag{A-18}$$

Multiple sinks

Now a graph with $M \geq 2$ sinks and $N > M$ strongly connected components will be considered. Since a sink component does not update its state based on the information of other components, the corresponding adjacency matrix of such a graph can be constructed as

$$A = \left[\begin{array}{cccc|cccc} A_{11} & \mathbb{0}_{n_1 \times n_2} & \cdots & \mathbb{0}_{n_1 \times n_M} & \mathbb{0}_{n_1 \times n_{M+1}} & \mathbb{0}_{n_1 \times n_{M+2}} & \cdots & \mathbb{0}_{n_1 \times n_N} \\ \mathbb{0}_{n_2 \times n_1} & A_{22} & \cdots & \mathbb{0}_{n_2 \times n_M} & \mathbb{0}_{n_2 \times n_{M+1}} & \mathbb{0}_{n_2 \times n_{M+2}} & \cdots & \mathbb{0}_{n_2 \times n_N} \\ \vdots & \vdots & \ddots & \vdots & \vdots & \vdots & \ddots & \vdots \\ \mathbb{0}_{n_M \times n_1} & \mathbb{0}_{n_M \times n_2} & \cdots & A_{MM} & \mathbb{0}_{n_M \times n_{M+1}} & \mathbb{0}_{n_M \times n_{M+2}} & \cdots & \mathbb{0}_{n_M \times n_N} \\ \hline A_{(M+1)1} & A_{(M+1)2} & \cdots & A_{(M+1)M} & A_{(M+1)(M+1)} & \mathbb{0}_{n_{M+1} \times n_{M+2}} & \cdots & \mathbb{0}_{n_{M+1} \times n_N} \\ A_{(M+2)1} & A_{(M+2)2} & \cdots & A_{(M+2)M} & A_{(M+2)(M+1)} & A_{(M+2)(M+2)} & \cdots & \mathbb{0}_{n_{M+2} \times n_N} \\ \vdots & \vdots & \ddots & \vdots & \vdots & \vdots & \ddots & \vdots \\ A_{N1} & A_{N2} & \cdots & A_{NM} & A_{N(M+1)} & A_{N(M+2)} & \cdots & A_{NN} \end{array}\right] \tag{A-19}$$

or in short

$$A = \left[\begin{array}{c|c} A_{sink} & \mathbb{0}_{n_s \times n_r} \\ \hline A_c & A_r \end{array}\right], \quad n_s = \sum_{i=1}^{M} n_i, \; n_r = \sum_{i=M+1}^{N} n_i. \tag{A-20}$$

When considering the convergence of the A matrix, it can be concluded that this system will not result in a consensus. In fact, the sink components converge to possibly different values, as can be seen from the convergence of A_{sink},

$$\lim_{k \to \infty} A_{sink}^k = \begin{bmatrix} \mathbb{1}_{n_1} w_1^\top & \mathbb{0}_{n_1 \times n_2} & \cdots & \mathbb{0}_{n_1 \times n_M} \\ \mathbb{0}_{n_2 \times n_1} & \mathbb{1}_{n_2} w_2^\top & \cdots & \mathbb{0}_{n_2 \times n_M} \\ \vdots & \vdots & \ddots & \vdots \\ \mathbb{0}_{n_M \times n_1} & \mathbb{0}_{n_M \times n_2} & \cdots & \mathbb{1}_{n_M} w_M^\top \end{bmatrix} \tag{A-21}$$

and the convergence of the states of these components is equal to

$$\lim_{k \to \infty} \begin{bmatrix} \mathbf{x}_1(k) \\ \mathbf{x}_2(k) \\ \vdots \\ \mathbf{x}_M(k) \end{bmatrix} = \begin{bmatrix} \mathbb{1}_{n_1} w_1^\top \mathbf{x}_1(0) \\ \mathbb{1}_{n_2} w_2^\top \mathbf{x}_2(0) \\ \vdots \\ \mathbb{1}_{n_M} w_M^\top \mathbf{x}_M(0) \end{bmatrix} \tag{A-22}$$

which is not strictly equal to each other. Similar to the result found for the case with one sink, the convergence of the states is only dependent on the initial states of the sink nodes. Following an analogous approach and defining $D := \lim_{k \to \infty} A_{sink}^k$, this results in

$$\lim_{k \to \infty} \mathbf{x}(k) = \left[\begin{array}{c|c} D & \mathbb{0}_{n_s \times n_r} \\ \hline (I_{n_r} - A_r)^{-1} A_c D & \mathbb{0}_{n_r \times n_r} \end{array}\right] \mathbf{x}(0). \tag{A-23}$$

Since this is not equal for all $x_i(k)$ for every possible $\mathbf{x}(0)$, a graph containing two or more sinks does not necessarily yield consensus.

Strongly connected and periodic

In case of a strongly connected, periodic graph $\mathcal{G}(\mathcal{V},\mathcal{E})$, the adjacency matrix A is irreducible but not primitive, as discussed in Chapter A-1. Furthermore since the graph is strongly connected, it can be determined that

$$\sum_{k=k^*}^{\infty} A^k \succ \mathbb{0}_{n\times n}, \quad \forall k^* \geq 0 \tag{A-24}$$

but also

$$\exists i,j>0, \quad s.t.\ \mathbb{e}_i^\top A^k \mathbb{e}_j = 0, \quad \forall k \geq 0 \tag{A-25}$$

therefore A^k does not converge for $k \to \infty$. This can also be seen from its spectral properties, since $\lambda = \rho(A) = 1$ is not strictly greater than the absolute value of the other eigenvalues, i.e. $\lambda \geq |\mu(A)|$. Meaning that any other eigenvalue with absolute value of one (for example $\lambda = -1$) can exist. These eigenvalues do not converge for $k \to \infty$, i.e. $\lim_{k\to\infty} \lambda^k$ does not exist for $\lambda \neq 1$ with $|\lambda| = 1$.

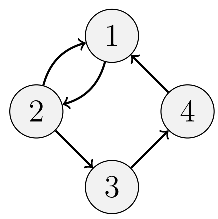

Figure A-6: Example of a strongly connected periodic digraph with a common period of 2.

For example, for the graph given in Figure A-6 the adjacency matrix is equal to

$$A = \begin{bmatrix} 0 & 1 & 0 & 0 \\ \frac{1}{2} & 0 & \frac{1}{2} & 0 \\ 0 & 0 & 0 & 1 \\ 1 & 0 & 0 & 0 \end{bmatrix}. \tag{A-26}$$

The eigenvalues of this adjacency matrix are equal to

$$\lambda(A) = \begin{bmatrix} 1 \\ -1 \\ \frac{1}{2}\sqrt{2}\,\imath \\ -\frac{1}{2}\sqrt{2}\,\imath \end{bmatrix}, \quad \imath = \sqrt{-1} \tag{A-27}$$

hence the matrix has at least one eigenvalue that does not converge. In fact

$$\lim_{k\to\infty} A^{2k} = \begin{bmatrix} \frac{2}{3} & 0 & \frac{1}{3} & 0 \\ 0 & \frac{2}{3} & 0 & \frac{1}{3} \\ \frac{2}{3} & 0 & \frac{1}{3} & 0 \\ 0 & \frac{2}{3} & 0 & \frac{1}{3} \end{bmatrix} \quad \text{(A-28)}$$

$$\lim_{k\to\infty} A^{2k+1} = \begin{bmatrix} 0 & \frac{2}{3} & 0 & \frac{1}{3} \\ \frac{2}{3} & 0 & \frac{1}{3} & 0 \\ 0 & \frac{2}{3} & 0 & \frac{1}{3} \\ \frac{2}{3} & 0 & \frac{1}{3} & 0 \end{bmatrix} \quad \text{(A-29)}$$

This concludes that a periodic graph does not result in consensus, or more general it does not result in a converging state value.

A-2-2 Continuous-time consensus

Consider Equation (A-6) once more. In order to determine the states convergence to a certain value the difference of the updated state with the current state can be calculated, i.e.

$$\Delta \mathbf{x}(k) = \mathbf{x}(k+1) - \mathbf{x}(k) = A\mathbf{x}(k) - I_n\mathbf{x}(k) = -L\mathbf{x}(k), \quad \text{(A-30)}$$

with L being the Laplacian matrix of a row-stochastic adjacency matrix A, as described in Section A-1. With small enough time periods for k, this system describes a continuous-time system as discussed in [2] with

$$\dot{\mathbf{x}}(t) = -L\mathbf{x}(t), \quad \text{(A-31)}$$

resulting in

$$\mathbf{x}(t) = \mathrm{e}^{-Lt}\mathbf{x}(0). \quad \text{(A-32)}$$

For the analysis of the spectrum of the Laplacian matrix, multiple graph properties will again be considered. We start with a strongly connected and aperiodic graph.

Strongly connected and aperiodic

Considering a strongly connected and aperiodic graph $\mathcal{G}(\mathcal{V}, \mathcal{E})$ with primitive row-stochastic adjacency matrix $A \in \mathbb{R}^{n\times n}$, it can be concluded that $(1, \mathbb{1}_n)$ is an eigenpair. Furthermore its spectral radius is equal to $\rho(A) = 1$ and for all other eigenvalues it is know that $|\mu(A)| < 1$. Therefore, with the Laplacian matrix being equal to $L = I_n - A$, it is known that $(0, \mathbb{1}_n)$ is an eigenpair of L and $\{\mu(-L)\} < 0$, with $\{\cdot\}$ denoting the real part of an argument. As a result the Jordan form of the Laplacian can be constructed as follows:

$$L = T \begin{bmatrix} \lambda & \mathbb{0}_{1\times(n-1)} \\ \mathbb{0}_{(n-1)\times 1} & \tilde{L} \end{bmatrix} T^{-1}, \quad \text{(A-33)}$$

Similarly to Section A-2-1, the transformation matrices will be defined as $T = [v_1, v_2, \ldots, v_n]$ and $T^{-1} = [w_1, w_2, \ldots, w_n]^\top$. Furthermore it is known that $v_1 = \mathbb{1}_n$ and w_1 is the left eigenvector of A with eigenvalue $\lambda = 1$. Also note that w_1 is the eigenvector of L with eigenvalue $\lambda = 0$ and $w_1^\top \mathbb{1}_n = 1$. As a result the Laplacian matrix converges to

$$\lim_{t\to\infty} \mathrm{e}^{-Lt} = \begin{bmatrix} \mathbb{1}_n & \tilde{v} \end{bmatrix} \left(\lim_{t\to\infty} \begin{bmatrix} \mathrm{e}^{-\lambda t} & \mathbb{0}_{1\times(n-1)} \\ \mathbb{0}_{(n-1)\times 1} & \mathrm{e}^{-\tilde{L}t} \end{bmatrix} \right) \begin{bmatrix} w_1^\top \\ \tilde{w}^\top \end{bmatrix} \tag{A-34}$$

$$= \begin{bmatrix} \mathbb{1}_n & \tilde{v} \end{bmatrix} \begin{bmatrix} 1 & 0 \\ 0 & 0 \end{bmatrix} \begin{bmatrix} w_1^\top \\ \tilde{w}^\top \end{bmatrix} \tag{A-35}$$

$$= \mathbb{1}_n w_1^\top, \tag{A-36}$$

yielding a state consensus of

$$\lim_{t\to\infty} \mathbf{x}(t) = \lim_{t\to\infty} \mathrm{e}^{-Lt}\mathbf{x}(0) = \mathbb{1}_n \left(w_1^\top \mathbf{x}(0) \right). \tag{A-37}$$

Weakly connected and aperiodic

Now considering the weakly connected and aperiodic case, first the graph containing a globally reachable node will be discussed (a graph containing at most one sink).

One sink

Considering the adjacency matrix containing one sink, as defined in Equation (A-15), and using it to construct the Laplacian matrix yields

$$L = \begin{bmatrix} L_{11} & \mathbb{0}_{n_1\times n_2} & \cdots & \mathbb{0}_{n_1\times n_m} \\ -A_{21} & L_{22} & \cdots & \mathbb{0}_{n_2\times n_m} \\ \vdots & \vdots & \ddots & \vdots \\ -A_{m1} & -A_{m2} & \cdots & L_{mm} \end{bmatrix}. \tag{A-38}$$

Since A_{11} is row-stochastic and primitive, the Laplacian matrix L_{11} converges for $\mathrm{e}^{-L_{11}t}$ with $t \to \infty$. Additionally, since matrices A_{jj} for $j \geq 2$ are row-substochastic, thus $\rho(A_{jj}) < 1$, the resulting Laplacian L_{jj} is invertible. Furthermore, since $L\mathbb{1}_n = \mathbb{0}_n$, it can be found that $L_{jj}^{-1} \sum_{i=1}^{j-1} A_{ji}\mathbb{1}_{n_i} = \mathbb{1}_{n_j}$. Following a similar approach as in Section A-2-1 then yields

$$
\begin{aligned}
\dot{\mathbf{x}}_1(t) &= -L_{11}\mathbf{x}_1(t) & &\rightarrow \lim_{t\to\infty} \mathbf{x}_1(t) = \mathbb{1}_{n_1} w_1^\top \mathbf{x}_1(0)\\
\dot{\mathbf{x}}_2(t) &= A_{21}\mathbf{x}_1(t) - L_{22}\mathbf{x}_2(t) & &\rightarrow \lim_{t\to\infty} \mathbf{x}_2(t) = L_{22}^{-1} A_{21}\mathbb{1}_{n_1}(w_1^\top \mathbf{x}_1(0))\\
& & &\qquad\qquad\qquad = \mathbb{1}_{n_2} w_1^\top \mathbf{x}_1(0)\\
&\vdots\\
\dot{\mathbf{x}}_j(t) &= \sum_{i=1}^{j-1} A_{ji}\mathbf{x}_i(t) - L_{jj}\mathbf{x}_j(t) & &\rightarrow \lim_{t\to\infty} \mathbf{x}_j(t) = L_{jj}^{-1} \sum_{i=1}^{j-1} A_{ji}\mathbb{1}_{n_i}(w_1^\top \mathbf{x}_1(0))\\
& & &\qquad\qquad\qquad = \mathbb{1}_{n_j} w_1^\top \mathbf{x}_1(0).
\end{aligned}
$$

Therefore, we get the analogous result

$$
\lim_{t\to\infty} \mathrm{e}^{-Lt} = \mathbb{1}_n \begin{bmatrix} w_1^\top & \mathbb{0}_{1\times(n-n_1)} \end{bmatrix} \tag{A-39}
$$

Multiple sinks

In this section the case of a weakly connected and aperiodic graph with $M \geq 2$ sinks will be discussed. With the adjacency matrix equal to the matrix given in (A-19), the Laplacian matrix has the following structure

$$
L = \left[\begin{array}{cccc|cccc}
L_{11} & \mathbb{0}_{n_1\times n_2} & \cdots & \mathbb{0}_{n_1\times n_M} & \mathbb{0}_{n_1\times n_{M+1}} & \mathbb{0}_{n_1\times n_{M+2}} & \cdots & \mathbb{0}_{n_1\times n_N}\\
\mathbb{0}_{n_2\times n_1} & L_{22} & \cdots & \mathbb{0}_{n_2\times n_M} & \mathbb{0}_{n_2\times n_{M+1}} & \mathbb{0}_{n_2\times n_{M+2}} & \cdots & \mathbb{0}_{n_2\times n_N}\\
\vdots & \vdots & \ddots & \vdots & \vdots & \vdots & \ddots & \vdots\\
\mathbb{0}_{n_M\times n_1} & \mathbb{0}_{n_M\times n_2} & \cdots & L_{MM} & \mathbb{0}_{n_M\times n_{M+1}} & \mathbb{0}_{n_M\times n_{M+2}} & \cdots & \mathbb{0}_{n_M\times n_N}\\
\hline
-A_{(M+1)1} & -A_{(M+1)2} & \cdots & -A_{(M+1)M} & L_{(M+1)(M+1)} & \mathbb{0}_{n_{M+1}\times n_{M+2}} & \cdots & \mathbb{0}_{n_{M+1}\times n_N}\\
-A_{(M+2)1} & -A_{(M+2)2} & \cdots & -A_{(M+2)M} & -A_{(M+2)(M+1)} & L_{(M+2)(M+2)} & \cdots & \mathbb{0}_{n_{M+2}\times n_N}\\
\vdots & \vdots & \ddots & \vdots & \vdots & \vdots & \ddots & \vdots\\
-A_{N1} & -A_{N2} & \cdots & -A_{NM} & -A_{N(M+1)} & -A_{N(M+2)} & \cdots & L_{NN}
\end{array}\right] \tag{A-40}
$$

or rewriting it to a compact form

$$
L = \left[\begin{array}{c|c} L_{sink} & \mathbb{0}_{n_s\times n_r}\\ \hline -A_c & L_r \end{array}\right], \quad n_s = \sum_{i=1}^{M} n_i,\ n_r = \sum_{i=M+1}^{N} n_i. \tag{A-41}
$$

Following a similar approach as in the discrete-time section, the following convergence result can be obtained with $D := \lim_{t\to\infty} \mathrm{e}^{-L_{sink}t}$

$$
\lim_{t\to\infty} \mathbf{x}(t) = \left[\begin{array}{c|c} D & \mathbb{0}_{n_s\times n_r}\\ \hline L_r^{-1}A_cD & \mathbb{0}_{n_r\times n_r} \end{array}\right] \mathbf{x}(0). \tag{A-42}
$$

The system evolution does not necessarily result in consensus, yielding the same result as in the discrete-time case.

Strongly connected and periodic

In the case of a strongly connected and periodic graph, the discrete-time system evolution does not result in a consensus. This is due to the eigenvalues with an absolute value of $|\mu(A)| = 1$ but not equal to $\lambda = 1$. However, since the Laplacian matrix is equal to $L = I_n - A$, the real part of these eigenvalues will be smaller than zero. Therefore the non-converging eigenvalues do not pose a problem in the continuous-time case. Revisiting the example of Figure A-6 results in the following Laplacian matrix

$$L = \begin{bmatrix} 1 & -1 & 0 & 0 \\ -\frac{1}{2} & 1 & -\frac{1}{2} & 0 \\ 0 & 0 & 1 & -1 \\ -1 & 0 & 0 & 1 \end{bmatrix}. \tag{A-43}$$

With the eigenvalues being equal to

$$\lambda(L) = \begin{bmatrix} 0 \\ 2 \\ 1 + \frac{1}{2}\sqrt{2}\,\imath \\ 1 - \frac{1}{2}\sqrt{2}\,\imath \end{bmatrix}, \quad \imath = \sqrt{-1} \tag{A-44}$$

which, except for the simple eigenvalue of $\lambda = 0$, all have positive real parts. Therefore also for the periodic case, the continuous-time approach converges to

$$\lim_{t\to\infty} \mathrm{e}^{-Lt} = \mathbb{1}_n w_1^\top, \tag{A-45}$$

with w_1 being the left-eigenvector corresponding to the eigenvalue of $\lambda = 1$. For the given example, the limit is:

$$\lim_{t\to\infty} \mathrm{e}^{-Lt} = \mathbb{1}_n \begin{bmatrix} \frac{1}{3} & \frac{1}{3} & \frac{1}{6} & \frac{1}{6} \end{bmatrix} \tag{A-46}$$

A-2-3 Time-varying topology

In the previous sections the graph topology was considered time-invariant, meaning that it was kept constant during the consensus finding problem. However, in some cases the graph could vary over time. Assuming that the nodes and node-ordering remains the same over time, a time-varying graph can be expressed as $\mathcal{G}(k)\,(\mathcal{V}, \mathcal{E}(k))$. The discussion whether a graph structure results in a consensus is similar for time-varying graphs, with the added constraint that periodicity and connectivity properties should hold for all possible graph topologies [2]. For example, if the graph $\mathcal{G}(k)$ can have a set amount of topologies, i.e. $\mathcal{G}(k) \in \{\mathcal{G}_1, \mathcal{G}_2, \ldots, \mathcal{G}_m\}$, then the findings in the strongly connected and aperiodic section hold if all graphs $\mathcal{G}_j$ with $j \in \{1, 2, \ldots, m\}$ are strongly connected and aperiodic.

Defining $\mathcal{G}(k) := \mathcal{G}_{s_k}$ with $s_k \in \{1, 2, \ldots, m\}$ being a switching parameter depending on time instant k, with corresponding adjacency matrix A_{s_k}, the following analogies can be made:

	Time-invariant graph	Time-varying graph
Irreducible	$\sum_{k=0}^{n-1} A^k \succ \mathbb{0}_{n\times n}$	$\sum_{k=0}^{\infty} \left(\prod_{j=0}^{k} A_{s_j}\right) \succ \mathbb{0}_{n\times n}$
Primitive $(k > k^*)$	$A^k \succ \mathbb{0}_{n\times n}$	$\prod_{j=0}^{k} A_{s_j} \succ \mathbb{0}_{n\times n}$

Note that the selection parameter s_k might not be known in advance for some problems. To prove stability in these cases, either the inequalities must hold for all possible s_k, or all A_{s_k} must be irreducible/primitive.

Furthermore the proof in the weakly connected and aperiodic case with one sink also holds for the time-varying case as long as the sink nodes are consistent throughout all possible graph topologies, i.e., there exists a set of nodes $\mathcal{V}_{gr} \subseteq \mathcal{V}$ such that $\mathcal{V}_{gr}$ is globally reachable for all possible topologies $\mathcal{G}_{s_k}$.

A-3 Network-decentralized control

In this chapter network-decentralized control problems will be discussed. These frameworks consider multiple nodes, possibly subject to local dynamics, which interact with one another through edges. Section A-3-1 will discuss a subset of network-decentralized systems, namely compartmental systems. Section A-3-2 will provide proofs to stabilize such a compartmental system. Sections A-3-3 and A-3-4 will refer to more general network systems, with the first discussing linear systems and the latter nonlinear systems.

As an example for a compartmental system a water distribution network can be considered. In this network a certain water-supply demand for several compartments must be reached, this is done by controlling the flow through pipes between the compartments and through a certain supply from the environment. Modelling the compartments as nodes and the pipes as edges, a graph with the structure of Figure A-7 can be constructed.

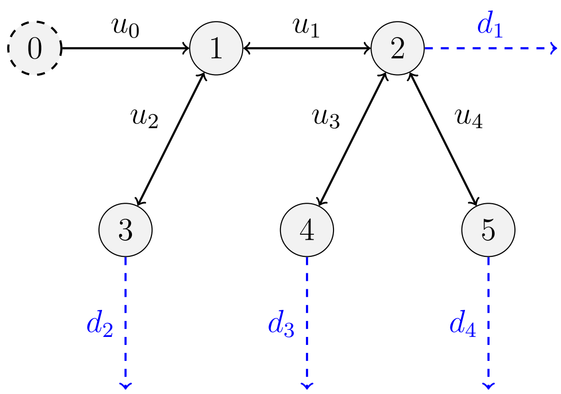

Figure A-7: Example of a compartmental flow graph, with environment node 0 and compartments 1 through 5. The blue dashed lines indicate the supply demand for certain compartments and the control edges are denoted by u_i.

The control goal in this example would be to exactly fulfil the demand by designing control strategies for each link u_i. Doing this in a network-decentralized way implies that a control action u_i can only be a function of the state of the compartments connected to it, for example $u_1 = \phi(x_1, x_2)$.

A-3-1 Compartmental systems

As described in Figure A-7, a compartmental system consists of multiple nodes interacting with each other through links. A more detailed depiction of a single node can be seen in Figure A-8.

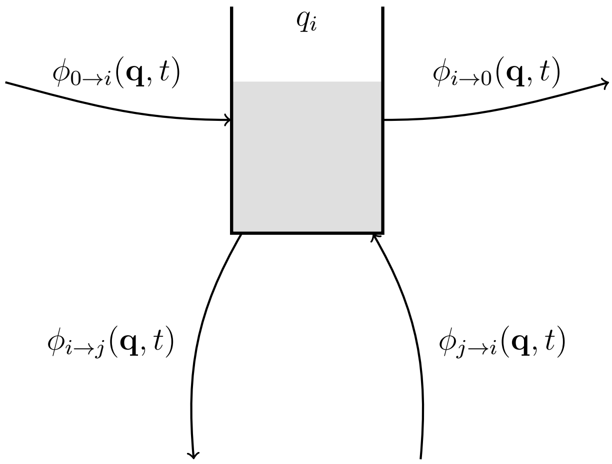

Figure A-8: A single node with in- and outgoing edges for a compartmental system.

With the state of the node being q_i, the flow rate $\dot{q}_i$ is equal to

$$\dot{q}_i(t) = \sum_{j\neq i} \Big(\phi_{j\to i}(\mathbf{q}, t) - \phi_{i\to j}(\mathbf{q}, t)\Big) - \phi_{i\to 0}(\mathbf{q}, t) + \phi_{0\to i}(\mathbf{q}, t). \tag{A-47}$$

Since compartmental systems are assumed to be positive systems (a negative water level for example does not make sense) and the flow functions $\phi(\cdot)$ are directional and therefore assumed to be strictly flowing in the depicted direction, the following two restrictions should be made [1]:

$$\phi_{i\to j}(\mathbf{q}, t) \geq 0 \quad \forall(\mathbf{q}, t) \tag{A-48}$$

$$\phi_{i\to j}(\mathbf{q}, t) = 0 \quad \text{if } q_i(t) = 0 \tag{A-49}$$

In the case that $q_i(t_0) = 0$, applying the two assumptions yields $\dot{q}_i(t_0) = \sum_{j\neq i} \phi_{j\to i}(\mathbf{q}, t_0) + \phi_{0\to i}(\mathbf{q}, t) \geq 0$. Therefore the state vector $\mathbf{q}(t)$ is non-negative for a non-negative initial state $\mathbf{q}(0) \succeq \mathbb{0}$.

Furthermore, when considering a decentralized compartmental flow system, the flow rates can only be a function of the compartments connected to them; $\phi_{i\to j} = \phi_{i\to j}(q_i, q_j, t)$, a network decentralized control. Additionally the environment state q_0 is unknown, therefore the flows going to and coming from the environment are not a function of this state, i.e. $\phi_{0\to i} = \phi_{0\to i}(q_i, t)$ and $\phi_{i\to 0} = \phi_{i\to 0}(q_i, t)$.

A-3-2 Network-decentralized stability

For the discussion of stabilizability of compartmental systems, the system of Figure A-8 will be considered. The flows along the edges will be numbered in arbitrary order and named u_k for $k \in \{1, 2, \ldots, m\}$ with m the number of edges. Furthermore the compartments will be subject to internal dynamics $\dot{\mathbf{q}}_i = A_i\mathbf{q}_i$ and an uncontrollable demand $\mathbf{d}$. An example of such a system is depicted in Figure A-9.

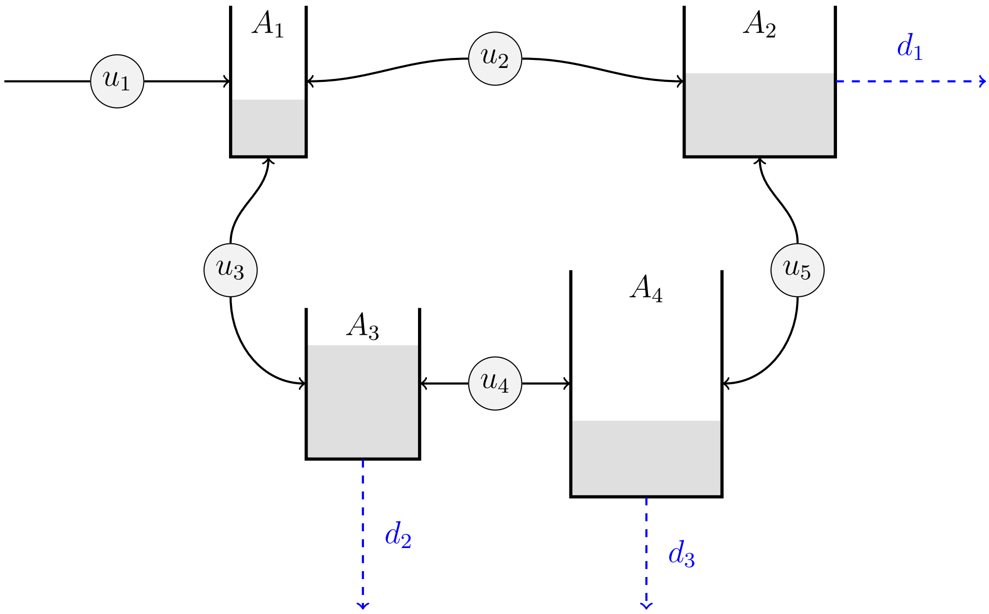

Figure A-9: Compartmental flow graph example with internal dynamics.

In this case the dynamics of, for example, compartment 2 will be equal to

$$\dot{\mathbf{q}}_2 = A_2\mathbf{q}_2 + B_{22}u_2 + B_{25}u_5 + E_2\mathbf{d}. \tag{A-50}$$

Defining $\mathbf{q} = [\mathbf{q}_1^\top, \ldots, \mathbf{q}_n^\top]^\top$, $\mathbf{u} = [u_1^\top, \ldots, u_n^\top]^\top$, $E = [E_1^\top, \ldots, E_n^\top]^\top$ and $A = \text{blockdiag}\{A_1, \ldots, A_n\}$ the dynamics of the system as a whole can be described as

$$\dot{\mathbf{q}}(t) = A\mathbf{q}(t) + B\mathbf{u}(t) + E\mathbf{d}(t) \tag{A-51}$$

with B being a structered matrix equal to

$$B = \begin{bmatrix} B_{11} & B_{12} & B_{13} & \mathbb{0} & \mathbb{0} \\ \mathbb{0} & B_{22} & \mathbb{0} & \mathbb{0} & B_{25} \\ \mathbb{0} & \mathbb{0} & B_{33} & B_{34} & \mathbb{0} \\ \mathbb{0} & \mathbb{0} & \mathbb{0} & B_{44} & B_{45} \end{bmatrix}. \tag{A-52}$$

Note that the structure of this matrix is similar to that of the incidence matrix corresponding to the graph, as mentioned in Section A-1.

In the following subsections three notions of stability will be discussed, which is based on the results of [6]. A system is considered stabilizable if (A, B) is stabilizable. Node-stabilizability requires that every subsystem i is stabilizable, thus $(A_i, [B_{i1}, B_{i2}, \dots, B_{im}])$ is stabilizable $\forall i$. Furthermore a control of the form $\mathbf{u} = -K\mathbf{q}$ is said to be a network-decentralized control if the feedback matrix K has the same structural zero blocks as $B^\top$. Resulting in network-decentralized stability if the system can be stabilized by means of such a network-decentralized control. Note that network-decentralized stabilizability implies stabilizability and node-stabilizability and that node-stabilizability implies stabilizability. Hence it will be assumed that the system is at least stabilizable. Furthermore the trivial case where all subsystems only contain stable eigenvalues will not be discussed. In the following subsections the case of the systems having distinct unstable eigenvalues and the case of a common unstable eigenvalue will be analysed.

Distinct unstable eigenvalues

In this case the subsystems A_i can contain unstable eigenvalues, but two different subsystems do not share the same unstable eigenvalues. Under this assumption stabilizability and node-stabilizability are equivalent. In other words, if (A, B) is stable then (A_i, B_i) is also stable $\forall i$. Since stability of (A, B) implies $\text{rank}[\lambda I - A|G] = n$ for all unstable eigenvalues λ, with $A = \text{diag}[A_1, A_2, \dots, A_n]$ and $B = [B_1^\top, B_2^\top, \dots, B_n^\top]^\top$. Rewriting this formula to explicitly denote subsystem i results in

$$\text{rank} \left[\begin{array}{cc|c} \lambda I - A_i & \mathbb{0} & B_i \\ \mathbb{0} & \lambda I - \tilde{A}_i & \tilde{B}_i \end{array}\right] = n \tag{A-53}$$

with $\tilde{A}_i$ and $\tilde{B}_i$ being the matrices A and B with the removal of A_i and B_i. With λ equal to an unstable eigenvalue of A_i it must hold that $[\lambda I - \tilde{A}_i|\tilde{B}_i]$ has full rank, due to the subsystems not sharing unstable eigenvalues. Furthermore, due to the assumed stability of (A, B) it must hold that $[\lambda I - A_i|B_i]$ has full rank, following from Equation (A-53). Therefore (A_i, B_i) is a stabilizable pair for all i, and as such the system is node-stabilizable.

The assumption of distinct eigenvalues also concludes that (node) stabilizability implies stabilizability by means of a network-decentralized control. For the proof of this statement refer to Appendix D-1, based on [6]. However the mentioned feedback might not be the most efficient, potentially not exploiting all inputs. For a more suitable feedback control scheme, the following Lyapunov equation can be solved

$$\min ||K||_2 \ : \ (A - BK)^\top P + P(A - BK) < 0, \quad K \in \mathcal{S}(B^\top), \ P > 0 \tag{A-54}$$

with $K \in \mathcal{S}(B^\top)$ meaning that K has the same structural blocks as $B^\top$.

Common unstable eigenvalue

In the case of a common unstable eigenvalue λ shared by the subsystems, the LMI in Equation (A-54) will be considered once more.

$$(A - BK)^\top P + P(A - BK) < 0, \quad K \in \mathcal{S}(B^\top),\ P > 0. \tag{A-55}$$

Setting the feedback matrix K equal to

$$K = \gamma B^\top P, \quad P = \text{blockdiag}\{P_1, P_2, \ldots, P_n\} > 0 \tag{A-56}$$

then results in the following LMI

$$\left(A - \gamma B B^\top P\right)^\top P + P\left(A - \gamma B B^\top P\right) < 0. \tag{A-57}$$

Note that defining K in this way implicitly ensures that the feedback has the same structural blocks as $B^\top$, $K \in \mathcal{S}(B^\top)$. Furthermore, defining

$$S = P^{-1} = \text{blockdiag}\{P_1^{-1}, P_2^{-1}, \ldots, P_n^{-1}\} > 0 \tag{A-58}$$

yields

$$SA^\top + AS - 2\gamma B B^\top < 0. \tag{A-59}$$

Theorem A.4. *If a system with common unstable eigenvalues λ with associated Jordan blocks of dimension 1 is stabilizable, the LMI of Equations* (A-58) *and* (A-59) *have a structured solution.*

Proof: See Appendix D-2.

Example

Consider a network system with $n = 5$ compartments as discussed in [6] and as depicted in Figure A-10.

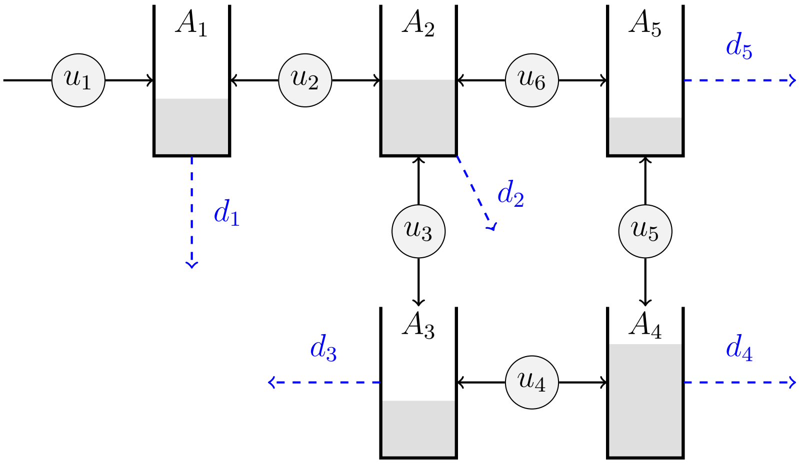

Figure A-10: Compartmental flow graph example with internal dynamics.

The system evolution is described by the matrices

$$A_i = \begin{bmatrix} -\alpha_i & \beta_i & 0 \\ \alpha_i & -\beta_i & 0 \\ 0 & 1 & 0 \end{bmatrix}, \quad \alpha = \begin{bmatrix} 15 \\ 20 \\ 16 \\ 16.7 \\ 14 \end{bmatrix}, \beta = \begin{bmatrix} 0 \\ 0 \\ 12 \\ 0 \\ 22 \end{bmatrix} \tag{A-60}$$

and

$$B = \begin{bmatrix} B_u & -B_d & \mathbb{0} & \mathbb{0} & \mathbb{0} & \mathbb{0} \\ \mathbb{0} & B_u & -B_d & \mathbb{0} & \mathbb{0} & -B_d \\ \mathbb{0} & \mathbb{0} & B_d & -B_u & \mathbb{0} & \mathbb{0} \\ \mathbb{0} & \mathbb{0} & \mathbb{0} & B_d & B_u & \mathbb{0} \\ \mathbb{0} & \mathbb{0} & \mathbb{0} & \mathbb{0} & -B_u & B_d \end{bmatrix}, \quad B_u = \begin{bmatrix} 1 \\ 0 \\ 0 \end{bmatrix}, B_d = \begin{bmatrix} 0 \\ 1 \\ 0 \end{bmatrix} \tag{A-61}$$

and the external demand is

$$E = I, \quad d_i = \begin{bmatrix} 0 \\ -1 \\ 0 \end{bmatrix} \tag{A-62}$$

resulting in the overall networked system dynamics

$$\dot{\mathbf{x}}(t) = A\mathbf{x}(t) + B\mathbf{u}(t) + E\mathbf{d}. \tag{A-63}$$

Since the systems share only one unstable eigenvalue $\lambda = 0$ with ascent one, the system can be regulated by means of decentralized control. Solving the LMI defined in Equations (A-58) and (A-59), a control law equal to $u = \gamma B^\top P$ stabilizes the system. In order to obtain a certain minimum convergence rate, the A matrix in Equation (A-59) can be substituted by $A+\sigma I$; a value of $\sigma = 0.15$ was used in the following simulations.

Using the MATLAB LMI toolbox, the LMI was solved for γ and P. With initial states equal to

$$x_1(0) = \begin{bmatrix} -8.80 \\ 3.63 \\ -9.15 \end{bmatrix},\ x_2(0) = \begin{bmatrix} -8.57 \\ 0.43 \\ -8.06 \end{bmatrix},\ x_3(0) = \begin{bmatrix} 6.36 \\ 6.35 \\ 4.44 \end{bmatrix},\ x_4(0) = \begin{bmatrix} -7.00 \\ 3.19 \\ 0.37 \end{bmatrix},\ x_5(0) = \begin{bmatrix} 9.45 \\ 2.97 \\ 6.00 \end{bmatrix} \tag{A-64}$$

the system indeed stabilizes, resulting in the response shown in Figure A-11.

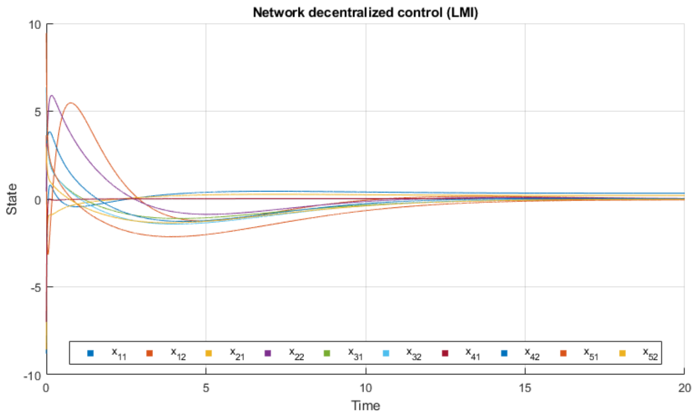

Figure A-11: Stabilization of a network system with a shared unstable eigenvalue of $\lambda = 0$ by means of a network decentralized control scheme.

A-3-3 Network-decentralized estimation

In this section the state-estimation of agents in a decentralized network will be discussed, based on [8]. The dynamics of each agent is defined as

$$\dot{\mathbf{q}}_i(t) = A_i \mathbf{q}_i(t) + B_i \mathbf{u}_i(t), \quad i \in \{1, \dots, n\}, \tag{A-65}$$

connected to a set of arcs $\mathcal{C}_i$ where each arc describes a local measurement of the connected states. Defining the states connected to arc j as $\mathcal{N}_j$, the measurement associated with this arc is defined as

$$\mathbf{y}_j(t) = \sum_{k \in \mathcal{N}_j} C_{jk} \mathbf{q}_k(t) \tag{A-66}$$

with the block-structured matrix $C^\top$ having the same zero/non-zero structure as the incidence matrix of the graph.
Furthermore each agent contains a local estimator

$$\dot{\hat{\mathbf{q}}}_i(t) = A_i \hat{\mathbf{q}}_i(t) + B_i \mathbf{u}_i(t) + \sum_{k \in \mathcal{C}_i} L_{ik}(\hat{\mathbf{y}}_k(t) - \mathbf{y}_k(t)) \tag{A-67}$$

where

$$\hat{\mathbf{y}}_j(t) = \sum_{k \in \mathcal{N}_j} C_{jk} \hat{\mathbf{q}}_k(t) \tag{A-68}$$

being the estimated measurement.

With $A = \text{blockdiag}\{A_1, \ldots, A_n\}$, $B = \text{blockdiag}\{B_1, \ldots, B_n\}$, C being a block-structured matrix with blocks C_{jk}, and the observer matrix L, the dynamics of all agents can be described as:

$$\dot{\mathbf{q}}(t) = A\mathbf{q}(t) + B\mathbf{u}(t) \tag{A-69}$$
$$\mathbf{y}(t) = C\mathbf{q}(t) \tag{A-70}$$
$$\dot{\hat{\mathbf{q}}}(t) = A\hat{\mathbf{q}}(t) + B\mathbf{u}(t) + LC\hat{\mathbf{q}}(t) - L\mathbf{y}(t)). \tag{A-71}$$

The system is said to be network-decentralized detectable if an observer matrix with structure $L \in \mathcal{S}(C^\top)$ exists such that the error dynamics $\mathbf{e}(t) = \mathbf{q}(t) - \hat{\mathbf{q}}(t)$ is asymptotically stable. This is true for systems where A_i do not share unstable eigenvalues and (A, C) is detectable [8]. A way of finding such an observer matrix, is by means of the Lyapunov inequality

$$A^\top P + PA - 2\gamma C^\top C < 0, \quad P > 0 \tag{A-72}$$

when solved for P yields $L = -\gamma P^{-1} C^\top$. If the Lyapunov matrix has a block-diagonal structure, $P = \text{blockdiag}\{P_1, \ldots, P_n\}$, then the resulting observer matrix fulfils $L \in \mathcal{S}(C^\top)$.

Detectability of homogeneous systems

In order to discuss the case of A_i sharing unstable eigenvalues, a homogeneous system will be considered. In this system the individual agents share the same internal dynamics, $A_i = A_1$ and $C_{ij} \in \{-1, 0, 1\} \cdot C_1$. Or more specifically, with $B_\mathcal{G}$ the incidence matrix of the corresponding graph, and $\otimes$ denoting the Kronecker product

$$A = I_n \otimes A_1 \tag{A-73}$$
$$C = B_\mathcal{G}^\top \otimes C_1. \tag{A-74}$$

A necessary assumption is that (A_1, C_1) is detectable, which will be referred to as being node-detectable. Furthermore A_1 is considered to have at least one unstable eigenvalue, in order to exclude the trivial case of an asymptotically stable system matrix.

Furthermore the system is said to be externally connected if all internally connected components are connected to the outside environment. This implies that at least one column per internally connected component of C contains just one non-zero block, $\pm C_1$; which entails that $B_\mathcal{G}$ has full rank.

Theorem A.5. *A node-detectable, homogeneous system with one or more unstable eigenvalues is network-decentralized detectable if and only if it is externally connected.*

Proof: In view of the homogeneity of the system, a suitable solution to the Lyapunov, if it exists, is of the form $P = \text{blockdiag}\{P_1, \dots, P_1\}$. Since $C^\top C$ is positive semi-definite, there exists a $\gamma > 0$ such that

$$z^\top \left[A^\top P + PA - 2\gamma C^\top C\right] z < 0, \quad z \notin \ker(C) \tag{A-75}$$

therefore a solution to the Lyapunov inequality exists for $Cz \neq \mathbb{0}$. Since $B_\mathcal{G}$ has full rank, $z \in \ker(C)$ implies $z \in \ker(C_1)$. Due to the detectability of (A_1, C_1) the Lyapunov inequality has a solution for the individual subsystems, and therefore also for the full system. As a result the system is network-decentralized detectable [8].

If the system, however, is not externally connected, $B_\mathcal{G}$ does not have full rank. More specifically, take $z = \left[z_1^\top, \dots, z_1^\top\right]$ with z_1 the eigenvector of A_1 corresponding to the unstable eigenvalue λ, then

$$\begin{bmatrix} \lambda I - A \\ C \end{bmatrix} z = 0 \tag{A-76}$$

and as a result λ is an unobservable eigenvalue of the system, according to the Popov criterion.

Example

Consider a network of $n = 16$ agents as introduced in [8], with a square communication graph $\mathcal{G}(\mathcal{V}, \mathcal{E})$ as depicted in Figure A-12.
The adjacency matrix for this graph is equal to

$$B_\mathcal{G} = \begin{bmatrix} b & \mathbb{0} & \mathbb{0} & \mathbb{0} \\ \tilde{B} & \mathbb{0} & \mathbb{0} & \mathbb{0} \\ \mathbb{0} & \tilde{B} & \mathbb{0} & \mathbb{0} \\ \mathbb{0} & \mathbb{0} & \tilde{B} & \mathbb{0} \\ \mathbb{0} & \mathbb{0} & \mathbb{0} & \tilde{B} \\ I & -I & \mathbb{0} & \mathbb{0} \\ \mathbb{0} & I & -I & \mathbb{0} \\ \mathbb{0} & \mathbb{0} & I & -I \end{bmatrix}, \qquad \begin{aligned} b &= \begin{bmatrix} 1 & 0 & 0 & 0 \end{bmatrix} \\ \tilde{B} &= \begin{bmatrix} 1 & -1 & 0 & 0 \\ 0 & 1 & -1 & 0 \\ 0 & 0 & 1 & -1 \end{bmatrix} \end{aligned} \tag{A-77}$$

The agents are set still, meaning that their dynamics are equal to $\dot{q}_i = 0$. Furthermore the measurement they receive along the graph edges is equal to $y_{ij} = q_i - q_j$ if an edge exists between nodes i and j, hence $C_i = 1$ and $C = B_\mathcal{G}$. This results in the total system dynamics of

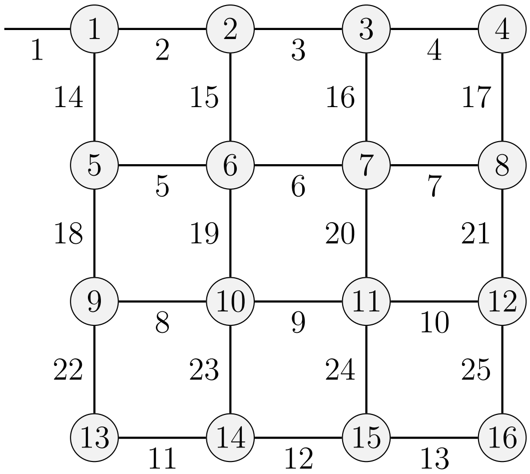

Figure A-12: Example of a network system consisting of 16 agents in a square graph.

$$\dot{\mathbf{q}}(t) = \mathbb{0} \tag{A-78}$$

$$\mathbf{y}(t) = C\mathbf{q}(t) \tag{A-79}$$

$$\dot{\hat{\mathbf{q}}}(t) = LC\hat{\mathbf{q}}(t) - L\mathbf{y}(t)). \tag{A-80}$$

Due to the absence of state dynamics, the inequality from Equation (A-72) simplifies to:

$$-2\gamma C^\top C < 0 \tag{A-81}$$

Hence the estimation converges for arbitrary $\gamma > 0$ and $P > 0$, therefore setting them to $\gamma = 0.1$ and $P = I$ yields $L = -0.1C^\top$. Implementing this estimation feedback for the system with an initial estimation of $\hat{q}_i(0) = 0.5$ and an actual state chosen randomly between 0 and 1 then yields the response shown in Figure A-13.
The trajectories indeed converge to zero for all agents.

A-3-4 Network-decentralized robust control

In the previous sections a linear network-decentralized system was considered. However, for the analysis of robust control with input limitations, the following non-linear system will be considered as metioned in [7]:

$$\dot{\mathbf{q}}(t) = S\tilde{\boldsymbol{\phi}}(\mathbf{q}) + B\mathbf{u}(t) + \mathbf{d}(t). \tag{A-82}$$

Where the control u along the graph arcs is bounded, $\mathbf{u}^- \leq \mathbf{u} \leq \mathbf{u}^+$, S and B are subsets of the incidence matrix $B_\mathcal{G}$, and the unknown function vector $\tilde{\boldsymbol{\phi}}(\cdot)$ describes the flow across the arcs of the corresponding network graph. The function is assumed to be smooth and has a positive derivative. Furthermore, the sub-functions $\tilde{\phi}_i(\cdot)$ are only a function of the connecting nodes, i.e.:

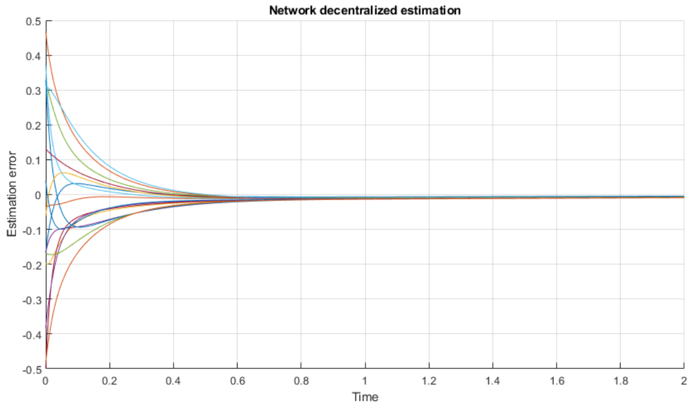

Figure A-13: Estimation of a network of systems by means of a network decentralized estimation feedback.

$$\tilde{\boldsymbol{\phi}}(\mathbf{q}) = \tilde{\boldsymbol{\phi}}(-S^\top \mathbf{q}). \tag{A-83}$$

It is assumed that the demand vector is constant, $\mathbf{d}(t) = \mathbf{d}$, and an equilibrium state $\bar{\mathbf{q}}$ corresponding to an equilibrium input $\bar{\mathbf{u}}$ such that $\mathbf{u}^- \leq \bar{\mathbf{u}} \leq \mathbf{u}^+$ exists:

$$\mathbb{0}_n = S\tilde{\boldsymbol{\phi}}(-S^\top \bar{\mathbf{q}}) + B\bar{\mathbf{u}}(t) + \mathbf{d}. \tag{A-84}$$

Defining $\mathbf{z}(t) = \mathbf{q}(t) - \bar{\mathbf{q}}$, $\mathbf{v}(t) = \mathbf{u}(t) - \bar{\mathbf{u}}$ and $\boldsymbol{\phi}(\mathbf{z}) = \tilde{\boldsymbol{\phi}}(\mathbf{z} + \bar{\mathbf{q}}) - \tilde{\boldsymbol{\phi}}(\bar{\mathbf{q}})$ then yields

$$\dot{\mathbf{z}}(t) = S\boldsymbol{\phi}(-S^\top \mathbf{z}) + B\mathbf{v}(t). \tag{A-85}$$

Now consider the saturated control scheme $\mathbf{v} = \text{sat}\left(-\gamma B^\top \mathbf{z}\right)$, where the saturation function $\text{sat}(\mathbf{x})$ clips the value of $\mathbf{x}$ such that $(\mathbf{u}^- - \bar{\mathbf{u}}) \leq \mathbf{x} \leq (\mathbf{u}^+ - \bar{\mathbf{u}})$, i.e.:

$$\text{sat}(\mathbf{x}) = \begin{cases} \mathbf{u}^- - \bar{\mathbf{u}} & \mathbf{x} < \mathbf{u}^- - \bar{\mathbf{u}} \\ \mathbf{u}^+ - \bar{\mathbf{u}} & \mathbf{x} > \mathbf{u}^+ - \bar{\mathbf{u}} \\ \mathbf{x} & \text{otherwise} \end{cases}$$

To prove that such a control scheme yields (asymptotic) stability, first it will be shown that

$$B\text{sat}(-\gamma B^\top \mathbf{z}) = -\gamma B D_v(\mathbf{z}) B^\top \mathbf{z} \tag{A-86}$$
$$S\boldsymbol{\phi}(-S^\top \mathbf{z}) = -S D_\phi(\mathbf{z}) S^\top \mathbf{z} \tag{A-87}$$

for some bounded positive definite diagonal matrix functions $D_v(\mathbf{z})$ and $D_\phi(\mathbf{z})$. For the saturation function it holds that there exists a value for d_i such that $\text{sat}(x_i) = d_i x_i$; with d_i equal to 1 if x_i is within the saturation range. As a result, for the earlier mentioned control scheme there exists a diagonal matrix $D_v(\mathbf{z})$ with $0 < [D_v]_{ii} \leq 1$, such that $\text{sat}(-\gamma B^\top \mathbf{z}) = -\gamma D_v(\mathbf{z}) B^\top \mathbf{z}$.

In order to show the equality for $S\boldsymbol{\phi}(-S^\top \mathbf{z})$, note that for a strictly increasing function f with $f(0) = 0$ it holds that

$$f(\xi) = \int_0^\xi f'(\sigma)\mathrm{d}\sigma = \left[\int_0^1 f'(\lambda\xi)\mathrm{d}\lambda\right]\xi, \quad \xi\lambda = \sigma. \tag{A-88}$$

With $f(\cdot) = \phi_i(\cdot)$ and $\xi = S_i^\top \mathbf{z}$ this equates to

$$S_i\phi_i(-S_i^\top \mathbf{z}) = -S_i \left[\int_0^1 \phi_i'(\lambda S_i^\top \mathbf{z})\mathrm{d}\lambda\right] S_i^\top \mathbf{z} = -S_i[D_\phi(\mathbf{z})]_{ii} S_i^\top \mathbf{z} \tag{A-89}$$

with $[D_\phi]_{ii}$ strictly positive and bounded, showing that $\boldsymbol{\phi}(-S^\top \mathbf{z}) = -D_\phi(\mathbf{z})S^\top \mathbf{z}$.

Now the state dynamics from Equation (A-85) can be rewritten as

$$\dot{\mathbf{z}}(t) = \begin{bmatrix} S & B \end{bmatrix} \begin{bmatrix} -D_\phi(\mathbf{z}) & \mathbb{0} \\ \mathbb{0} & -\gamma D_v(\mathbf{z}) \end{bmatrix} \begin{bmatrix} S^\top \\ B^\top \end{bmatrix} \mathbf{z} \doteq A(\mathbf{z})\mathbf{z}(t) \tag{A-90}$$

where matrix $A(\mathbf{z})$ has strictly negative diagonal entries and non-negative off-diagonal entries. Furthermore matrix $A(\mathbf{z})$ is diagonally dominant and strictly diagonally dominant if the system is connected to the environment (B containing a column with just one non-zero entry). Since $A(\mathbf{z})$ is (strictly) diagonally dominant, it is Lyapunov stable [27]. If the graph corresponding to the system is strongly connected, $A(\mathbf{z})$ is irreducible. Therefore an externally- and strongly connected graph implies an irreducible, strictly diagonally dominant matrix $A(\mathbf{z})$ with negative diagonal entries, and as such $\dot{\mathbf{z}}(t) = A(\mathbf{z})\mathbf{z}(t)$ is asymptotically stable [27].

Example

Consider a data transmission system consisting of 5 macro-nodes (routers) with internal switching dynamics, as discussed in [7] and shown in Figure A-14.
The macro-nodes need to process a certain demand denoted by the blue dashed lines, this is done by controlling the flow between the macro-nodes. The internal dynamics of a macro-node can be represented by

$$\dot{x}_i = A_i x_i + [B\mathbf{u}]_i + d_i. \tag{A-91}$$

The internal dynamics of the macro-nodes are based on probabilities that a packet is transferred between the internal nodes. With parameters α_{AA}, α_{AB}, α_{AC} and α_{AD} defined as the probability that a packet is send from node IA to nodes AA, AB, AC and AD respectively; vice versa for the parameters $\alpha_{AA'}$, α_{BA}, α_{CA} and α_{DA}. The switching probability matrix is

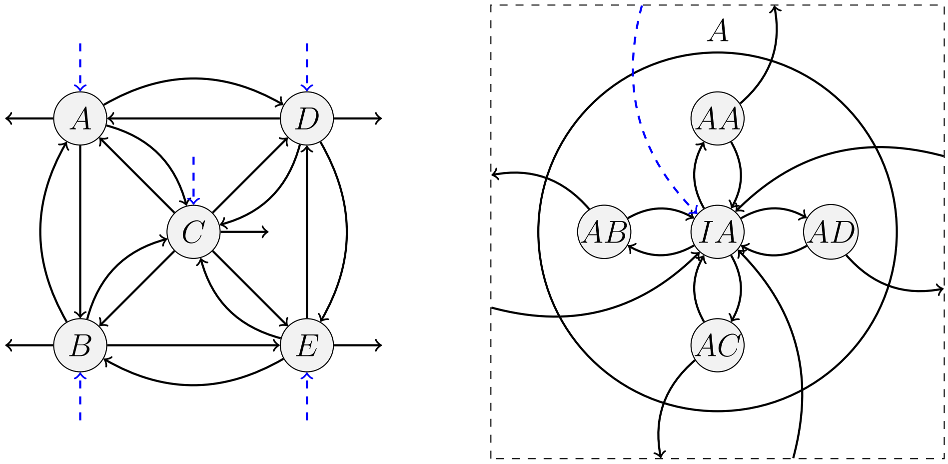

Figure A-14: The 5 macro-nodes of the communication network (left) and the internal dynamics per macro-node (right).

$$A_A = \begin{bmatrix} -(\alpha_{AA}+\alpha_{AB}+\alpha_{AC}+\alpha_{AD}) & \alpha_{BA} & \alpha_{CA} & \alpha_{DA} & \alpha_{AA'} \\ \alpha_{AB} & -\alpha_{BA} & 0 & 0 & 0 \\ \alpha_{AC} & 0 & -\alpha_{CA} & 0 & 0 \\ \alpha_{AD} & 0 & 0 & -\alpha_{DA} & 0 \\ \alpha_{AA} & 0 & 0 & 0 & -\alpha_{AA'} \end{bmatrix} \tag{A-92}$$

likewise for the other macro-nodes.

Defining $A = \text{blockdiag}(A_A, A_B, A_C, A_D, A_E)$ and $\mathbf{d} = [d_A^\top, d_B^\top, d_C^\top, d_D^\top, d_E^\top]^\top$ then yields

$$\dot{\mathbf{x}} = A\mathbf{x} + B\mathbf{u} + \mathbf{d}. \tag{A-93}$$

Three different control strategies were applied to this system, which are discussed in detail in [7]:

- $\mathbf{u} = \text{sat}(-\gamma B^\top \mathbf{x})$
- $\mathbf{u} = \text{sat}(-\gamma B^\top H \mathbf{x})$
- $\mathbf{u} = \text{sat}(-\gamma \tilde{B}^\top \mathbf{x})$

where $H = \text{blockdiag}(\frac{1}{5}\mathbb{1}_{5\times5}, \frac{1}{5}\mathbb{1}_{5\times5}, \frac{1}{6}\mathbb{1}_{6\times6}, \frac{1}{5}\mathbb{1}_{5\times5}, \frac{1}{5}\mathbb{1}_{5\times5})$ and $\tilde{B} = \min(B, 0)$. Furthermore the saturation function is set to clip the input between 0 and 1.

With $\gamma = 3$, probability parameters $\alpha_{AA} = \alpha_{AB} = \alpha_{AC} = \alpha_{AD} = 1$, $\alpha_{BA} = \alpha_{CA}, = \alpha_{DA} = 0.25$ and $\alpha_{AA'} = 0.05$ (similarly for the other macro nodes) and a demand of

$$d_A = \begin{bmatrix} 0.6 \\ 0 \\ 0 \\ 0 \\ 0 \end{bmatrix}, \quad d_B = \begin{bmatrix} 0.2 \\ 0 \\ 0 \\ 0 \\ 0 \end{bmatrix}, \quad d_C = \begin{bmatrix} 0.7 \\ 0 \\ 0 \\ 0 \\ 0 \\ 0 \end{bmatrix}, \quad d_D = \begin{bmatrix} 0.5 \\ 0 \\ 0 \\ 0 \\ 0 \end{bmatrix}, \quad d_E = \begin{bmatrix} 1.2 \\ 0 \\ 0 \\ 0 \\ 0 \end{bmatrix} \tag{A-94}$$

where the demand d_D increased by a factor 3 at $t = 150$. The resulting response is shown if Figure A-15.

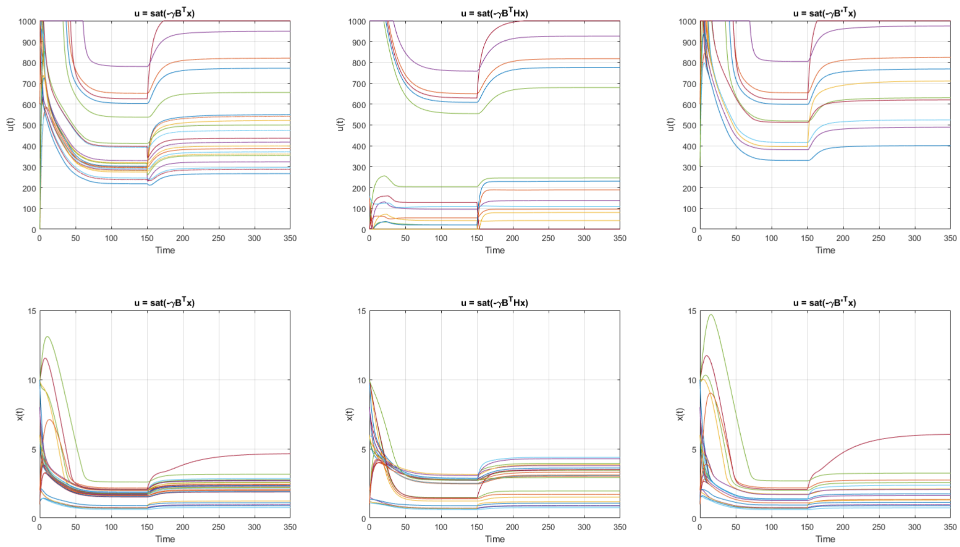

Figure A-15: Response of the data transmission system with different types of saturated feedback control.

As can be seen from the responses in Figure A-15, all control methods result in a stabilized system. Furthermore the H-saturated control results in a faster convergence.

A-4 Game theory

In this section the concept of game theory will be discussed. The first section will briefly detail generalized Nash equilibrium problems (GNEP), followed by proximal dynamics, and ending with a section discussing dynamical games.

A-4-1 Generalized Nash equilibrium problems

A GNEP is the problem of finding a solution to the minimization

$$\forall v : \quad \min_{x^v} \theta_v(x^v, \mathbf{x}^{-v}) \quad s.t. \; x^v \in X_v(\mathbf{x}^{-v}), \tag{A-95}$$

where $\mathbf{x}^{-v}$ is the vector of states where the vth vector is omitted. This minimization problem differs from standard Nash equilibrium problems due to the feasible set of x^v depending on the other states as well, $X_v(\mathbf{x}^{-v})$. The set of solutions for agent v is denoted by $\mathcal{S}_v(\mathbf{x}^{-v})$. In essence, the GNEP is the problem to find a vector $\bar{\mathbf{x}}$ such that $\bar{x}^v \in \mathcal{S}_v(\mathbf{x}^{-v})$ for all v. Defining the solution set for all states as $\mathcal{S}(\mathbf{x}) := \Pi_{v=1}^{N} \mathcal{S}_v(\mathbf{x}^{-v})$ then $\bar{\mathbf{x}}$ is a solution to the GNEP if and only if $\bar{\mathbf{x}} \in \mathcal{S}(\bar{\mathbf{x}})$.

A way of finding (a subset of) solutions to the GNEP is by using the concept of quasi-variational inequality. Given the set of feasible states $\mathbf{X}(\mathbf{x}) := \cap_v X_v(\mathbf{x}^{-v})$ and the gradient of the cost-functions $\mathbf{F}(\mathbf{x}) := (\nabla_{x^v} \theta_v(x^v, \mathbf{x}^{-v}))_{v=1}^{N}$, the quasi-variational inequality problem denoted as $QVI(\mathbf{X}(\mathbf{x}), \mathbf{F}(\mathbf{x}))$ then consists of finding an equilibrium $\bar{\mathbf{x}} \in \mathbf{X}(\mathbf{x})$ such that

$$(\mathbf{y} - \bar{\mathbf{x}})^\top \mathbf{F}(\bar{\mathbf{x}}) \geq 0 \quad \forall \mathbf{y} \in \mathbf{X}(\mathbf{x}). \tag{A-96}$$

Solutions obtained using the quasi-variational inequality approach are a subset of the solution set of the original GNEP, these solutions are referred to as variational equilibria.
Now referring to the feasible set of states $X_v(\mathbf{x}^{-v})$, which can be reformulated as

$$X_v(\mathbf{x}^{-v}) = \{x^v \in \mathbb{R}^v \ : \ \mathbf{g}^v(x^v, \mathbf{x}^{-v}) \leq 0\}. \tag{A-97}$$

If the constraints $\mathbf{g}^v$ are equal for all v, i.e. $\mathbf{g}^1 = \mathbf{g}^2 = \cdots = \mathbf{g}^N = \mathbf{g}(\mathbf{x})$, and $\mathbf{g}(\mathbf{x})$ is component-wise convex with respect to the states x_v, the system is called jointly convex.

A-4-2 Proximal dynamics

With the definition GNEPs as given in previous section, methods to solve game-theoretic problems can be discussed. In this section a way to solve multi-agent games by means of proximal mappings will be analysed, as in [13] and references therein. Such a proximal mapping is defined as $\text{prox}_f(x) := \arg\min_{y \in \mathbb{R}^n} f(y) + \frac{1}{2}\|x - y\|^2$.

Local constraints

Consider a game with N agents, with an adjacency matrix A corresponding to the directed communication graph. Through this communication graph the agents seek an equilibrium state for the game

$$\min_{x^v} \theta_v(x^v, A\bar{\mathbf{x}}), \quad s.t. \ x^v \in X_v(\mathbf{x}^{-v}). \tag{A-98}$$

For simplicity first a game with only local constraints will be considered, $X_v(\mathbf{x}^{-v}) = X_v$. In this case the game simplifies to

$$\min_{x^v \in X_v} \theta_v(x^v, \mathbb{e}_v^\top A\bar{\mathbf{x}}). \tag{A-99}$$

Using an indicator function for the feasible set X_v such that $\imath_{X_v}(x^v)$ equals zero if $x^v \in X_v$ and infinity if $x^v \notin X_v$ and adding a proximal term to penalize the distance between the local state and the average state of the other agents, then yields

$$\min_{x^v \in \mathbb{R}} \theta_v(x^v, \mathbb{e}_v^\top A\bar{\mathbf{x}}) + \imath_{X_v}(x^v) + \frac{1}{2}\|x^v - \mathbb{e}_v^\top A\bar{\mathbf{x}}\|^2. \tag{A-100}$$

However, since finding the equilibrium state of agent v requires that the equilibrium of the other states is known, finding the solution to this problem is not trivial. Defining $f^v := \theta_v(x^v, \mathbb{e}_v^\top A\bar{\mathbf{x}}) + \imath_{X_v}(x^v)$, the equilibrium can be obtained iteratively using

$$x^v(k+1) = \text{prox}_{f^v}(\mathbb{e}_v^\top A\mathbf{x}(k)). \tag{A-101}$$

This iteration method is stable if the adjacency matrix A is an averaged adjacency matrix. This implies that the linear matrix inequality

$$\begin{bmatrix} (2\eta - 1)I + (1-\eta)(A^\top + A) & A^\top \\ A & I \end{bmatrix} \geq 0, \quad \eta \in (0,1) \tag{A-102}$$

holds. A sufficient condition is that the adjacency matrix is doubly stochastic and all self loops are present.

If not all self loops are present, the iteration does not guarantee to converge to a network equilibrium. Instead the following approach can be used

$$x^v(k+1) = (1-\alpha)x^v(k) + \alpha \ \text{prox}_{f^v}(\mathbb{e}_v^\top A\mathbf{x}(k)), \quad \alpha \in (0,1). \tag{A-103}$$

Local constraints and jointly convex

Now that the system with only local constraints can be solved, jointly convex constraints $\mathbf{g}(x^v, \mathbf{x}^{-v}) \leq 0$ can be added, resulting in $X_v(\mathbf{x}^{-v}) = \{x^v \in \mathbb{R}^v \ : \ \mathbf{g}^v(x^v, \mathbf{x}^{-v}) \leq 0\}$. Due to the addition of coupling constraints, the optimisation problem cannot be solved using the previously mentioned iteration methods. Instead an extended network equilibrium problem will be considered, defined as:

$$\bar{x}^v = \arg\min_{x^v \in \mathbb{R}} f^v + \frac{1}{2}\|x^v - \mathbb{e}_v^\top A\bar{\mathbf{x}}\|^2 + \bar{\lambda}^\top \mathbf{g}^v(x^v, \bar{\mathbf{x}}^{-v}) \tag{A-104}$$

$$\bar{\lambda} = \arg\min_{\xi \in \mathcal{L}} -\xi^\top \mathbf{g}(\bar{\mathbf{x}}). \tag{A-105}$$

Where the dual variables λ are bounded by a set $\mathcal{L} := [0, \hat{\lambda}]$ with $\hat{\lambda} > 0$. Furthermore it is assumed that jointly convex constraints are separable, meaning that $\mathbf{g}(\mathbf{x}) = \sum_{v=1}^N \mathbf{g}^v(x^v) \leq 0$. In this case the separated constraints can be added to the local constraints with $\mathbf{g}^v(x^v) \leq \zeta^v$ and $\sum_{v=1}^N \zeta^v \leq 0$ as the affine coupling constraint. Note that affine coupling constraints are separable, therefore the following constraints will be considered:

$$\mathbf{g}(\mathbf{x}) := C\mathbf{x} + c = \begin{bmatrix} C_1 & C_2 & \cdots & C_N \end{bmatrix} \mathbf{x} + c \tag{A-106}$$

Which can be separated as $\mathbf{g}(\mathbf{x}) = c + \sum_{v=1}^{N} C_v x^v \leq 0$, thus $C_v x^v \leq \zeta^v$ with $c + \sum_{v=1}^{N} \zeta^v \leq 0$.

For the dual variables the proximal mapping can also be used by rewriting the problem as

$$\begin{aligned} \bar{\lambda} &= \arg\min_{\xi \in \mathcal{L}} -\xi^\top \mathbf{g}(\bar{\mathbf{x}}) + \frac{1}{2}\|\xi - \bar{\lambda}\|^2 && \text{(A-107)} \\ &= \text{prox}_{\iota_{\mathcal{L}}}\left(\bar{\lambda} + \mathbf{g}(\bar{\mathbf{x}})\right) && \text{(A-108)} \\ &= \text{proj}_{\mathcal{L}}\left(\bar{\lambda} + \mathbf{g}(\bar{\mathbf{x}})\right). && \text{(A-109)} \end{aligned}$$

As a result the following mappings can be defined

$$\begin{aligned} \boldsymbol{\mathcal{F}} &:= \text{diag}(\text{prox}_{f^1}, \ldots, \text{prox}_{f^N}, \text{proj}_{\mathcal{L}}) && \text{(A-110)} \\ \boldsymbol{\mathcal{G}} &:= \begin{bmatrix} A & -C^\top \\ C & I \end{bmatrix} \cdot + \begin{bmatrix} \mathbb{0} \\ c \end{bmatrix} && \text{(A-111)} \end{aligned}$$

which results in the following iteration method

$$\begin{bmatrix} \mathbf{x}(k+1) \\ \lambda(k+1) \end{bmatrix} = (\boldsymbol{\mathcal{F}} \circ \boldsymbol{\mathcal{G}}) \begin{bmatrix} \mathbf{x}(k) \\ \lambda(k) \end{bmatrix}. \tag{A-112}$$

However, since in general $\begin{bmatrix} A & -C^\top \\ C & I \end{bmatrix} > 1$ the iteration may fail to converge. As such a distributed protocol can be used, such as the following forward-backward-forward distributed protocol:

$$\begin{aligned} \begin{bmatrix} \tilde{\mathbf{x}}(k) \\ \tilde{\lambda}(k) \end{bmatrix} &= ((1-\alpha)\text{Id} + \alpha\boldsymbol{\mathcal{G}}) \begin{bmatrix} \mathbf{x}(k) \\ \lambda(k) \end{bmatrix} && \text{(A-113)} \\ \begin{bmatrix} \mathbf{x}(k+\frac{1}{2}) \\ \lambda(k+\frac{1}{2}) \end{bmatrix} &= \boldsymbol{\mathcal{F}}_\alpha\left(\begin{bmatrix} \tilde{\mathbf{x}}(k) \\ \tilde{\lambda}(k) \end{bmatrix}\right) && \text{(A-114)} \\ \begin{bmatrix} \tilde{\mathbf{x}}(k+\frac{1}{2}) \\ \tilde{\lambda}(k+\frac{1}{2}) \end{bmatrix} &= ((1-\alpha)\text{Id} + \alpha\boldsymbol{\mathcal{G}}) \begin{bmatrix} \mathbf{x}(k+\frac{1}{2}) \\ \lambda(k+\frac{1}{2}) \end{bmatrix} && \text{(A-115)} \\ \begin{bmatrix} \mathbf{x}(k+1) \\ \lambda(k+1) \end{bmatrix} &= \begin{bmatrix} \tilde{\mathbf{x}}(k+\frac{1}{2}) \\ \tilde{\lambda}(k+\frac{1}{2}) \end{bmatrix} + \alpha\,(\text{Id} - \boldsymbol{\mathcal{G}}) \begin{bmatrix} \mathbf{x}(k) \\ \lambda(k) \end{bmatrix} && \text{(A-116)} \end{aligned}$$

where $\boldsymbol{\mathcal{F}}_\alpha = \text{diag}(\text{prox}_{\alpha f^1}, \ldots, \text{prox}_{\alpha f^N}, \text{proj}_{\mathcal{L}})$.

Note that the dual variable λ should converge to the same value for each agent. As such in this protocol the variable shall be updated by an agent with full information on the coupling constraing $g(\mathbf{x})$. Either an extra communication graph $\mathcal{G}_c(\mathcal{V}, \mathcal{E}_c)$ is introduced which is fully connected, or the individual agents reach a consensus on the dual variable. For the latter approach, the study of consensus as described in Chapter A-2 is of use.

A-4-3 Dynamical Cournot competition

Game theory plays a prevalent role in economics; for example in Cournot competition problems where the problem to find a supply-demand equilibrium arises. Consider such a Cournot competition consisting of n producers and consumers as mentioned in [15]. In this model both producers and consumers have a certain goal. Denoting producer i by P_{gi} and consumer i by P_{di}, the model can be described as

$$\bar{P}_{gi} = \arg\max_{P_{gi}\geq 0} P_{gi} \cdot p(P_{gi}, \bar{\mathbf{P}}_{-gi}) - C_{gi}(P_{gi}) \tag{A-117}$$

$$\bar{P}_{di} = \arg\max_{P_{di}\geq 0} U_i(P_{di}) - P_{di} \cdot \bar{p} \tag{A-118}$$

where U_i is continuously differentiable with $U_i'(0) > 0$ and C_{gi} is convex, non-decreasing and continuously differentiable with $C_{gi}(0) = 0$. Given a price $\bar{p} = p(\bar{P}_{gi}, \bar{\mathbf{P}}_{-gi})$, the consumer maximisation problem results in

$$\bar{P}_{dj} = \begin{cases} (U_i')^{-1}(\bar{p}) & \text{if } \bar{p} < U_i'(0) \\ 0 & \text{if } \bar{p} \geq U_i'(0) \end{cases}. \tag{A-119}$$

Both maximization problems are linked by a supply-demand balancing, meaning that

$$\mathbb{1}_n \mathbf{P}_g = \mathbb{1}_n \mathbf{P}_d. \tag{A-120}$$

Linear-quadratic functions

With the general Cournot competition explained, the linear-quadratic model will be considered. This model simplifies the general case with

$$U_i(P_{di}) = -\tfrac{1}{2} P_{di} Q_{di} P_{di} + b_{di} P_{di} \tag{A-121}$$

$$C_{gi}(P_{gi}) = \tfrac{1}{2} P_{gi} Q_{gi} P_{gi} + b_{gi} P_{gi} \tag{A-122}$$

resulting in

$$\bar{P}_{dj} = \begin{cases} Q_{di}^{-1}(b_{di} - \bar{p}) & \text{if } \bar{p} < b_{di} \\ 0 & \text{if } \bar{p} \geq b_{di} \end{cases}. \tag{A-123}$$

Now assuming that $\bar{p} < \min_i b_{di}$, the expression can be inverted to

$$\bar{p} = \beta^\star - \alpha^\star \mathbb{1}_n^\top \mathbf{P}_d \tag{A-124}$$

with

$$\beta^\star = \frac{\mathbb{1}_n^\top Q_d^{-1}\mathbf{b}_d}{\mathbb{1}_n^\top Q_d^{-1}\mathbb{1}_n}, \quad \alpha^\star = \frac{1}{\mathbb{1}_n^\top Q_d^{-1}\mathbb{1}_n}. \tag{A-125}$$

Now defining the price function on the producers' end as

$$p(P_{gi}, \mathbf{P}_{-gi}) = \beta - \alpha P_{gi} - \alpha \mathbb{1}_n^\top \mathbf{P}_{-gi} \tag{A-126}$$

resulting in the solution

$$\bar{\mathbf{P}}_g = (\alpha(I_n + \mathbb{1}_{n\times n}) + Q_g)^{-1} (\mathbb{1}_n \beta - \mathbf{b}_g). \tag{A-127}$$

Rewriting the solutions with implicitly including the price and using $\star$ to denote the Cournot-Nash equilibrium then yields

$$p^\star = \beta - \alpha \mathbb{1}_n^\top \mathbf{P}_g^\star \tag{A-128}$$

$$\mathbf{P}_g^\star = (\alpha I_n + Q_g)^{-1} (\mathbb{1}_n p^\star - \mathbf{b}_g) \tag{A-129}$$

$$\mathbf{P}_d^\star = Q_d^{-1}(\mathbf{b}_d - \mathbb{1}_n p^\star) \tag{A-130}$$

Note that in general $\alpha \neq \alpha^\star$ and $\beta \neq \beta^\star$, and as a result there is a mismatch in the supply-demand balancing. More specifically it can be seen that

$$\mathbb{1}_n^\top \mathbf{P}_d^\star = \mathbb{1}_n^\top Q_d^{-1}\mathbf{b}_d - \mathbb{1}_n^\top Q_d^{-1}\mathbb{1}_n \beta + \mathbb{1}_n^\top Q_d^{-1}\mathbb{1}_n \alpha \mathbb{1}_n^\top \mathbf{P}_g^\star \tag{A-131}$$

$$= \frac{\beta^\star - \beta}{\alpha^\star} + \frac{\alpha}{\alpha^\star}\mathbb{1}_n^\top \mathbf{P}_g^\star. \tag{A-132}$$

To resolve this issue, a dynamical system will be introduced which, with a correct feedback control, leads to a balanced system.

Cournot network dynamics

Consider a network of n agents with an undirected graph $\mathcal{G}(\mathcal{V}, \mathcal{E})$, where the neighbour set of node i is defined as $\mathcal{N}_i = \{j \in \mathcal{V} \ : \ \{i,j\} \in \mathcal{E}\}$. The following second-order dynamics will be introduced

$$m_i \ddot{x}_i + d_i \dot{x}_i - \sum_{j \in \mathcal{N}_i} \nabla H_{ij}(x_i - x_j) = P_{gi} - P_{di}, \quad m_i, d_i > 0 \tag{A-133}$$

where $H_{ij} : \mathbb{R} \to \mathbb{R}$ is continously differentiable and convex with $H_{ij}(x) \geq H_{ij}(0)$. Note that a mismatch in production and consumption means that the state of node i drifts from its unforced behaviour.

With B as the incidence matrix of graph $\mathcal{G}$, the dynamics can be rewritten as

$$\dot{\mathbf{x}} = \mathbf{y} \tag{A-134}$$

$$M\dot{\mathbf{y}} = -D\mathbf{y} - B\nabla H(B^\top \mathbf{x}) + \mathbf{P}_g - \mathbf{P}_d \tag{A-135}$$

where $M = \text{diag}(m_i)$, $D = \text{diag}(d_i)$ and $\nabla H = \text{col}(\nabla H_{ij})$. Note that if (x, y) is an equilibrium of the system so is $(x + c\mathbb{1}_n, y)$, since $B^\top \mathbb{1}_n = \mathbb{0}_n$. As a result a change of coordinates is introduced, namely

$$\zeta_i = x_i - x_n \tag{A-136}$$

or defining $E^\top = [I_{n-1},\ -\mathbb{1}_{n-1}]$

$$\boldsymbol{\zeta} = E^\top \mathbf{x}. \tag{A-137}$$

With B_ζ being the incidence matrix with the n-th row removed, the function H_ζ can be defined such that $H(B_\zeta^\top \boldsymbol{\zeta}) = H_\zeta(\boldsymbol{\zeta})$, and as such $B_\zeta \nabla H(B_\zeta^\top \boldsymbol{\zeta}) = \nabla H_\zeta(\boldsymbol{\zeta})$. Doing so leads to the following dynamics

$$\dot{\boldsymbol{\zeta}} = E^\top \mathbf{y} \tag{A-138}$$

$$M\dot{\mathbf{y}} = -D\mathbf{y} - E\nabla H_\zeta(\boldsymbol{\zeta}) + \mathbf{P}_g - \mathbf{P}_d. \tag{A-139}$$

Now given constant demand and supply vectors $\mathbf{P}_d = \bar{\mathbf{P}}_d$ and $\mathbf{P}_g = \bar{\mathbf{P}}_g$, the point $(\bar{\boldsymbol{\zeta}}, \bar{\mathbf{y}})$ is an equilibrium with

$$\bar{\mathbf{y}} = \mathbb{1}_n \frac{(\bar{\mathbf{P}}_g - \bar{\mathbf{P}}_d)^\top \mathbb{1}_n}{\mathbb{1}_n^\top D \mathbb{1}_n} \tag{A-140}$$

$$\nabla H_\zeta(\bar{\boldsymbol{\zeta}}) = E^\dagger \left(\bar{\mathbf{P}}_g - \bar{\mathbf{P}}_d - D\bar{\mathbf{y}}\right) \tag{A-141}$$

with $E^\dagger = (E^\top E)^{-1} E^\top$.

Now a feedback can be introduced that regulates the production and demand to the Cournot-Nash solution, $\mathbf{P}_g = \mathbf{P}_g^\star$ and $\mathbf{P}_d = \mathbf{P}_d^\star$. Note that regulating the production and pricing results in a certain demand, given an estimated price $p_i(t)$ for consumer i the demand follows as

$$P_{di}(t) = Q_{di}^{-1}(b_{di} - p_i(t)). \tag{A-142}$$

Since the price $p_i(t)$ is required for the entire network, an extra communication layer will be introduced denoted by $\mathcal{G}_c(\mathcal{V}, \mathcal{E}_c)$ with neighbour set $\mathcal{N}_i^c$, analogously to Section A-4-2. Using the communication layer, the following pricing and production update can be introduced

$$\tau_i \dot{p}_i = -k_i y_i - Q_{di}^{-1} y_i - \sum_{j \in \mathcal{N}_i^c} \rho_{ij}(p_i - p_j) \tag{A-143}$$

$$P_{gi} = k_i(p_i - b_{gi}) \tag{A-144}$$

with $\tau_i > 0$ the time constant, $k_i > 0$ the controller gain and ρ_{ij} the weight of the edges of the communication layer. With $T = \text{diag}(\tau_i)$, $K = \text{diag}(k_i)$ and L_c the Laplacian matrix of $\mathcal{G}_c$, the overall system becomes

$$\dot{\boldsymbol{\zeta}} = E^\top \mathbf{y} \tag{A-145}$$
$$M\dot{\mathbf{y}} = -D\mathbf{y} - E\nabla H_\zeta(\boldsymbol{\zeta}) + K(\mathbf{p} - \mathbf{b}_g) + Q_d^{-1}(\mathbf{p} - \mathbf{b}_d) \tag{A-146}$$
$$T\dot{\mathbf{p}} = -L\mathbf{p} - K\mathbf{y} - Q_d^{-1}\mathbf{y} \tag{A-147}$$

The equilibrium of this feedback system $(\bar{\boldsymbol{\zeta}}, \bar{\mathbf{y}}, \bar{\mathbf{p}})$ now becomes

$$\bar{\mathbf{y}} = \mathbb{0}_n \tag{A-148}$$
$$\bar{\mathbf{p}} = \mathbb{1}_n \frac{\mathbb{1}_n^\top K\mathbf{b}_g + \mathbb{1}_n^\top Q_d^{-1}\mathbf{b}_d}{\mathbb{1}_n^\top K\mathbb{1}_n + \mathbb{1}_n^\top Q_d^{-1}\mathbb{1}_n} \tag{A-149}$$
$$\bar{\mathbf{P}}_g = K(\bar{\mathbf{p}} - \mathbf{b}_g) \tag{A-150}$$
$$\bar{\mathbf{P}}_d = Q_d^{-1}(\mathbf{b}_d - \bar{\mathbf{p}}) \tag{A-151}$$
$$\nabla H_\zeta(\bar{\bar{\boldsymbol{\zeta}}}) = E^\dagger\left(\bar{\mathbf{P}}_g - \bar{\mathbf{P}}_d\right) \tag{A-152}$$

Note that if $K = (\alpha^\star I_n + Q_g)^{-1}$, then it follows that $\bar{\mathbf{P}}_g = (\alpha^\star I_n + Q_g)^{-1}(\bar{\mathbf{p}} - \mathbf{b}_g) = \mathbf{P}_g^\star$. Furthermore the price equilibrium can be rewritten as $\bar{\mathbf{p}} = \mathbb{1}_n(\beta^\star - \alpha^\star \mathbb{1}_n^\top \mathbf{P}_g^\star) = \mathbf{p}^\star$.

To discuss the stability of this feedback control, the following Lyapunov function will be considered

$$V = \tfrac{1}{2}(\mathbf{y} - \bar{\mathbf{y}})^\top M(\mathbf{y} - \bar{\mathbf{y}}) + \tfrac{1}{2}(\mathbf{p} - \bar{\mathbf{p}})^\top T(\mathbf{p} - \bar{\mathbf{p}}) + \mathcal{H}(\boldsymbol{\zeta}) \tag{A-153}$$
$$\mathcal{H}(\boldsymbol{\zeta}) = H(\boldsymbol{\zeta}) - H(\bar{\boldsymbol{\zeta}}) - (\boldsymbol{\zeta} - \bar{\boldsymbol{\zeta}})^\top \left.\frac{\partial H}{\partial \boldsymbol{\zeta}}\right|_{\bar{\zeta}} \tag{A-154}$$

Due to the convexity of H, the Bregman distance $\mathcal{H}$ is non-negative and equal to zero if $\boldsymbol{\zeta} = \bar{\boldsymbol{\zeta}}$. Furthermore the time-derivative of the Lyapunov function is equal to

$$\dot{V} = -(\mathbf{y} - \bar{\mathbf{y}})^\top D(\mathbf{y} - \bar{\mathbf{y}}) - (\mathbf{p} - \bar{\mathbf{p}})^\top L(\mathbf{p} - \bar{\mathbf{p}}). \tag{A-155}$$

Since V is positive definite and $\dot{V}$ is non-positive, the solutions are bounded. Furthermore the equilibrium $(\bar{\boldsymbol{\zeta}}, \bar{\mathbf{y}}, \bar{\mathbf{p}})$ is unique and equal to the Cournot-Nash equilibrium under the earlier mentioned assumptions on K.

A-5 Summary

The fields of network dynamics and consensus, network-decentralized control and game theory were discussed in the previous chapters. These concepts will be used in the master thesis research following this literature review. In this chapter a quick summary will be given.

Summary: consensus

The study of consensus in multi-agent system describes the approach to obtain a certain agreement between participants on the value of a variable, as discussed in Chapter A-2. A useful tool to assist the analysis of consensus finding problems is graph theory. Consider a system with N participants described by a graph $\mathcal{G}(\mathcal{V},\mathcal{E})$. The adjacency matrix will be denoted by $A_{\mathcal{G}}$ and the Laplacian matrix by $L_{\mathcal{G}}$. The consensus finding problem then yields both a continuous-time formulation:

$$\dot{\mathbf{x}}(t) = -L\mathbf{x}(t) \tag{A-156}$$

and a discrete-time formulation:

$$\mathbf{x}(k+1) = A\mathbf{x}(k) \tag{A-157}$$

Whether these iterations yield consensus depends on the graph properties, mainly periodicity and connectivity. These properties can be determined looking at the adjacency matrix corresponding to the graph. They can be assessed using the following table, with the strongest assumption leading (i.e. if the graph is primitive then it is both strongly connected and aperiodic, even though it is also irreducible):

		Strongly connected	Aperiodic
primitive:	$A_{\mathcal{G}}^k \succ \mathbb{0},\ k > k^*$	✓	✓
irreducible:	$\sum_{k=1}^{N} A_{\mathcal{G}}^k \succ \mathbb{0}$	✗	✓
non-negative:	$A_{\mathcal{G}} \succeq \mathbb{0}$	✗	✗

The periodicity and connectivity then leads to a consensus (or not) according to

Discrete-/Continuous-time	Strongly connected	Weakly connected one sink	Weakly connected multiple sinks
Periodic	✓/✓	✓/✓	✗/✗
Aperiodic	✗/✓	✗/✓	✗/✗

Summary: network-decentralized control

To briefly summarize the findings of Chapter A-3, consider a linear network-decentralized system with N subsystems where every subsystem has a state $\mathbf{q}_i(t)$. The susbsystems are connected through edges, which can be described using a graph $\mathcal{G}(\mathcal{V},\mathcal{E})$. The incidence matrix of the graph will be defined as $B_{\mathcal{G}}$. For the notion of controllability, the control between subsystems can be modelled using the graph edges. Where the state flow between two subsystems is determined by the control action $u_j(t)$. As a result, the overall system can be described as

$$\dot{\mathbf{q}}(t) = A\mathbf{q}(t) + B\mathbf{u}(t) + E\mathbf{d}(t), \quad B \in \mathcal{S}(B_{\mathcal{G}}) \tag{A-158}$$

with $\mathbf{d}(t)$ being an external demand vector.

Decentralized stability

Using a control law $\mathbf{u}(t) = -K\mathbf{q}(t)$ with $K \in \mathcal{S}(B_{\mathcal{G}}^{\top})$ (which ensures the control is network-decentralized), the stabilizability of the system can be analysed. First it is assumed that the system in general is stable, meaning that (A, B) is stable. Since an unstable system cannot be stabilized when introducing more limitations to the control scheme. In case of distinct unstable eigenvalues of the subsystem dynamics A_i, a suitable feedback matrix K can be determined by solving the Lyapunov equation

$$\min ||K||_2 \ : \ (A - BK)^{\top} P + P(A - BK) < 0, \quad K \in \mathcal{S}(B_{\mathcal{G}}^{\top}), \ P > 0. \tag{A-159}$$

In case of a single common unstable eigenvalue between the subsystems, the structure of the K matrix will implicitly be defined by setting $K = \gamma B^{\top} P$, with P having a block-diagonal structure. Then defining $S = P^{-1}$, a suitable control law can be found by solving

$$SA^{\top} + AS - 2\gamma BB^{\top} < 0 \tag{A-160}$$

for S. This LMI has a structured solution under the given assumptions.

Robust control

Consider a similar (possibly non-linear) network system of N subsystems but with uncontrollable flow between edges described by the unknown functions $\tilde{\boldsymbol{\phi}}_j(\mathbf{x})$. Yielding the system dynamics

$$\dot{\mathbf{q}}(t) = S\tilde{\boldsymbol{\phi}}(-S^{\top}\mathbf{q}) + B\mathbf{u}(t) + E\mathbf{d}(t) \tag{A-161}$$

where $[S, B] \in \mathcal{S}(B_{\mathcal{G}})$ up to a possible reordering of edges. The control $\mathbf{u}(t)$ will be restricted in view of possible actuator limitations, hence $\mathbf{u}^{-} \leq \mathbf{u} \leq \mathbf{u}^{+}$. Assuming a constant demand vector $\mathbf{d}(t) = \mathbf{d}$, the system reaches an equilibrium $(\bar{\mathbf{q}}, \bar{\mathbf{u}})$ (under the assumption that $\bar{\mathbf{u}}$ fulfils the imposed restriction) when

$$\mathbb{0}_n = S\tilde{\boldsymbol{\phi}}(-S^{\top}\bar{\mathbf{q}}) + B\bar{\mathbf{u}}(t) + E\mathbf{d}. \tag{A-162}$$

Analysis of the system around this equilibrium then leads to the conclusion that a control law of the form $\mathbf{u}(t) = \mathrm{sat}(-\gamma B^{\top}(\mathbf{q}(t) - \bar{\mathbf{q}}) + \bar{\mathbf{u}})$ yields a stable system (where $\mathrm{sat}(\cdot)$ clips the signal such that the control does not exceed the limitations).

Estimation

Instead of control along the edges of the graph, measurements can be taken as well. Consider again a system of N participants with graph $\mathcal{G}(\mathcal{V}, \mathcal{E})$. Each system once more has an internal state $\mathbf{q}_i(t)$, but also an internal control action $\mathbf{u}_i(t)$. Leading to the overall dynamics

$$\dot{\mathbf{q}}(t) = A\mathbf{q}(t) + B\mathbf{u}(t) \quad B = \mathrm{blockdiag}\{B_1, \ldots, B_n\}. \tag{A-163}$$

Each agent has no direct information about their own state $\mathbf{q}_i(t)$. However, along the edges of the graph the difference in output between the connecting agents will be measured, resulting in

$$\mathbf{y}(t) = C\mathbf{q}(t), \quad C \in \mathcal{S}(B_{\mathcal{G}}^\top). \tag{A-164}$$

Using these measurements an estimation of the state can be made, defined as $\hat{\mathbf{q}}(t)$. Introducing an observer matrix $L \in \mathcal{S}(B\mathcal{G})$, this leads to the following dynamics

$$\dot{\mathbf{q}}(t) = A\mathbf{q}(t) + B\mathbf{u}(t) \tag{A-165}$$

$$\mathbf{y}(t) = C\mathbf{q}(t) \tag{A-166}$$

$$\dot{\hat{\mathbf{q}}}(t) = A\hat{\mathbf{q}}(t) + B\mathbf{u}(t) + LC\hat{\mathbf{q}}(t) - L\mathbf{y}(t)). \tag{A-167}$$

The error dynamics $\mathbf{e}(t) = \mathbf{q}(t) - \hat{\mathbf{q}}(t)$ is asymptotically stable with an observer feedback of $L = -\gamma P^{-1}C^\top$ where P solves

$$A^\top P + PA - 2\gamma C^\top C < 0, \quad P > 0. \tag{A-168}$$

The inequality has a solution for homogeneous systems where (A, C) is detectable and the system is externally connected, thus $B_{\mathcal{G}}$ has full rank.

Summary: game theory

Consider a multi-agent game with N agents, each having a state $x_v \in \mathbb{R}^{n_v}$. A game theory problem as introduced in Chapter A-4 can then be defined as finding a vector $\bar{\mathbf{x}} = [\bar{x}_1^\top, \ldots, \bar{x}_N^\top]^\top$ such that

$$\bar{x}_v \in \arg\min_{x_v \in \mathbb{R}^{n_v}} \theta_v(x_v, \bar{\mathbf{x}}_{-v}), \quad s.t.\ \bar{x}_v \in X_v(\bar{\mathbf{x}}_{-v}) \tag{A-169}$$

with $\theta_v(\cdot)$ the objective function of the agent and $X_v(\cdot)$ a certain constraint on the state of the agent. A way of defining this constraint set is by means of constraint functions $\mathbf{g}_v(\cdot)$, such that

$$X_v(\mathbf{x}_{-v}) := \{x_v \in \mathbb{R}^{n_v} : \mathbf{g}_v(x_v, \mathbf{x}_{-v}) \leq 0\}. \tag{A-170}$$

The game is said to be jointly convex if the constraints for all agents are equal, thus $\mathbf{g}_1 = \mathbf{g}_2 = \cdots = \mathbf{g}_N = \mathbf{g}(\mathbf{x})$, and the constraint function $\mathbf{g}(\cdot)$ is component-wise convex.

Proximal dynamics

Consider a decentralized multi-agent game with N agents with graph $\mathcal{G}(\mathcal{V}, \mathcal{E})$ and adjacency matrix $A_{\mathcal{G}}$, where

$$\bar{x}_v = \arg\min_{x_v \in X_v} \theta_v(x_v, \mathbb{e}_v^\top A_{\mathcal{G}}\bar{\mathbf{x}}) \tag{A-171}$$

with local constraints X_v. The local constraints can be included implicitly by defining

$$\imath_{X_v}(x_v) := \begin{cases} 0 & \text{if } x_v \in X_v \\ \infty & \text{if } x_v \notin X_v \end{cases} \tag{A-172}$$

and redefining the game as

$$\min_{x^v \in \mathbb{R}} \theta_v(x_v, \mathbb{e}_v^\top A_\mathcal{G}\bar{\mathbf{x}}) + \imath_{X_v}(x_v) + \frac{1}{2}\|x_v - \mathbb{e}_v^\top A_\mathcal{G}\bar{\mathbf{x}}\|^2. \tag{A-173}$$

Defining $f_v := \theta_v(x_v, \mathbb{e}_v^\top A\bar{\mathbf{x}}) + \imath_{X_v}(x_v)$, the solution to this problem can be obtained using the following iterative approach for each agent

$$x_v(k+1) = (1-\alpha)x_v(k) + \alpha \ \text{prox}_{f_v}(\mathbb{e}_v^\top A_\mathcal{G}\mathbf{x}(k)), \quad \alpha \in (0,1). \tag{A-174}$$

Where α can be set to $\alpha = 1$ if matrix $A_\mathcal{G}$ is averaging.

With the addition of jointly convex constraints, the problem needs to be redefined. By adding the dual variables λ, an extended network equilibrium problem can be defined as

$$\bar{x}_v = \arg\min_{x_v \in \mathbb{R}} f_v + \frac{1}{2}\|x_v - \mathbb{e}_v^\top A_\mathcal{G}\bar{\mathbf{x}}\|^2 + \bar{\lambda}^\top \mathbf{g}_v(x_v, \bar{\mathbf{x}}_{-v}) \tag{A-175}$$

$$\bar{\lambda} = \arg\min_{\xi \in \mathcal{L}} -\xi^\top \mathbf{g}(\bar{\mathbf{x}}). \tag{A-176}$$

If the jointly convex constraint functions are separable, the local constraints can be extended with $\mathbf{g}_v(x_v) \leq \zeta_v$ and the coupled constraints simplify to $\sum_{v=1}^N \zeta_v \leq 0$. With the mappings

$$\boldsymbol{\mathcal{F}} := \text{diag}(\text{prox}_{f_1}, \ldots, \text{prox}_{f_N}, \text{proj}_\mathcal{L}) \tag{A-177}$$

$$\boldsymbol{\mathcal{G}} := \begin{bmatrix} A & -C^\top \\ C & I \end{bmatrix} \cdot + \begin{bmatrix} \mathbb{0} \\ c \end{bmatrix} \tag{A-178}$$

the iteration method

$$\begin{bmatrix} \mathbf{x}(k+1) \\ \lambda(k+1) \end{bmatrix} = (\boldsymbol{\mathcal{F}} \circ \boldsymbol{\mathcal{G}}) \begin{bmatrix} \mathbf{x}(k) \\ \lambda(k) \end{bmatrix} \tag{A-179}$$

can be introduced. This approach results in a stable equilibrium if $\begin{bmatrix} A & -C^\top \\ C & I \end{bmatrix} < 1$. However generally that is not the case. As a result a forward-backward-forward distributed protocol is introduced:

$$\begin{bmatrix}\tilde{\mathbf{x}}(k)\\ \tilde{\lambda}(k)\end{bmatrix} = ((1-\alpha)\mathrm{Id} + \alpha\boldsymbol{\mathcal{G}})\begin{bmatrix}\mathbf{x}(k)\\ \lambda(k)\end{bmatrix} \tag{A-180}$$

$$\begin{bmatrix}\mathbf{x}(k+\frac{1}{2})\\ \lambda(k+\frac{1}{2})\end{bmatrix} = \boldsymbol{\mathcal{F}}_\alpha\left(\begin{bmatrix}\tilde{\mathbf{x}}(k)\\ \tilde{\lambda}(k)\end{bmatrix}\right) \tag{A-181}$$

$$\begin{bmatrix}\tilde{\mathbf{x}}(k+\frac{1}{2})\\ \tilde{\lambda}(k+\frac{1}{2})\end{bmatrix} = ((1-\alpha)\mathrm{Id} + \alpha\boldsymbol{\mathcal{G}})\begin{bmatrix}\mathbf{x}(k+\frac{1}{2})\\ \lambda(k+\frac{1}{2})\end{bmatrix} \tag{A-182}$$

$$\begin{bmatrix}\mathbf{x}(k+1)\\ \lambda(k+1)\end{bmatrix} = \begin{bmatrix}\tilde{\mathbf{x}}(k+\frac{1}{2})\\ \tilde{\lambda}(k+\frac{1}{2})\end{bmatrix} + \alpha\,(\mathrm{Id} - \boldsymbol{\mathcal{G}})\begin{bmatrix}\mathbf{x}(k)\\ \lambda(k)\end{bmatrix} \tag{A-183}$$

where $\boldsymbol{\mathcal{F}}_\alpha = \mathrm{diag}(\mathrm{prox}_{\alpha f_1}, \ldots, \mathrm{prox}_{\alpha f_N}, \mathrm{proj}_{\mathcal{L}})$.

Cournot dynamics

Consider the Cournot competition with N producers and consumers:

$$\bar{P}_{gi} = \arg\max_{P_{gi}\geq 0} P_{gi}\cdot p(P_{gi}, \bar{\mathbf{P}}_{-gi}) - C_{gi}(P_{gi}) \tag{A-184}$$

$$\bar{P}_{di} = \arg\max_{P_{di}\geq 0} U_i(P_{di}) - P_{di}\cdot \bar{p} \tag{A-185}$$

where

$$U_i(P_{di}) = -\tfrac{1}{2}P_{di}Q_{di}P_{di} + b_{di}P_{di} \tag{A-186}$$

$$C_{gi}(P_{gi}) = \tfrac{1}{2}P_{gi}Q_{gi}P_{gi} + b_{gi}P_{gi}. \tag{A-187}$$

Defining the price function $p(P_{gi}, \mathbf{P}_{-gi})$ as

$$p(P_{gi}, \mathbf{P}_{-gi}) = \beta - \alpha P_{gi} - \alpha\mathbb{1}_n^\top\mathbf{P}_{-gi} \tag{A-188}$$

the Cournot-Nash equilibrium results in

$$p^\star = \beta - \alpha\mathbb{1}_n^\top\mathbf{P}_g^\star \tag{A-189}$$

$$\mathbf{P}_g^\star = (\alpha I_n + Q_g)^{-1}(\mathbb{1}_n p^\star - \mathbf{b}_g) \tag{A-190}$$

$$\mathbf{P}_d^\star = Q_d^{-1}(\mathbf{b}_d - \mathbb{1}_n p^\star). \tag{A-191}$$

In general there is a mismatch between production and consumption, $\mathbb{1}_n\mathbf{P}_g \neq \mathbb{1}_n\mathbf{P}_d$, unless $\alpha = \alpha^\star$ and $\beta = \beta^\star$ with

$$\alpha^\star = \frac{1}{\mathbb{1}_n^\top Q_d^{-1}\mathbb{1}_n}, \quad \beta^\star = \frac{\mathbb{1}_n^\top Q_d^{-1}\mathbf{b}_d}{\mathbb{1}_n^\top Q_d^{-1}\mathbb{1}_n}. \tag{A-192}$$

To steer the network equilibrium in the balanced direction, state dynamics will be introduced. With a network of N agents, graph $\mathcal{G}(\mathcal{V}, \mathcal{E})$ and incidence matrix $B_{\mathcal{G}}$, defining $\mathbf{x} = [x_1, \ldots, x_N]^\top$ with node states x_v then results in the following dynamics:

$$\dot{\mathbf{x}} = \mathbf{y} \tag{A-193}$$
$$M\dot{\mathbf{y}} = -D\mathbf{y} - B_{\mathcal{G}}\nabla H(B_{\mathcal{G}}^{\top}\mathbf{x}) + \mathbf{P}_g - \mathbf{P}_d \tag{A-194}$$

To avoid drift in the equilibrium with respect to states $\mathbf{x}$, the dynamics will be reformulated to

$$\dot{\boldsymbol{\zeta}} = E^{\top}\mathbf{y} \tag{A-195}$$
$$M\dot{\mathbf{y}} = -D\mathbf{y} - E\nabla H_{\zeta}(\boldsymbol{\zeta}) + \mathbf{P}_g - \mathbf{P}_d. \tag{A-196}$$

with $E = [I_{n-1},\ -\mathbb{1}_{n-1}^{\top}]^{\top}$ and $\boldsymbol{\zeta} = E^{\top}\mathbf{x}$.

Now a feedback control will be introduced which adjusts the price $\mathbf{p}$. Resulting in the controlled dynamics

$$\dot{\boldsymbol{\zeta}} = E^{\top}\mathbf{y} \tag{A-197}$$
$$M\dot{\mathbf{y}} = -D\mathbf{y} - E\nabla H_{\zeta}(\boldsymbol{\zeta}) + K(\mathbf{p} - \mathbf{b}_g) + Q_d^{-1}(\mathbf{p} - \mathbf{b}_d) \tag{A-198}$$
$$T\dot{\mathbf{p}} = -L\mathbf{p} - K\mathbf{y} - Q_d^{-1}\mathbf{y} \tag{A-199}$$

which leads to a balanced system if $K = (\alpha^{\star} I_n + Q_g)^{-1}$, which requires limited information of the system.

Appendix B

Perron-Frobenius Theorem

In this appendix a number of proofs for the spectral analysis of non-negative matrices will be discussed.

B-1 Real dominant eigenvalue

In this section it will be shown that for a primitive matrix A the dominant eigenvector λ is real and positive, $\lambda \in \mathbb{R}_{>0}$, and therefor equal to the spectral radius $\rho(A)$. For readability the assumption will be made that $\rho(A) = 1$, however this does not generalize the proof. Any matrix with a non-zero spectral radius can be rescaled with $\alpha \in \mathbb{R}_{>0}$ such that $\rho\left(\frac{A}{\alpha}\right) = 1$ but for readability this fraction is omitted from the proof and instead the assumption is made. Furthermore the absolute signs $|\cdot|$ are considered component-wise.

Define $k \geq k^*$ (thus $A^k \succ 0$), since $\rho(A) = 1$ it is also true that $\rho(A^k) = 1$. Now consider the eigenpair $(\lambda, \mathbf{v})$ with $|\lambda^k| = \rho(A^k) = 1$, the following (in)equalities hold.

$$|\mathbf{v}| = |\lambda^k||\mathbf{v}| = |\lambda^k \mathbf{v}| = |A^k \mathbf{v}| \preceq |A^k||\mathbf{v}| = A^k|\mathbf{v}| \tag{B-1}$$

thus

$$|\mathbf{v}| \preceq A^k|\mathbf{v}| \tag{B-2}$$

The aim is to show that the inequality (B-2) strictly holds at equality, i.e. $|\mathbf{v}| = A^k|\mathbf{v}|$ (or $A^k|\mathbf{v}| - |\mathbf{v}| = \mathbb{0}_n$). Rewriting Equation (B-2) results in $A^k|\mathbf{v}| - |\mathbf{v}| \succeq \mathbb{0}_n$. By contradiction, assume that atleast one of the components is not strictly equal to zero, then $A^k\left(A^k|\mathbf{v}| - |\mathbf{v}|\right) \succ \mathbb{0}_n$. Since $|\mathbf{v}| \neq \mathbb{0}_n$, $A^k|\mathbf{v}| \succ \mathbb{0}_n$ and $\exists\epsilon \in \mathbb{R}_{>0}$ such that $A^k\left(A^k|\mathbf{v}| - |\mathbf{v}|\right) \succ \epsilon A^k|\mathbf{v}|$. Rewriting this inequality yields $\frac{A^k}{1+\epsilon}A^k|\mathbf{v}| \succ A^k|\mathbf{v}|$ and by extension $\lim_{l\to\infty}\left(\frac{A^k}{1+\epsilon}\right)^l A^k|\mathbf{v}| = \frac{\rho(A^k)}{1+\epsilon}A^k|\mathbf{v}| \succ A^k|\mathbf{v}|$. However, since $\frac{\rho(A^k)}{1+\epsilon} < 1$ this statement implies that $A^k|\mathbf{v}| \prec \mathbb{0}_n$ which is in contradiction with the earlier statement about $A^k|\mathbf{v}|$. Therefore $A^k\left(A^k|\mathbf{v}| - |\mathbf{v}|\right)$ does not have a non-zero component and as such $|\mathbf{v}| = A^k|\mathbf{v}|$.

The eigenpair $(1, |\mathbf{v}|)$ is an eigenpair of the primitive matrix A, with $\rho(A) = 1$ and the dominant eigenvector can be selected positive.

B-2 Simple dominant eigenvalue

In this section it will be shown that for a primitive matrix A the dominant eigenvalue $\lambda = \rho(A) = 1$ is simple. Since the eigenpair $(\lambda, \mathbf{v})$ exists with $\mathbf{v} \succ \mathbb{0}_n$ it also holds that $\mathbf{v} = A^k\mathbf{v}$, and as a result

$$||\mathbf{v}||_\infty = ||A^k\mathbf{v}||_\infty \geq ||A^k||_\infty \cdot \min \mathbf{v}, \quad \rightarrow \quad ||A^k||_\infty \leq \frac{||\mathbf{v}||_\infty}{\min \mathbf{v}} \tag{B-3}$$

Therefore A^k is bounded and as such its Jordan decomposition $A^k = VJ^kV^{-1}$. Assume that the algebraic multiplicity of λ is larger than 1, thus contradicting the fact that λ is simple, then the Jordan-block corresponding to λ is equal to

$$J_\lambda = \begin{bmatrix} \lambda & 1 & 0 & \cdots & 0 \\ 0 & \lambda & 1 & \cdots & 0 \\ 0 & 0 & \lambda & \cdots & 0 \\ \vdots & \vdots & \vdots & \ddots & \vdots \\ 0 & 0 & 0 & \cdots & \lambda \end{bmatrix} \tag{B-4}$$

which for an algebraic multiplicity of $m_a(\lambda) = 2$ with $\lambda = 1$ results in

$$J_\lambda = \begin{bmatrix} 1 & 1 \\ 0 & 1 \end{bmatrix} \tag{B-5}$$

yielding

$$J_\lambda^k = \begin{bmatrix} 1 & k \\ 0 & 1 \end{bmatrix} \tag{B-6}$$

which is not bounded for $k \rightarrow \infty$. As a result the algebraic multiplicity is equal to $m_a(\lambda) = 1$, thus the dominant eigenvalue $\lambda = \rho(A) = 1$ is simple.

Appendix C

Row-substochastic matrix

In this section a spectral analysis for row-substochastic matrices will be done. More specifically, considering a row-substochastic matrix A, if A is irreducible then it also is convergent. A matrix is said to be convergent if

$$\lim_{k\to\infty} A^k = \mathbb{0}_{n\times n}. \tag{C-1}$$

In order to prove that a row-substochastic, irreducible matrix is convergent, the following useful statements will be discussed:

(i) if $\mathbb{e}_i^\top A^k \mathbb{1}_n < 1$, then $\mathbb{e}_i^\top A^{k+1}\mathbb{1}_n < 1$,

(ii) if $\mathbb{e}_i^\top A^k \mathbb{e}_j > 0$ and $\mathbb{e}_j^\top A^k \mathbb{1}_n < 1$, then $\mathbb{e}_i^\top A^{k+1}\mathbb{1}_n < 1$,

(iii) $\exists k$ such that $A^k\mathbb{1}_n \prec \mathbb{1}_n$.

Since A is row-substochastic it can be concluded that $A\mathbb{1}_n \preceq \mathbb{1}_n$ and as a result

$$\mathbb{e}_i^\top A^{k+1}\mathbb{1}_n = \mathbb{e}_i^\top A^k \left(A\mathbb{1}_n\right) \leq \mathbb{e}_i^\top A^k\mathbb{1}_n < 1 \tag{C-2}$$

confirming statement (i). Furthermore, since $0 \leq \mathbb{e}_j^\top A^k \mathbb{1}_n < 1$, the following inequality holds

$$A^k\mathbb{1}_n \preceq \mathbb{1}_n - \left(1 - \mathbb{e}_j^\top A^k \mathbb{1}_n\right)\mathbb{e}_j \tag{C-3}$$

since at index $i \neq j$ the inequality yields $\mathbb{e}_i^\top A^k\mathbb{1}_n \leq 1$ and at index j it results in $\mathbb{e}_j^\top A^k\mathbb{1}_n \leq \mathbb{e}_j^\top A^k\mathbb{1}_n$ which holds for equality. Using Equation (C-3), the following result can be obtained

$$\mathbb{e}_i^\top A^{k+1}\mathbb{1}_n = \mathbb{e}_i^\top A\left(A^k\mathbb{1}_n\right) \leq \underbrace{\mathbb{e}_i^\top A\mathbb{1}_n}_{\leq 1} - \underbrace{\left(1 - \mathbb{e}_j^\top A^k\mathbb{1}_n\right)\mathbb{e}_i^\top A^k \mathbb{e}_j}_{>0} < 1. \tag{C-4}$$

Finally, if the matrix is irreducible, i.e. $\sum_{k=0}^{n-1} A^k \succ \mathbb{0}_{n\times n}$, there exists a k such that $\mathbb{e}_i^\top A^k \mathbb{e}_j > 0$ and following statement (i) and (ii) $\exists k$ such that $\mathbb{e}_i^\top A^{k+l}\mathbb{1}_n < 1, \quad \forall l \in \mathbb{Z}_{>0}$.

As a result $A^k \mathbb{1}_n \prec \mathbb{1}_n$, proving statement (iii).

Defining $\lambda = \max_i \left(\mathbb{e}_i^\top A^k \mathbb{1}_n \right)$ and $k^* = ak + b$ with $a, b \in \mathbb{Z}_{>0}$, the following result can be obtained

$$A^{k^*} \mathbb{1}_n = A^{ak} A^b \mathbb{1}_n \preceq A^{ak} \mathbb{1}_n = \left(A^k \right)^a \mathbb{1}_n \preceq \lambda^a \mathbb{1}_n. \tag{C-5}$$

Note that $\lambda < 1$ following statement (iii), therefore as $a \to \infty$ then $\lambda^a \to 0$ and as such $A^{k^*} \to \mathbb{0}_{n \times n}$ as $k^* \to \infty$. Therefor it is proven that if a matrix A is irreducible and row-stochastic, then it is convergent as well. Additionally it can be concluded that $\rho(A) < 1$.

The previous proof also holds for reducible row-stochastic matrices, as long as for all nodes i with $\mathbb{e}_i^\top A \mathbb{1}_n = 1$ there exists a path to a node j with $\mathbb{e}_j^\top A \mathbb{1}_n < 1$.

Appendix D

Network-decentralized control

In this appendix proofs regarding network systems will be given.

D-1 Distinct eigenvalues

Under the assumption of distinct eigenvalues of subsystems in a linear system with block-diagonal state matrix, the notions of (node) stabilizability and stabilizability by means of a network-decentralized control are equivalent.

Assume that the system is node-stabilizable, applying a Kalman-like transformation of the m_1 subsystems of (A, B) connected to u_1 then yields

$$[A||B] = \left[\begin{array}{cc|c|cc|c||cc} S_1 & R_1 & \cdots & \mathbb{0} & \mathbb{0} & \mathbb{0} & V_1 & X \\ \mathbb{0} & U_1 & \cdots & \mathbb{0} & \mathbb{0} & \mathbb{0} & \mathbb{0} & \tilde{B}_1 \\ \hline \vdots & \vdots & \ddots & \vdots & \vdots & \vdots & \vdots & \vdots \\ \hline \mathbb{0} & \mathbb{0} & \cdots & S_{m_1} & R_{m_1} & \mathbb{0} & V_{m_1} & X \\ \mathbb{0} & \mathbb{0} & \cdots & \mathbb{0} & U_{m_1} & \mathbb{0} & \mathbb{0} & \tilde{B}_{m_1} \\ \hline \mathbb{0} & \mathbb{0} & \cdots & \mathbb{0} & \mathbb{0} & \Delta & \mathbb{0} & \tilde{B} \end{array}\right] \tag{D-1}$$

with (S_i, V_i) a stabilizable pair, U_i the matrices containing the unreachable unstable eigenvalues (with respect to u_1), $(\Delta, \tilde{B})$ the part of (A, B) not connected to u_1 and X the negligible entries. Reordering the entries of Equation (D-1) then yields

$$[A||B] = \left[\begin{array}{ccc|ccc|c||cc} S_1 & \cdots & \mathbb{0} & R_1 & \cdots & \mathbb{0} & \mathbb{0} & V_1 & X \\ \vdots & \ddots & \vdots & \vdots & \ddots & \vdots & \vdots & \vdots & \vdots \\ \mathbb{0} & \cdots & S_p & \mathbb{0} & \cdots & R_{m_1} & \mathbb{0} & V_{m_1} & X \\ \hline \mathbb{0} & \cdots & \mathbb{0} & U_1 & \cdots & \mathbb{0} & \mathbb{0} & \mathbb{0} & \tilde{B}_1 \\ \vdots & \ddots & \vdots & \vdots & \ddots & \vdots & \vdots & \vdots & \vdots \\ \mathbb{0} & \cdots & \mathbb{0} & \mathbb{0} & \cdots & U_{m_1} & \mathbb{0} & \mathbb{0} & \tilde{B}_{m_1} \\ \hline \mathbb{0} & \cdots & \mathbb{0} & \mathbb{0} & \cdots & \mathbb{0} & \Delta & \mathbb{0} & \tilde{B} \end{array}\right] \tag{D-2}$$

Since the (S_i, V_i) entries are stabilizable pairs, due to the assumption of node-stabilizability, the following feedback results in stability

$$\Phi_1 = \begin{bmatrix} S_1 & \cdots & \mathbb{0} \\ \vdots & \ddots & \vdots \\ \mathbb{0} & \cdots & S_{m_1} \end{bmatrix} + \begin{bmatrix} V_1 \\ \vdots \\ V_{m_1} \end{bmatrix} \begin{bmatrix} \tilde{K}_1 & \cdots & \tilde{K}_{m_1} \end{bmatrix} \tag{D-3}$$

yielding the block-triangular form

$$[\hat{A}||B] = \left[\begin{array}{cc||cc} \Phi_1 & X & \Gamma_{11} & \Gamma_{12} \\ \mathbb{0} & \Phi_2 & \mathbb{0} & \Gamma_{22} \end{array}\right] \tag{D-4}$$

With the unstable part $[\Phi_2||\Gamma_{22}]$ equal to

$$[\Phi_2||\Gamma_{22}] = \left[\begin{array}{cccc||c} U_1 & \cdots & \mathbb{0} & \mathbb{0} & \tilde{B}_1 \\ \vdots & \ddots & \vdots & \vdots & \vdots \\ \mathbb{0} & \cdots & U_{m_1} & \mathbb{0} & \tilde{B}_{m_1} \\ \mathbb{0} & \cdots & \mathbb{0} & \Delta & \tilde{B} \end{array}\right] \tag{D-5}$$

This part still includes the remaining inputs u_2 to u_m, and due to the assumption of node-stabilizability the unstable parts U_1 to U_{m_1} must be stabilizable by the remaining inputs. Repeating the process for input u_2 then yields a stable Φ_2 with remaining unstable part $[\Phi_3||\Gamma_{33}]$, this can be repeated for every input and terminates successfully. As a result the statement that (node) stabilizability implies stabilizability by means of a network-decentralized control is true.

D-2 Common eigenvalues

In case of the subsystems of a network system having a single common unstable eigenvalue λ with ascent 1, stabilizability of the system implies there is a structured solution of the LMI given by

$$SA^\top + AS - 2\gamma BB^\top < 0 \tag{D-6}$$

with

$$S = P^{-1} = \text{blockdiag}\{P_1^{-1}, P_2^{-1}, \dots, P_n^{-1}\} > 0. \tag{D-7}$$

To proof this, each individual subsystem A_i will undergo a transformation T_i such that $T_i^{-1}A_iT_i = \text{blockdiag}\{\lambda I_{m_i}, A_i^S\}$. Where A_i^S contains the stable part of matrix A_i. Due to A_i^S being stable, a valid Lyapunov matrix is the identity I, yielding

$$A_i^{S\top} + A_i^S = -Q_i < 0. \tag{D-8}$$

Doing this for each subsystem and grouping the unstable blocks and stable blocks seperatly then yields

$$\hat{A} = T^{-1}AT = \begin{bmatrix} \lambda I & \mathbb{0} \\ \mathbb{0} & \hat{A}^S \end{bmatrix}, \quad \hat{B} = T^{-1}B = \begin{bmatrix} \hat{B}^\lambda \\ \hat{B}^S \end{bmatrix}. \tag{D-9}$$

In view of the assumed stability, $(\hat{A}, \hat{B})$ must be stabilizable. Therefore the popov criterion rank $\left[\lambda I - \hat{A}, \hat{B}\right] = n$ must hold, implying that $\hat{B}^\lambda$ must have full row rank. Resulting in $\hat{B}^\lambda \hat{B}^{\lambda^\top} > 0$. Furthermore, since the stable part $\hat{A}^S$ does not require a feedback control for stabilizability, matrix K can be defined as

$$\hat{K} = \gamma \left[\hat{B}^{\lambda^\top}, 0\right] \hat{P} \tag{D-10}$$

Furthermore, the following candidate structured matrix will be considered

$$\hat{S} = \begin{bmatrix} I & \mathbb{0} \\ \mathbb{0} & \mu I \end{bmatrix} \tag{D-11}$$

yielding

$$\hat{P} = \begin{bmatrix} I & \mathbb{0} \\ \mathbb{0} & \frac{1}{\mu} I \end{bmatrix}. \tag{D-12}$$

Resulting in the following equation:

$$\hat{S}(\hat{A} - \hat{B}\hat{K})^\top + (\hat{A} - \hat{B}\hat{K})\hat{S} = \begin{bmatrix} 2\left(\lambda I - \gamma \hat{B}^\lambda \hat{B}^{\lambda^\top}\right) & -\gamma \hat{B}^\lambda \hat{B}^{S^\top} \\ -\gamma \hat{B}^S \hat{B}^{\lambda^\top} & -\mu \hat{Q} \end{bmatrix}. \tag{D-13}$$

Since $\hat{B}^\lambda \hat{B}^{\lambda^\top} > 0$, a γ can be chosen such that $\left(\lambda I - \gamma \hat{B}^\lambda \hat{B}^{\lambda^\top}\right) < 0$. Subsequently, choosing μ large enough such that the resulting matrix is diagonally dominant then ensures that

$$\hat{S}(\hat{A} - \hat{B}\hat{K})^\top + (\hat{A} - \hat{B}\hat{K})\hat{S} < 0 \tag{D-14}$$

thus a structured solutiong to the LMI exists.

In order to find the solution for the LMI of the original system, $\hat{S}$ must undergo some backwards transformations. Considering the original LMI

$$SA^\top + AS - 2\gamma BB^\top < 0 \tag{D-15}$$

and the transformed LMI

$$\hat{S}\hat{A}^\top + \hat{A}\hat{S} - 2\gamma\hat{B}\hat{B}^\top < 0. \tag{D-16}$$

Using the definition that $\hat{A} = T^{-1}AT$ and $\hat{B} = T^{-1}B$, and substituting those in Equation (D-16) then results in

$$\begin{aligned} \hat{S}\left(T^{-1}AT\right)^\top + \left(T^{-1}AT\right)\hat{S} - 2\gamma\left(T^{-1}B\right)\left(T^{-1}B\right)^\top &= \\ \hat{S}T^\top A^\top {T^{-1}}^\top + T^{-1}AT\hat{S} - 2\gamma T^{-1}BB^\top {T^{-1}}^\top &= \\ T^{-1}\left(T\hat{S}T^\top A^\top + AT\hat{S}T^\top - 2\gamma BB^\top\right){T^{-1}}^\top &< 0 \end{aligned}$$

therefor

$$T\hat{S}T^\top A^\top + AT\hat{S}T^\top - 2\gamma BB^\top < 0 \tag{D-17}$$

taking $S = T\hat{S}T^\top$ then yields the original LMI from Equation (D-15). Therefore to obtain the appropriate matrix P for the original system, the following equation applies:

$$P = {T^{-1}}^\top \begin{bmatrix} I & \mathbb{0} \\ \mathbb{0} & \frac{1}{\mu}I \end{bmatrix} T^{-1} \tag{D-18}$$

Bibliography

[1] F. Bullo, *Lectures on network systems.* Createspace, 2018.

[2] R. Olfati-Saber, J. A. Fax, and R. M. Murray, "Consensus and Cooperation in Networked Multi-Agent Systems," *Proceedings of the IEEE*, vol. 95, no. 1, p. 215–233, 2007.

[3] Y. Cao, W. Yu, W. Ren, and G. Chen, "An Overview of Recent Progress in the Study of Distributed Multi-Agent Coordination," *IEEE Transactions on Industrial Informatics*, vol. 9, no. 1, p. 427–438, 2013.

[4] J. Qin, Q. Ma, Y. Shi, and L. Wang, "Recent Advances in Consensus of Multi-Agent Systems: A Brief Survey," *IEEE Transactions on Industrial Electronics*, vol. 64, no. 6, p. 4972–4983, 2017.

[5] W. Ren, R. Beard, and E. Atkins, "A survey of consensus problems in multi-agent coordination," *Proceedings of the 2005, American Control Conference, 2005.*

[6] F. Blanchini, E. Franco, and G. Giordano, "Network-Decentralized Control Strategies for Stabilization," *IEEE Transactions on Automatic Control*, vol. 60, no. 2, p. 491–496, 2015.

[7] F. Blanchini, E. Franco, G. Giordano, V. Mardanlou, and P. L. Montessoro, "Compartmental flow control: Decentralization, robustness and optimality," *Automatica*, vol. 64, p. 18–28, 2016.

[8] G. Giordano, F. Blanchini, E. Franco, V. Mardanlou, and P. L. Montessoro, "The Smallest Eigenvalue of the Generalized Laplacian Matrix, with Application to Network-Decentralized Estimation for Homogeneous Systems," *IEEE Transactions on Network Science and Engineering*, vol. 3, no. 4, p. 312–324, 2016.

[9] J. F. Nash, "Equilibrium points in n-person games," *Proceedings of the National Academy of Sciences*, vol. 36, no. 1, p. 48–49, 1950.

[10] G. Debreu, "A Social Equilibrium Existence Theorem," *Proceedings of the National Academy of Sciences*, vol. 38, no. 10, p. 886–893, 1952.

[11] K. J. Arrow and G. Debreu, "Existence of an Equilibrium for a Competitive Economy," *Econometrica*, vol. 22, no. 3, p. 265, 1954.

[12] F. Facchinei and C. Kanzow, "Generalized Nash Equilibrium Problems," *Annals of Operations Research*, vol. 175, no. 1, p. 177–211, 2009.

[13] S. Grammatico, "Proximal Dynamics in Multiagent Network Games," *IEEE Transactions on Control of Network Systems*, vol. 5, no. 4, p. 1707–1716, 2018.

[14] F. Salehisadaghiani and L. Pavel, "Distributed Nash equilibrium seeking: A gossip-based algorithm," *Automatica*, vol. 72, p. 209–216, 2016.

[15] C. D. Persis and N. Monshizadeh, "A feedback control algorithm to steer networks to a Cournot-Nash equilibrium," *IEEE Transactions on Control of Network Systems*, p. 1–1, 2019.

[16] R. Rajamani, "Transform Solutions to LTI Systems," *http://www.me.umn.edu/courses/me3281/notes/TransformSolutionsToLTISystems Part4.pdf*.

[17] R. A. Horn and C. R. Johnson, "Matrix Analysis," *Cambridge University Press*, 1990.

[18] R. Opie, "Pitch Control Critical for Wind Power."

[19] J. Zhang, M. Cheng, Z. Chen, and X. Fu, "Pitch angle control for variable speed wind turbines," *2008 Third International Conference on Electric Utility Deregulation and Restructuring and Power Technologies*, 2008.

[20] A. Hwas and R. Katebi, "Wind turbine control using pi pitch angle controller," *IFAC Proceedings Volumes*, vol. 45, no. 3, p. 241–246, 2012.

[21] R. Tiwari and R. B. N, "Comparative analysis of pitch angle controller strategies for pmsg based wind energy conversion system," *International Journal of Intelligent Systems and Applications*, vol. 9, p. 62–73, Aug 2017.

[22] D. Petković and S. Shamshirband, "Soft methodology selection of wind turbine parameters to large affect wind energy conversion," *International Journal of Electrical Power & Energy Systems*, vol. 69, p. 98–103, 2015.

[23] Z. Shao, Y. Wu, L. Li, S. Han, and Y. Liu, "Multiple wind turbine wakes modeling considering the faster wake recovery in overlapped wakes," *Energies*, vol. 12, no. 4, p. 680, 2019.

[24] Kimerius, "Aerodynamics of Wind Turbines."

[25] J. L. Gross and J. Yellen, "Handbook of Graph Theory," 2003.

[26] A. Maheshwari, "Perron-Frobenius Theorem," *https://people.scs.carleton.ca/~maheshwa/courses/3801/Projects17/PF-thm-report.pdf*, 2017.

[27] J. Willems, "Lyapunov functions for diagonally dominant systems," *Automatica*, vol. 12, no. 5, p. 519–523, 1976.